Design and development of energy-efficient transmission for wireless IoT modules

Nikesh Man Shakya

université PARIS-SACLAY

TELECOM SudParis

NNT : 2019SACLL001

Thèse de doctorat

Design and Development of Energy-efficient Transmission for Wireless IoT Modules

Thèse de doctorat de l'Université Paris-Saclay
préparée à Télécom SudParis

Ecole doctorale n°580 Sciences et technologies de l'information et de la communication (STIC)
Spécialité de doctorat : Informatique

Thèse présentée et soutenue à Meudon, le 06/02/2019, par

NIKESH MAN SHAKYA

Composition du Jury :

M. Nazim AGOULMINE Professeur, Université d'Évry Val d'Essonne	Président
M. Stefano SECCI Professeur, CNAM	Rapporteur
M. Naceur MALOUCH Associate Professor, University Pierre et Marie Curie (UPMC)	Rapporteur
M. Nazim AGOULMINE Professeur, Université d'Évry Val d'Essonne	Examinateur
Mme. Maria POTOP-BUTUCARU Professeure, Campus Pierre et Marie Curie Sorbonne Université - LIP6	Examinateur
M. Noel CRESPI Professeur, Télécom SudParis	Directeur de thèse
M. Mehdi MANI Sr. Project Manager, Itron	Co-directeur de thèse

I. Acknowledgement

I would like to express my sincere gratitude to all those people who made my thesis possible. I am indebted to them for their incessant supervision, valuable suggestions, support and motivation for completion of this Thesis.

First of all, I would like to express my genuine appreciation and gratitude to Dr. Mehdi Mani, who offered his continuous advice and encouragement throughout the course of this thesis and having a belief on me and giving me an opportunity to purse my PhD here at ITRON. I am also indebted to my thesis director Prof. Noel Crespi for his advice, constant suggestions and support. I truly appreciate his esteemed guidance and timely inspirations.

Also, I would also like to thank both HR of ITRON, Leticia Royere and HR of TSP Veronique Guy for their support and guidance in solving the tedious administrative works. I appreciate the hospitality received from ITRON lab and all my colleagues during my thesis.

With profound love and respect, I would also like to thank my wife Mrs. Niraja Shakya and my parents Mr. Narendra Man Shakya and Mrs. Durga Shakya for supporting me along the way with their love, moral and emotional support.

Lastly, my sincere thanks to all the others who availed me directly or indirectly throughout the thesis period.

Thank you for all your encouragements!

II. Abstract

Radio Transmission is one of the major sources of energy consumption in today's rising IoT devices in low powered and lossy networks. Device longevity has become the foundation of the IoT's entire value proposition and is a key to unravel the next great wave of IoT. Transmission power and transmission bit-rate are the two radio parameters that principally impact the energy consumption along with the radio coverage, interference, link reliability, channel/spatial reuse etc. Transmitting at a constant high/low power or rate leads to an inefficient energy usage due to the varying, unstable and unpredictable radio links. Hence, the power/rate level should dynamically vary with such erratic radio conditions.

Transmission (TX) power/rate control algorithms for the constrained devices in IoT/WSN should have low overheads and must be energy efficient. They need to be adaptive and versatile to different environment conditions; yet be simple and easily implementable in the real sensor/IoT platform. Many dynamic Transmission Power and/or Rate Control algorithms have been proposed in the literature to economize the energy waste in the massive IoT deployments. But they fail to satisfy all these requirements alone. Each of them has its strengths and weaknesses. Therefore, there is a need of a new algorithm that performs an energy-efficient power and/or rate control which can be easily implemented in a real sensor platform.

This thesis presents REACT (Responsive Energy-efficient Adaptive Control of Transmission power and rate), a technique that considers more than one link quality information for better adaptation of TX power and rate. It has a self-learning, versatile and environment-adaptive control technique with a global aim to reduce the transmission energy consumption with insignificant compromise on the packet delivery ratio or throughput. It has least possible initial phase with zero overhead and has a responsive behavior that reacts appropriately to the varying radio conditions.

To attain this aim, we commenced with the study and the selection of a proper link quality estimation metric which is a crucial part in any power or rate control mechanism. ETX (Expected Transmission Count) from the sender-side and RSSI (Received Signal Strength Indicator) from receiver-side were used as a primary and a secondary metric respectively to provide multiple link information. Second, we designed and developed a responsive transmission power control at fixed bit-rate (REACT-P). We proved its efficiency comparing

with using the maximum constant power at constant rate (CPCR) and one of the dominant existing algorithms. Third, this design is extended considering the bit-rate to give rise to REACT or REACT-PR that offers higher energy savings by controlling both transmission power and rate.

We have evaluated our solutions using repetitive simulation and experimentation under both congested and un-congested environment. Simulation were performed in Cooja with TMote Sky motes whereas the experimentations were performed in Itron IoT device hardware compliant with IEEE802.15.4. The test results showed that, comparing to CPCR and REACT-P, with similar packet delivery ratio, REACT consumes much less energy, reduces interference, channel occupancy and aids to prolong the device lifetime. Even in the worst case, where all nodes transmit at the same time, the improvement in total energy consumption was 58% with REACT and 29% with REACT-P compared to CPCR. The nodes closer to the sink gain lifetime maximally than those farther away. The results also reveal that the improvement in the energy consumption improves with the decrease in the concurrent transmissions.

Although the scope of the algorithm was designed for the battery-operated devices, it is equally applicable to mains line powered devices as well as it can aid in reducing interference, channel occupancy and improve the throughput and latency

III. Abstract French

La transmission radio est une des principales sources de consommation d'énergie des objets connectés dans les réseaux IoT. La durée de vie des objets IoT est le facteur principal qui permet le développement massif d'une solution IoT. La puissance de transmission et le débit binaire de transmission sont les deux paramètres radio qui affectent principalement la consommation d'énergie avec la portée radio, le brouillage, la fiabilité des liaisons et la réutilisation des canaux/de l'espace. Les conditions variables des liaisons radios nécessite que le niveau de puissance/débit varie de manière dynamique pour s'aligner à de telles conditions instables.

Les algorithmes de contrôle de puissance/débit de transmission (TX) ne doivent pas poser des charges supplémentaires pour qu'ils soient applicable pour les appareils IoT avec des ressources d'énergie limitées. Ils doivent être adaptables et polyvalents aux différentes conditions environnementales et de l'autre côté, être simple et facilement implémentable dans les plateformes capteur/IoT. De nombreux algorithmes dynamiques de transmission de puissance et / ou de contrôle de débit ont été proposés dans la littérature pour économiser la consommation d'énergie. Mais ils ne parviennent pas à satisfaire toutes ces exigences. Chacun d'entre eux a ses forces et ses faiblesses. Par conséquence, il existe le besoin d'un nouvel algorithme qui effectue un contrôle de puissance et / ou de débit qui peut être facilement implémenté dans une véritable plateforme de réseau IoT.

Cette thèse présente REACT (Responsive Energy-efficient Adaptive Control of Transmission), une technique qui prend en compte plus d'une information de qualité de liaison pour une meilleure adaptation de la puissance et du débit TX. Il dispose d'une technique de contrôle à auto-apprentissage, polyvalente et adaptative pour l'environnement, avec un objectif global de réduction de la consommation d'énergie de transmission tout en maintenant une fiabilité similaire. Il possède la phase initiale la plus légère possible avec une surcharge nulle et un comportement réactif qui réagit de manière appropriée aux variations des conditions radio.

Pour atteindre cet objectif, nous avons commencé par l'étude et la sélection d'une métrique d'estimation de la qualité de la liaison qui constitue un élément crucial de tout mécanisme de contrôle de la puissance ou de la vitesse. ETX (nombre de transmissions prévu) du côté de l'expéditeur et RSSI du côté du récepteur ont été utilisés respectivement comme métrique

primaire et secondaire pour fournir des informations de liaison. Deuxièmement, nous avons conçu et développé un mécanisme de contrôle de puissance de transmission réactive à débit binaire fixe (REACT-P). Nous avons prouvé son efficacité en comparant l'utilisation de la puissance constante maximale à débit constant (CPCR) et l'un des algorithmes existants dominants. Troisièmement, cette conception est élargie en ajoutant l'option d'adaptation de débit donnant lieu à REACT ou REACT-PR qui permet de réaliser des économies d'énergie plus importantes en contrôlant à la fois la puissance et le débit.

Nous avons évalué nos solutions en utilisant à la fois la simulation et l'expérimentation dans les environnements encombré et non encombré. Les résultats des tests ont montré que, comparé à la CPCR et REACT-P, avec un taux de livraison de paquets similaire, REACT consomme beaucoup moins d'énergie, réduit les interférences, l'occupation des canaux et contribue à prolonger la durée de vie de l'appareil. Même dans le pire des cas, où tous les nœuds transmettent en même temps, l'amélioration de la consommation totale d'énergie était de 58% avec REACT et de 29% avec REACT-P par rapport à CPCR. Les nœuds les plus proches de point d'accès gagnent le maximum de durée de vie par rapport de ceux plus éloignés. Les résultats montrent également que l'amélioration de la consommation d'énergie diminue avec l'augmentation de nombre de transmissions simultanées.

IV. Table of Contents

I. Acknowledgement II

II. Abstract III

III. Abstract French V

IV. Table of Contents VII

V. List of Figures XI

VI. List of Tables XIV

VII. List of Abbreviations XV

1. Introduction 1

1.1 Internet of Things (IoT) 3

1.1.1 Background 3

1.1.2 IoT Predictions 5

1.1.3 Various Applications of IoT 8

1.1.4 An IoT Device 10

1.1.5 IoT Open Standard Protocol Stack 12

1.1.6 Power Sources for IoT Devices: A Big challenge 14

1.1.7 Energy Consumption in IoT: A Taxonomy 17

1.2 Thesis Motivation and Scope 18

1.3 Content of PhD 20

1.3.1 Research Objectives and Contributions 20

1.3.2 Structure of Thesis 22

2. Link Quality Estimation 25

2.1 Radio Link Quality 27

2.2 Signal-Based 28

2.2.1 RSSI 29

2.2.2 LQI 29

2.2.3 SNR and SINR 30

2.3 Statistics Based 30
2.3.1 Number of Neighbors 31
2.3.2 PRR 31
2.3.3 ETX 31
2.3.4 ETT 32
2.4 State of art and Review on signal and statistics-based metrics 32
2.4.1 Comparing Signal-based and Statistics based Metrics 33
2.5 Choice of Link Quality Metric 34
2.6 Conclusion 35
3. Transmission Power Control (TPC) 37
3.1 Introduction 39
3.1.1 Impacts of Transmission Power 39
3.1.2 Key Concept of TPC 40
3.1.3 Different Levels of TPC 41
3.1.4 Fundamental Blocks of TPC 42
3.1.5 Link Quality Estimation (LQE) 42
3.1.6 Control Mechanism 42
3.1.7 General Drawbacks of TPC Algorithms 43
3.2 Literature Review 44
3.3 Proposed Algorithm: REACT-P 46
3.3.1 Working Principle 46
3.3.2 REACT-P Block Diagram 50
3.3.3 Novelty 55
3.4 Implementation 56
3.4.1 Assumptions 58
3.4.2 Calculation of Transmission Time 58
3.4.3 Energy Consumption Model 58

3.4.4 Live Tool 59
3.5 Performance Metrics 61
3.5.1 Network TX Energy Consumption 61
3.5.2 PDR 61
3.5.3 Average TX Energy Consumption per Frame 62
3.6 Simulation 62
3.6.1 Setup 64
3.6.2 Parameters 64
3.6.3 Results and Discussions 66
3.7 Experimentation 71
3.7.1 Setup 71
3.7.2 Parameters 72
3.7.3 Results and Discussions 74
3.8 Conclusion 82
4. Transmission Rate Control 83
4.1 Introduction 85
4.1.1 Impacts of Transmission Bit Rate 86
4.2 Literature Review 88
4.3 Calculation of Transmission Time 90
4.4 Experimentation 90
4.4.1 Transmission Time 90
4.4.2 Experimentation at different TX Bit-Rates 92
4.5 Conclusion 93
5. Transmission Power and Rate Control 94
5.1 Introduction 96
5.2 Literature Review 97
5.3 Proposed Algorithm: REACT or REACT-PR 98

5.3.1 Working Principle 99
5.4 Performance Metrics 100
5.4.1 CCA Busy Count 100
5.4.2 Network Lifetime 101
5.4.3 Standard Deviation Error 101
5.5 Implementation 102
5.5.1 Initializing the Control Mechanism 102
5.5.2 Setting the Energy Level Array 102
5.5.3 Calculation of Remaining Lifetime of a Node 104
5.6 Experimentation 106
5.6.1 Parameters 106
5.6.2 Environment 107
5.6.3 Results and Discussion 108
5.7 Conclusion 119
6. Conclusion and Future Works 121
6.1 Conclusion 123
6.2 Future Works 125
7. Publications 127
8. References 129
9. Appendices 137
Appendix-A: Related Figures 137
Appendix-B: Sorted Energy level array in the ascending order 137
Appendix-C: Flowcharts of the proposed algorithm REACT 139

V. List of Figures

Figure 1-1: IoT Landscape 3
Figure 1-2: Number of connected devices from 2015 to 2025 [10] 6
Figure 1-3: Number of battery powered IoT devices [12] 6
Figure 1-4: Global share of IoT projects and trends [15] 7
Figure 1-5: Consumer and Bussiness IoT platforms [16] 7
Figure 1-6: Worldwide IoT Application Enablement and Device Management Platform Revenue [13] 8
Figure 1-7: Block diagram of a typical IoT device 11
Figure 1-8: Open wireless standard reference model for IoT 12
Figure 1-9: Tradeoffs in various IoT enabling communication technologies 14
Figure 1-10: Various energy saving techniques for WSN/IoTs 18
Figure 1-11: Research objectives addressed in each chapters 23
Figure 2-1: Various link quality metrics from various OSI layers 28
Figure 3-1: Key concept of transmission power control (TPC) 40
Figure 3-2: Fundamental blocks of TPC 42
Figure 3-3: Finite state transition diagram for REACT-P in run-time phase 48
Figure 3-4: REACT-P block diagram 51
Figure 3-5: Placement of REACT-P block in the IoT netstack 57
Figure 3-6: Live tool showing network metrics 60
Figure 3-7: Live tool showing power related metrics 61
Figure 3-8: Two simulation test networks 64
Figure 3-9: The % improvement in TX energy consumption at different distances and PSR 67
Figure 3-10: Throughput and PDR at different distances at 60% PSR 67
Figure 3-11: The % improvement in TX energy consumption for different numbers of nodes and link quality levels 68
Figure 3-12: Network Throughput and PDR at different PSR 69
Figure 3-13: Node 6's TX Energy consumption history and its average for a 25-node environment at 60% PSR 69
Figure 3-14: Mean energy consumption of ODTPC (left) and experimental setup (right) [64] 70

Figure 3-15: Mean energy consumption of REACT-P (left) and mimicked simulated setup 71
Figure 3-16: Itron wireless IoT Module 71
Figure 3-17: Experimentation floor deployment plan I 72
Figure 3-18: Transmission Power Amplifier Control Register for ATRF215 Tranceiver .. 73
Figure 3-19: Circuit connection to measure the current 74
Figure 3-20: Current consumption at different power levels for ATRF215 74
Figure 3-21: Timeline showing transmitting in different time slots (TSN) 76
Figure 3-22: Received Signal Strength (RSSI) of all clients over time 77
Figure 3-23: ETX and EWMA_ETX for a case of 2/7 at CPCR 78
Figure 3-24: Average energy consumed per frame and % Improvement in Total TX Energy 79
Figure 3-25: Total frame losses and PDR in a network 80
Figure 3-26: Average TX Energy consumed per client 81
Figure 3-27: Total TX Energy consumption of the clients 81
Figure 3-28: Client 8 adapting power over time with EWMA ETX with REACT-P 82
Figure 4-1 : Format of the MR-O-QPSK PHY PPDU 85
Figure 4-2: Format of the PHR for MR-O-QPSK 85
Figure 4-3: Rate Mode mapping for MR-OQPSK @100Kchips/sec 85
Figure 4-4: Reference Modulator diagram for MR-OQPSK [30] 86
Figure 4-5: Trade off between data rate, distance, SNR, and range [77] 88
Figure 4-6: Experimental PPDU frame duration for 142B MPDU frame at different rate modes 91
Figure 4-7: Agilent EXA Signal Analyzer in lab 92
Figure 4-8: Average network energy consumption and Total CCA busy counts at different bit-rates for the case of 2/7(a) and 4/7(b) 93
Figure 5-1: Tradeoffs in LLNs or LPWANs 96
Figure 5-2: Estimated Remaining Life Time (ERLT) calculation 105
Figure 5-3: REACT deployment plan 108
Figure 5-4: Average Energy consumed per unique frame received for CLient 7 at different rates and attenuation 109
Figure 5-5: PDR of client 7 at defferent rates and attenuation 109
Figure 5-6: Average network energy consumption and % improvement of REACT and REACT-P 112

Figure 5-7: Total frame losses and PDR in a network 112
Figure 5-8: Average network lifetime and % improvement 113
Figure 5-9: Network lifetime when different % of nodes are dead 114
Figure 5-10: Total CCA busy counts in a network 115
Figure 5-11: Energy consumed per TX frame for the case of 5/7 116
Figure 5-12: Total TX energy consumption per node 117
Figure 5-13: PDR per Node 117
Figure 5-14: Average Network Energy consumption and % improvement w.r.t. CPCR for different constant rates for 2/7 case. 118
Figure 5-15: Total CCA busy counts at different rates 119
Figure 9-1: Snapshot of COOJA simulator 137
Figure 9-2: FLowchart for initializing the control mechanism 140
Figure 9-3: Setting up energy level array 141
Figure 9-4: Flowchart to compare the energy levels used by qsort 142
Figure 9-5: Main function of Transmission power and rate control algortihm for REACT 146
Figure 9-6: Flowchart showing the bootstrap phase 148
Figure 9-7: Flowchart for calculating the ETT 149
Figure 9-8: Flowchart for calculating TX Energy consumption 149
Figure 9-9: Flowchart for claculating the path loss 150
Figure 9-10: Flowchart showing BEW Mechanism 150
Figure 9-11: Flowchart for the actions for increasing the power/energy level 151
Figure 9-12: Flowchart showing the process for decresing the power/energy level 152
Figure 9-13: Flowchart showing process for keeping the same level 152
Figure 9-14: Flowchart showing safe2Decrease Module 153
Figure 9-15: Flowchart showing out_of_coverage detection mechanism 154
Figure 9-16: Flowchart to update the last stable energy/power level 155
Figure 9-17: Flowchart to update the TX radio parameters (power, rate) 156

VI. List of Tables

Table 1-1: Various applications of IoT 8
Table 1-2: Various power sources choices for IoT devices 16
Table 2-1: Comparison table between Signal-based and Statistics-based link quality metrics 33
Table 3-1: Existing packet level TPC algorithms 44
Table 3-2: REACT-P Algorithm Parameters 57
Table 3-3: Algorithm parameters for Simulation 64
Table 3-4: REACT-P Simulation Parameters 65
Table 3-5: CC2420 Output power settings and typical current consumption @ 2.45GHz [47] 65
Table 3-6: Algorithm parmeters for experimentation 72
Table 3-7: REACT-P Experimentation Parameters 72
Table 3-8: Different settings for controlling the output power in ATRF215 transceiver ... 73
Table 3-9: Client IDs involved with different setup for REACT-P Test 75
Table 4-1: Different receiver sensitivities at different rate modes for MR-OQPSK 87
Table 4-2: Existing transmission rate control algorithms 88
Table 4-3: Calculated and Experimental frame duration at different rates 91
Table 5-1: Existing transmission power and rate control algorithms..... 97
Table 5-2: TX Energy consumed (µJoules) for different combination of power and rate levels 103
Table 5-3: Calculation of Remaining life time of Client 7 105
Table 5-4: Experimental parameters for one-sink-one-client setup 106
Table 5-5: Experimental parameters for 7 clients star topology setup..... 107
Table 5-6: Approximate distance of clients from sink for REACT deployment plan 108
Table 5-7: Client IDs involved with different setup for REACT Test..... 110
Table 9-1: Sorted Energy level array in ascending order for REACT 137

VII. List of Abbreviations

Acronym		Full Form
AC	:	Alternating Current
ACK	:	Acknowledgement
AIAD	:	Additive Increase Additive Decrease
AIMD	:	Additive Increase Multiplicative Decrease
BER	:	Bit Error Rate
BEW	:	Binary Exponential Window
CCA	:	Clear channel Assessment
CoAP	:	Constrained Application Protocol
COOJA	:	COntiki Os Java
CoRE	:	Constrained RESTful Environment
CPCR	:	Constant Power at Constant Rate
CSMA	:	Carrier Sense Multiple Access
CSMA/CA	:	Carrier Sense Multiple Access/ Collision Avoidance
CTS	:	Clear To Send
dB	:	Decibels
DBR	:	Discovery Beacon Request
DC	:	Direct Current
DGRM	:	Directed Graph Radio medium
EB	:	Enhanced Beacon
ERLT	:	Estimated Remaining Life Time
ETSI	:	European Telecommunication Standard Institute
ETT	:	Expected Transmission Time
ETX	:	Expected Transmission Count
EWMA	:	Exponential Weighted Moving Average
HTTP	:	Hyper Text Transfer Protocol
IEEE	:	Institute of Electrical and Electronics Engineering
IETF	:	Internet Engineering Task Force.
IoT	:	Internet of Things
LLN	:	Low Powered and Lossy Network
LoRA	:	Long Range
LPWAN	:	Low Power Wide Area Network

LQE	:	Link Quality Estimation
LQI	:	Link Quality Indicator
LSL	:	Last Stable Level
M2M	:	Machine to Machine
MAC	:	Medium Access Control Layer
MPDU	:	MAC Protocol Data Unit
MR-OQPSK	:	Multi-Rate-OQPSK
ODTPC	:	On Demand Transmission Power Control
OQPSK	:	Offset Quadrature Phase Shift Keying
OSI	:	Open System Interconnection
PAR	:	Packet Acknowledgement Rate
PCB	:	Printed Circuit Board
PDR	:	Packet Delivery Ratio
PER	:	Packet Error Ratio
PHY	:	Physical Layer
PPDU	:	PHY layer Protocol Data Unit
PRR	:	Packet Reception Ratio
PSDU	:	Physical layer Service Data Unit
PSR	:	Packet Reception Success Ratio
REACT	:	Responsive Energy-efficient Adaptive Control of Transmission Power and Rate
REACT-P	:	Responsive Energy-efficient Adaptive Control of Transmission Power
REACT-PR	:	Responsive Energy-efficient Adaptive Control of Transmission Power and Rate
RF	:	Radio Frequency
RISC	:	Reduced Instruction Set Computing
ROLL	:	Routing Over Low powered and Lossy Network
RPL	:	IPv6 Routing Protocol for LLNs
RSSI	:	Receive Signal Strength Indicator
RTS	:	Request To Send
RX	:	Reception
SFD	:	Start of Frame Delimiter

SHR	:	Synchronization Header
SINR	:	Signal to Interference plus Noise Ratio
SLP	:	Sleep/ideal state
SNR	:	Signal to Noise Ratio
TCP	:	Transport Control Protocol
TPC	:	Transmission Power Control
TSCH	:	Time Slotted Channel Hopping
TSN	:	Time Slot Number
TT	:	Transmission Time
TX	:	Transmission
UDP	:	User Datagram Protocol
Wi-SUN	:	Wireless Smart Ubiquitous Network
WLAN	:	Wireless Local Area Network
WSN	:	Wireless Sensor Network

1. Introduction

Contents

1.1 Internet of Things (IoT) 3

1.2 Thesis Motivation and Scope 18

1.3 Content of PhD 20

1.1 Internet of Things (IoT)

1.1.1 Background

The Internet of things (IoT) builds the potential for a world in which physical objects can communicate with one another or with humans intelligently and react with respect to the changes in the surrounding and become active participants in this smart world. Kevin Ashton first used the term Internet of Things in 1999 [1]. The number of connected things went increasing and in 2008, this number was greater than the people living on earth. Availability and affordability of such devices grow every year. Today, IoT is not only a technology but has also become an ecosystem. This technology has been existing for few decades but were not working together. With the advent of cheaper processing power, low power radio transceiver hardware, communication costs and some marketing, these forces have molded the IoT of today. Billions of gadgets/devices will gather data/information from nearly everything and, practically everyone. Almost any device with electronic components can be shaped for the IoT, and in the next five years, more will.

Raun has described IoT as: "*A world where the real, digital and the virtual are converging to create a smart environment that make energy, transport, home, industries, cities and many other areas more intelligent*" [2].

Figure 1-1: IoT Landscape

Figure 1-1 shows an IoT landscape including but not limited to implementation of IoT devices. IoT helps in modernizing infrastructure and improving operations, enhancing

efficiency and cost savings, business transformation services for more value-added services to consumers. The rise of the Internet of Things (IoT) is the most important advancement in the growing evolution of the smart world. The number of connected devices is increasing exponentially. As the next 10 billion IoT devices come online, the industry will face some challenging encounters, such as ensuring the device security, powering billions of sensors, etc.

IoT solutions can be divided into different categories based on their: i) Communication Technology ii) Network Topology and iii) Open-Standard stack versus proprietary solutions. Various communication technologies offer communication solutions for IoT devices, for example: Cellular Communication, Wired Networks, and RF Wireless networks (such as IEEE 802.15.4, Wi-Fi, NFC, Bluetooth)

In the last decade, star topology, combined with long range RF technology based on a proprietary network stack has been the mainstream solution deployed to harvest sensor data. In this solution, very similar to cellular networks, a gateway is installed on top of a pole, tower or a high-rise. To achieve long-distance coverage, low bit-rate RF technologies (in the order of 100 bits per second) are embedded in the gateway and at the endpoints. The communication may be unidirectional or bidirectional.

In parallel, there have been considerable advances in meshed sensor networking. Meshed topology provides scalability, self-healing, low powered, flexibility, reliability and reduced network infrastructure cost. Moreover, short-range RF technologies with much higher bit-rates (more than 100kbits/s) can be deployed in this topology. This means more real time data is collected and more service options can be offered.

Proprietary protocol stacks, tailored for various IoT applications, while usually robust and efficient, when it comes to their interoperability and openness to other systems, they limp. To unravel this issue, many standardization activities in IETF (Internet Engineering Task Force), IEEE and ETSI (European Telecommunications Standards Institute) are in process to provide open standard solutions[3]–[8]. There are dedicated alliances such as Wi-SUN which “promotes the adoption of open industry standards in wireless smart utility networks” [8]. Wi-SUN network is developed as per IEEE Standard 802.15.4e/g [5], [6] that defines PHY and MAC layer specifications. This permits multi-vendor products to interoperate seamlessly.

IPv6, together with wireless mesh, offers some ready solutions for large scale, low power and lossy sensor networks. IP-based devices can connect easily with existing IP networks, providing end to end connectivity. Recent advances in communications have made the IPv6 protocol possible and efficient for the use in Low Powered and Lossy Networks (LLNs) that are constituted by devices compatible with the IEEE802.15.4 standard.

1.1.2 IoT Predictions

Forecasting the future is not an easy task. There have been different estimates and forecasts from different firms depending on their own definition of IoT. Popular IoT forecast by Cisco of 50 Billion Devices by 2020 has been outdated [9]. According to IHS, It has been forecasted that the number of connected devices will grow from an installed base of 17 billion in 2016 to 125 billion in 2030 [10]. According to Machina Research [11], in August 2016, 11% of the connections in 2025 will use Low Power Wide Area (LPWA) connections. In [12], it has been roughly estimated that there will be around 23 billion battery operated IoT devices in 2025 as shown in Figure 1-3. With the involvement of battery, device lifetime would be a major challenge.

According to MachNation forecast data, 2018 [13] , IoT platform revenue will grow 89% in 2018. MachNation forecasts that IoT platform revenue in 2018 will reach USD3.3 billion to USD 64.6billion by 2026 (Figure 1-6). According to I-scoop, IoT spending is forecasted to surpass the $1 trillion mark in 2020 [14].

Figure 1-4 shows the top ten IoT segments based on 1600 real IoT projects in 2018 excluding the consumer IoT projects, done by IoT Analytics in January, 2018 [15]. IIoT (Industrial IoT) platforms is taking the lead in the IoT platform market as most platforms focus on industrial segments says IoT Analytics [16] as shown in Figure 1-5.

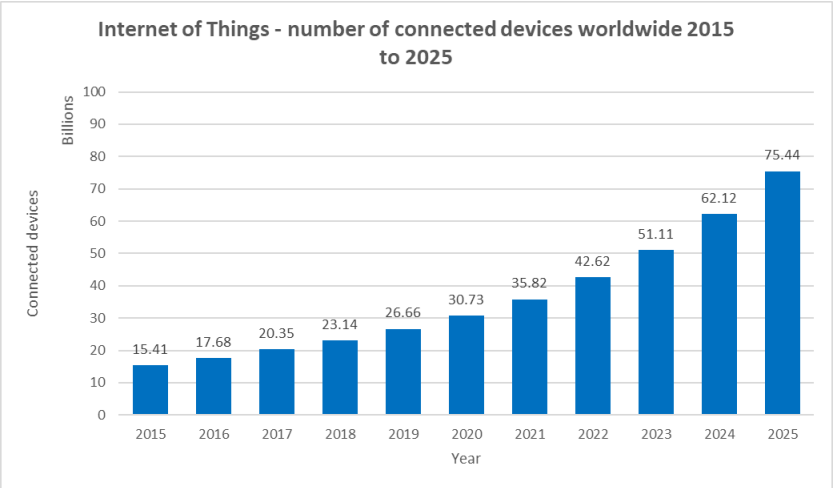

Figure 1-2: Number of connected devices from 2015 to 2025 [10]

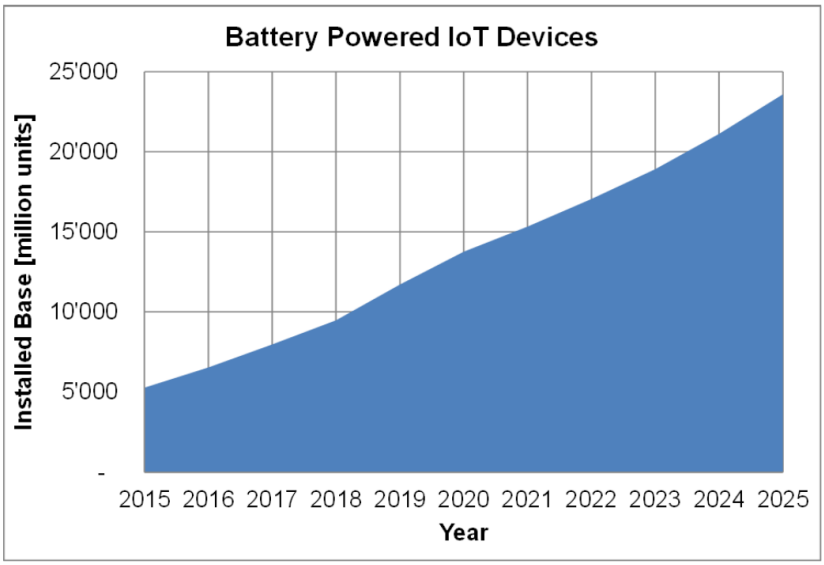

Figure 1-3: Number of battery powered IoT devices [12]

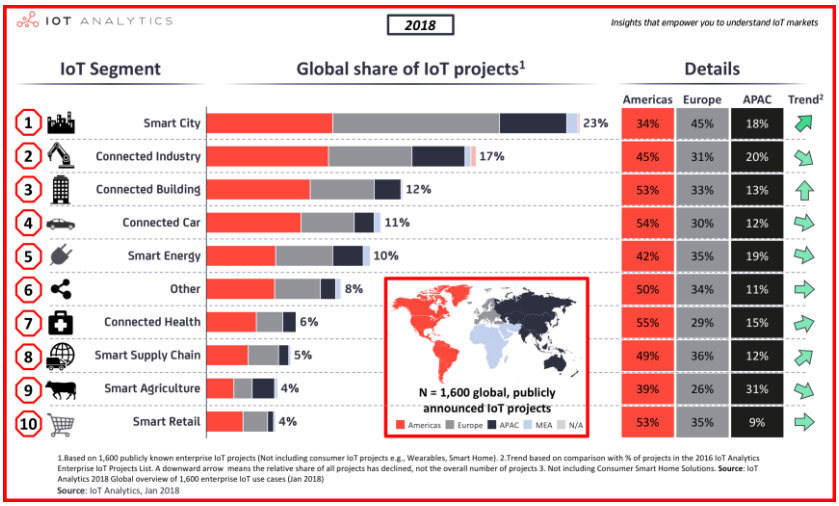

Figure 1-4: Global share of IoT projects and trends [15]

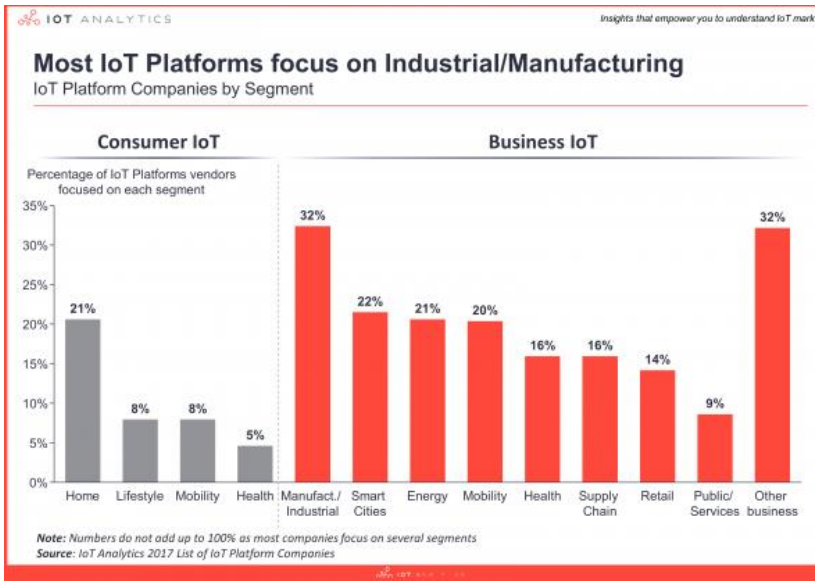

Figure 1-5: Consumer and Bussiness IoT platforms [16]

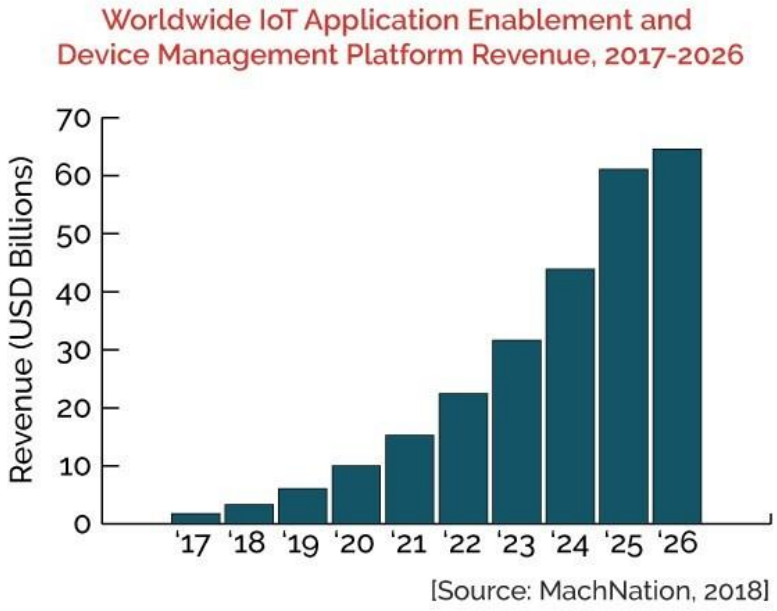

Figure 1-6: Worldwide IoT Application Enablement and Device Management Platform Revenue [13]

1.1.3 Various Applications of IoT

The applications of IoT are increasing day by day. From a small pill to big airplanes, simple smart kettles to complex man-less vehicles, everything has become a part of IoT. Table 1-1 lists some of the applications of IoT that are compiled from various sources [12], [15], [17]–[20].

Table 1-1: Various applications of IoT

Application Area	**Application**	**Edge Device**	**Power Source**
Smart Home	Home Automation	Smoke sensors, window	Battery
	Smart Lighting	Smart LED bulb, gateway	Mains
	Smart Appliances	Washing machine, dish cleaner, coffee machine, refrigerator, etc.	Mains
Health Care	Physical activity monitoring	Activity tracker, wearable devices	Battery
	Weight/cardiac monitoring	Smart body scale	Battery

	Sleep monitoring	Sleep sensor	Battery
	Dental health	Electrical toothbrush	Battery
	Emergency notification	Emergency tag(watch)	Battery
	Fall detection	Fall sensor	Battery
	Nutrition monitoring	Smart cup	Battery
Smart Grid	Metering application	Smart gas/water meter	Battery
		Electric meters	Mains
Smart mobility	Smart roads	Sensors in road	Battery
	Car-to-car communication	Various devices in the car	On-board
Smart Logistic	Product tracking/Item location	RFID tag	Battery
	Quality of storage, shipment and condition monitoring	Dedicated sensors	Battery
Smart Agriculture	Cattle monitoring/tracking	RFID tag, GPS transceiver	Battery
	Irrigation monitoring	Dedicated sensors	Battery
	Green Houses	Dedicated sensors	Battery
Smart City	Smart street lighting	Street lights	Mains
	Smart parking	Sensors in parking lot	Battery
	Air-quality Monitoring	Dedicated Sensors	Battery
Smart Security	Intrusion detection	Door, window sensors, smoke sensors,	Battery
	Perimeter Access Control	Presence sensors, proximity	Battery
	Explosive and hazardous gases/ radiation	Dedicated sensors	battery
Smart Environment monitoring	Air/Water quality monitoring	Dedicated sensors	Battery
	Flood monitoring	Dedicated sensors	Battery
	Forest fire monitoring	Dedicated sensors	Battery
	Landslide/avalanche prevention	Dedicated sensors	Battery

	Earthquake early detection	Dedicated sensors	Battery
	Snow level/ Glacier monitoring	Dedicated sensors	Battery
Underwater sensor networks	Aquatic life tracking/ sensing	Dedicated sensors	Battery
Underground sensor networks		Dedicated sensors	Battery

With an extensive range of IoT applications, a multitude of power source requirements come into play. Home appliances and industrial automation equipment both traditionally are connected to mains lines, making power readily available. Other applications which are deployed in unfavorable areas inconvenient for mains line power generates a necessity for autonomous power sources. It is obvious from the table above that, many IoT applications require the edge devices to run on battery. More details on this challenge on powering the IoT devices is explained in sub-section 1.1.6.

1.1.4 An IoT Device

Figure 1-7 shows a general block diagram of an IoT/Sensor Device. Processing platform may include one or more processors/chips, memory, one or more secondary storages, one or more input/output ports or devices. One of more communication interfaces may provide wired or wireless communication. It includes a power supply sub-system that may be mains line powered or battery powered. With the speedy advancement in IoT, it is important to remember that the key drivers behind IoT are the sensors, actuators and transceivers. In order to create smarter cities and smarter homes, edge intelligence is critical, without which, IoT would not scale. It would be beneficial by bringing some intellegence at the edge so that billions of IoT devices may be able to make their own decisions locally for various cases thereby reducing traffic and latency for making decisons. A connected object or thing can have few or thousands of sensors and actuators. Connected sensors and actuators have become the heart of IoT applications. They are giving our world a digital nervous system [18].

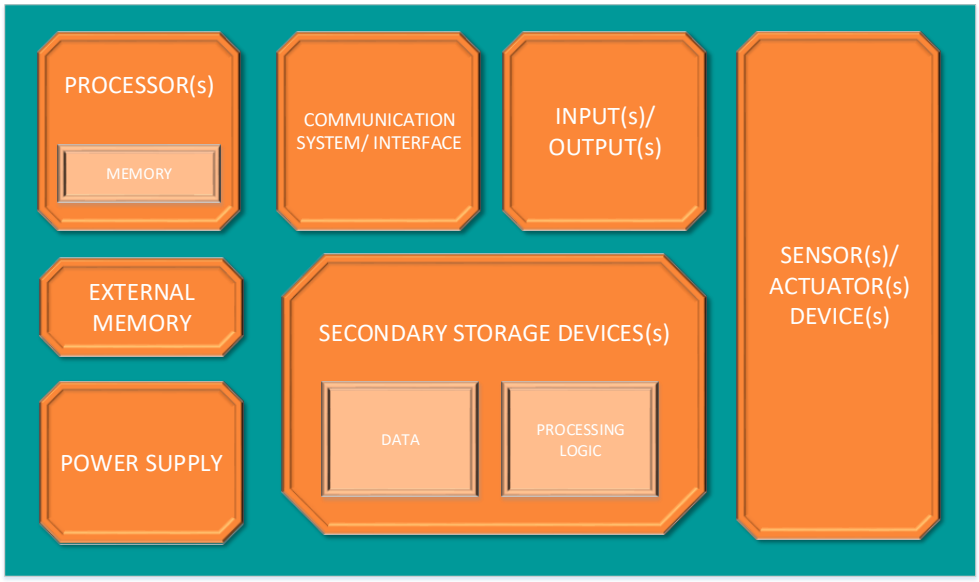

Figure 1-7: Block diagram of a typical IoT device

Sensors and actuators exist since long before the IoT in its current meaning and are ubiquitous in, for example, buildings, factories, energy and much more [18]. A sensor is a device that senses, detects, measures or specifies any physical quantity such as light, heat, sound, presence, pressure, motion, moisture, or similar entities, by converting them into any other form most being electrical pulses. As the sensors are basically the first source to capture raw data, it is clear that sensors are crucial IoT components and need to provide precise information but with strict power budget constraints. Actuators are just like sensors. While sensors sense, actuators act. They are there to trigger some actions in the physical world. In order to create a connected IoT network, the transceivers communicate to one another. As a basic home example, a sensor senses the occupancy of the room and the temperature and depending on control/management system, the actuator turns on/off the air-conditioning providing electricity savings.

The hardware together with software and external factors, such as the environment and the interaction with the network, dictate the power profile drain of each node [21]. Internet of Things (IoT) devices are supposed to be deployed 'everywhere' and to be accessed 'any time' from 'anywhere' [22]. Many of these devices perform control and monitoring tasks in the smart-x applications and hard to access or inconvenient areas. For successful realization of such applications, an IoT device should be tiny and autonomous while including sensing/actuating, processing and wireless communications capabilities. These limitations and simple requisites infer strict requirements for the energy storage and power management

of IoT devices to ensure their perpetual operation, given neither cable-power nor battery replacement are suitable options in those conditions, or simply because of convenience (quick "cable-free" and "no maintenance" installations are very tempting indeed).

1.1.5 IoT Open Standard Protocol Stack

There are many proprietary protocols in IoT to tackle the various challenges in the IoT. But when it comes to the concept of interoperability, they linger. Proprietary solutions suffer from vendor-locking. Although various alliances support these proprietary solutions, such as LoRA (Long Range) [23] , M2M (Machine to Machine) [7], Sigfox [24], Zigbee [25] Alliances but most of them are not standardized. It was predicted that by 2018, the “open data platform” will be emerged as the next frontier in IoT domain [19]. Wi-SUN (Wireless Smart Ubiquitous Networks) [8] is an alliance that promotes open standards. The following Figure 1-8 shows the protocol stack for a constrained IoT environment which are based on open standards.

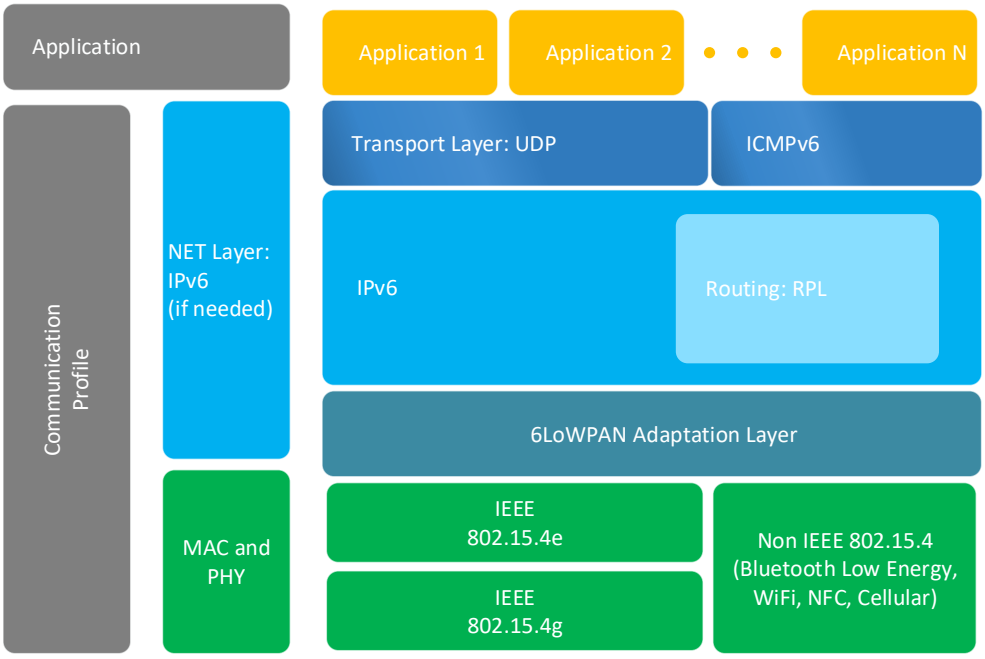

Figure 1-8: Open wireless standard reference model for IoT

The following sub-sections explain briefly about the various layers of the stack.

1.1.5.1 Application Layer

CoAP (Constrained Application Protocol), is a light-weight Web Transfer Protocol, standardized by IETF Constrained RESTful Environment (CoRE) in RFC 7252 [26]. It is specially designed for constrained devices and constrained networks for Internet of Things.

It can be transparently mapped to the HTTP (Hyper Text Transfer Protocol). CoAP runs on UDP (User Datagram Protocol) and has methods like GET, POST, PUT, and DELETE. It uses small and reduced set of headers.

1.1.5.2 Transport Layer

IoT devices mainly employ TCP (Transport Control Protocol) or UDP. As implementation of TCP is complex, it is difficult to employ on resource constrained devices like sensors. Hence, most of the IoT applications are better-suited with UDP protocols, which is much faster than TCP and have lower overheads. But UDP being connection-less protocol, it may need to be combined with application layer to improve its reliability.

1.1.5.3 Network Layer

This layer defines the overall routing of the data packets. It supports IPv6. IETF (Internet Engineering Task Force) RPL (Internet Engineering Task Force IPv6 Routing protocol for low power and lossy Networks, RFC 6550 [27]) from working group ROLL [3] is used as a routing protocol. In order to accommodate the large IPv6 packets over 802.15.4 MAC/PHY frames, 6LowPAN (IPv6 over Low Power Wireless Personal Area Network, RFC 4944 [28]) is used as an adaptation layer that provides encapsulation and header compression techniques. In the scope of this thesis, routing is not taken into account as the tests were performed on a Star network with a single sink.

1.1.5.4 PHY/MAC Layer

IEEE 802.15.4 is a standard for wireless communication between devices in constrained environment (low data rate, lossy) with limited resources (memory, power, bandwidth). It is standardized by IEEE similar to IEEE 802.11 for Wi-Fi or IEEE 802.3 for Ethernet. IEEE 802.15.4e [29] and IEEE 802.15.4g [30] are the enhanced MAC and PHY layers respectively based on IEEE 802.15.4 Standard.

This thesis mainly focuses on these two layers. In this research, we will be using IEEE 802.15.4e/g as the MAC/PHY layer. This PHY layer supports the multi-rate and multi-regional Offset Quadrature Phase Shift Keying (MR-OQPSK) PHY. The MAC layer IEEE 802.15.4e supports Time Slotted Channel Hopping (TSCH) and Carrier sense Multiple Access with collision avoidance (CSMA/CA) techniques.

Besides these, the protocols may consist of other technologies such as IEEE 802.11 Wi-Fi, 2G/3G/LTE/Cellular, Bluetooth Low Energy, Satellite, etc. Each of these technologies has its tradeoffs in terms of power consumption, range and bandwidth as shown in Figure 1-9.

Figure 1-9 illustrates the relative standby energy consumption of various wireless communication technologies (as well as Ethernet) and their typical data transfer rates and communication ranges. From this figure, it can be perceived that higher data rates and longer ranges tend to equate to higher standby energy consumption.

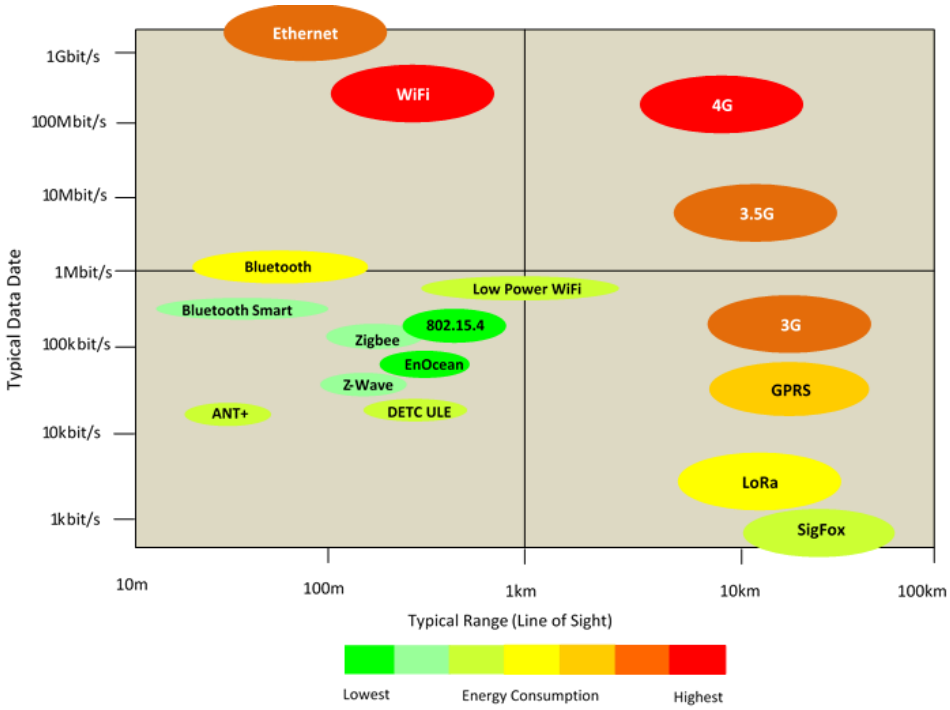

Figure 1-9: Tradeoffs in various IoT enabling communication technologies

1.1.6 Power Sources for IoT Devices: A Big challenge

Any electrical/electronic device requires power in order to operate. There are numerous potential alternatives for powering the devices [31], depending on the use case: nearby AC line, available DC line, energy harvesting and battery. There are basically 4 ways or their combination to power IoT devices.

1.1.6.1 AC Line:

Alternating Current (AC) line can provide unlimited power as required by the device and hence may seem to be the easiest choice. But the problem is that it requires the device to remain closer to the source and thus limits the portability/mobility of the IoT device. Also, there is a need of an AC/DC converter. These converters are large in size and expensive. A small AC/DC circuit can be built on-board on the IoT PCB (Printed Circuit Board) but this gives rise to safety and regulatory-approval issues due to the presence of direct line voltage, in addition to the cost and the size burden.

1.1.6.2 DC Line:

DC line can be a good choice if an IoT device is to be used near it such as in a home appliance. It is because a simple on-board DC/DC converter can be small in size, low-cost and reliable. It is necessary to ensure that the IoT device is able to consume the current from the DC line when it needs. This option also requires the IoT device to remain close to the source. Hence, although inline DC power sources are constant, they are often impractical in many instances.

1.1.6.3 Energy Harvesting:

Energy Harvesting is often a very good option, as it can be a hassle-free, moderate-cost and almost "free-ride" source. The three common harvested power sources include thermoelectric (thermopiles, thermo couples), kinetic or vibration (piezo), and photovoltaic (solar) systems. Unfortunately, energy harvesting is often impractical because there is no reliable or consistent source of energy to be scavenged, as some IoT devices are placed in dark and/or quiet places where the energy cannot be easily scavenged. This technology is not mature enough in terms of size and cost at this time. As they scavenge the energy from the ambient sources which are influenced by the weather conditions, energy harvesting devices cannot generate sufficient energy in a nonstop active mode; therefore, an alternative power source needs to be incorporated when using energy harvesting-powered devices. Hence, energy storage such as battery is still essential to guarantee smooth operation of an energy-harvesting IoT device.

1.1.6.4 Battery:

At first glance, this may seem like an unattractive option, since batteries eventually need to be replaced or recharged. However, if the battery is of proper size and type, it is actually often the most convenient choice because it provides flexibility, mobility and cost-effective

solution. For instance, a lithium cell with suitable attributes and capacity can offer several years of power at a low cost.

The first two choices require the IoT device to remain tethered and hence limits flexibility and mobility. Inline power sources are constant but may be often impractical or expensive in many instances.; the third has more freedom and can be a "something-for-nothing" source but the IoT device is still constrained by the placement of the harvesting transducer and lack of consistent power supply; and the battery-only option offers the greatest flexibility, cable-free installations and low cost, however, it will require periodic replacement.

The following table gives the glance on various power source choices for IoT devices [22]

Table 1-2: Various power sources choices for IoT devices

Technology	**Pros**	**Cons**
Non-rechargeable batteries	Convenience Cost	Replacement Ecology
Rechargeable batteries	Rechargeable	Limited charge-discharge cycles Feasible with energy harvesting
Printable batteries	Easy fabrication process Customizable cell (voltage, capacity, size) Thin and flexible	May damage at 40-50 °C Not mature enough
Solid-state batteries	Easy integration with IC Easy to miniaturize Thin and flexible	Low power density Not mature enough
Super capacitors	'Unlimited' charge-discharge cycles	Self-discharge
Energy harvesting	Continuously replenishes energy resources	Depends on ambient conditions (in some cases) Requires extra hardware and power conditioning Not mature enough

1.1.7 Energy Consumption in IoT: A Taxonomy

Many IoT edge devices run on battery and various applications require them to keep running for years. IoT applications requiring battery operated edge devices are the major driver for novel low energy/power consumption communication standards specifically developed for IoT. The consumers would not accept low battery lifetimes. It may be cost-prohibitive to substitute exhausted batteries or even impossible in certain hostile environment. Hence, prolonging the lifetime is very important. Therefore, when there is involvement of battery, the node's power becomes the most vital resource that must be used in a well-planned and efficient manner.

IoT applications can range from small sized healthcare surveillance systems to large scaled environmental monitoring or smart metering. A lot of research works have been done and are ongoing especially in optimizing the energy consumption covering several areas from physical to network layers of a protocol stack. There are various techniques of conserving the energy (energy saving techniques) in a wireless sensor network. The following presents the taxonomy of major existing approaches to tackle the energy consumption problem for battery-operated nodes. This taxonomy in Figure 1-10 is compiled from various sources [32]–[35]. These researches mention that the transmitting radio is the most dominant energy consumer. Hence, this thesis focuses on TX power and TX bit-rate control techniques to provide energy efficiency.

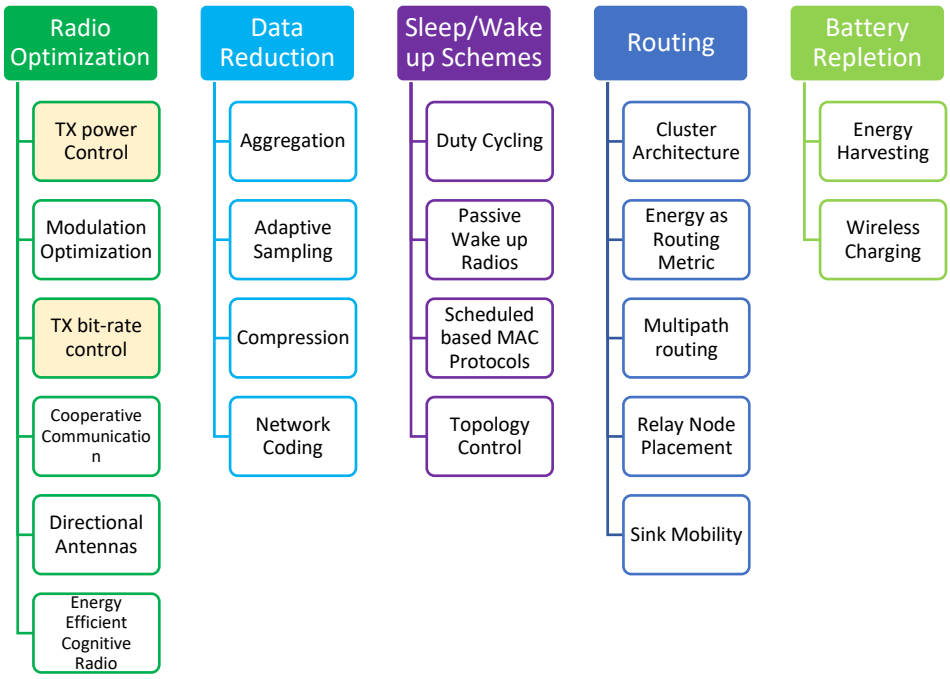

Figure 1-10: Various energy saving techniques for WSN/IoTs

1.2 Thesis Motivation and Scope

Although IoT has numerous potentials to save both time and resources for many applications, it has its own set of unique problems. A survey in 2015 shows that the major concerns are security, privacy, connectivity and device management [36]. A single IoT solution technology cannot suffice all the possible applications. Different factors must be considered when choosing connected devices and protocols for a particular IoT application.

IoT sensor nodes are often referred to as Constrained Network Devices. They are small devices with limited memory/buffer, limited processing capabilities and limited power resources or working on batteries that are deployed in a huge scale. Such nodes are often deployed in harsh, lossy environments [37], [38]. The network itself is constrained that has various traits like lossy and unreliable links, low data rates, duty-cycles and asymmetric links. Such class of a constrained network with constrained devices is known as Low-powered and Lossy Networks (LLNs) [3]. For such constrained devices and constrained network, energy consumption or the device lifetime becomes the major issue. When there are billions of connected devices deployed, recharging them over months is practically impossible. So, the main topic in the IoT is the battery life. Whoever is able to provide a technology that correctly manages the battery life is a clear winner and hence is the main scope of this thesis.

When energy efficiency becomes the most important factor, various energy saving techniques are needed which were discussed in Section 1.1.7 that points to an important outcome: Radio Transmission is one of the major sources of energy consumption in today's rising IoT devices in low powered and lossy networks. There are several parameters to optimize the energy consumption in IoT/WSN domain, but from this thesis point of view, transmission power and transmission bit-rate are the two radio parameters that principally impact the energy consumption along with the radio coverage, interference, link reliability, channel/spatial reuse, etc. They are the key factors influencing the connectivity, performance and the lifetime of a node/network. Transmitting at a constant high/low power or rate leads to an inefficient energy usage due to the varying, unstable and unpredictable radio links. Fortunately, there are some existing transmission Power and/or Rate Control algorithms that control the power or rate or both to provide energy savings. Each of them has its strengths and weaknesses. Some have initial overheads, and some are difficult to implement. Most existing solutions use single link quality metric for channel quality estimation. Some define static thresholds on their signal metrics that limit their adaptability. While some current power control algorithms were designed for sensor nodes, all the existing rate control and rate/power control solutions were addressed for the 802.11 WLAN. Most of them are validated via simulations only whereas some via experimentation. Some have defined unrealistic assumptions such as: not considering collisions or fading, having priori knowledge about the channel conditions, number of nodes, number of collisions, etc which are always not practical.

An efficient transmission (TX) power/rate control algorithm for the constrained devices in IoT/WSN should have low overheads and must be energy efficient. They need to be adaptive and versatile to different environment conditions; yet be simple and easily implementable in the real sensor/IoT platform. There is not a single existing solution that succeeds to satisfy all these requirements on their own. Due to aforementioned problems and design challenges for a reliable and robust transmission power/rate control techniques, there is a need of a new algorithm that performs an energy-efficient power and/or rate control which can be easily implemented in a real sensor platform.

The main scope of this thesis will be focused on the Low Powered and Lossy Network (LLNs) or Low Power Wide Area Networks (LPWANs) where the nodes themselves have limited power. This thesis focuses primarily on the applications of IoT that do not involve mobility of the end points, do not have very high traffic rates and are delay-tolerant. Some

examples of such applications may include: Smart metering, home automation, environmental monitoring and control, etc. This thesis focuses on a star network with long range communication where the deployed end-nodes send their packets to a central controller or sink based on event or periodically in a bubble-up fashion.

1.3 Content of PhD

1.3.1 Research Objectives and Contributions

Uncertainty in the radio links for a constrained wireless network is inevitable. The radio environment and the location where an IoT sensor node is deployed have a huge impact on the communication reliability. This would in turn effect the energy consumption of a node due to failures and need of retransmissions. Consequently, this will impact the node lifetime and hence the network lifetime. As discussed before, the evolution of IoT devices will increasingly involve batteries. Extending battery life clearly delivers economic benefits to IoT device manufacturers, management and end-users.

Hence, the overall research objective of the thesis is to reduce the energy consumption and prolong the device lifetime. Among the various techniques, this thesis focuses on controlling the transmission power and/or the transmission bit-rate as a means to improve the energy consumption while having similar reliability. There are various design goals that needs to be fulfilled in order to have an efficient control mechanism by bringing intelligence to the edge. They are summarized in the followings:

- The algorithm should have minimum communication overheads and short initial phase.
- The algorithm should be able to respond and adapt appropriately to the fast-fading as well as slow-fading environments. It should be versatile to different radio conditions.
- The algorithm must reduce energy consumption while maintaining similar reliability
- The algorithm should work well in both congested and uncongested environment.
- The developed algorithm should be simple and easy to implement in the real IoT platform without impacting too much the design and the other layers.

In order to develop a robust, reliable, responsive and energy-efficient power/rate control algorithm to fulfill the design goals defined earlier, following research objectives are addressed in this thesis:

RO1. Study of the impact of the transmission power and rate on the network

Before one can fully understand the transmission power/rate control mechanism, it is important to first understand the impacts of the transmission power and rate on the network. Hence, the first research objective was to understand the impacts of the power/rate on the various performance metrics such as energy consumption, interference, channel occupancy, packet delivery. In this research objective, it is shown how changing the transmission power and /or transmission bit-rate would help to reduce the transmission energy consumption while maintaining similar packet delivery performance.

RO2. Subjective analysis and selection of link quality metrics

It is equally necessary to understand link quality estimation technique and various available link quality metrics. They play a crucial role in the power or rate control mechanisms. The first contribution of this thesis is that it provides a rigorous analysis of the existing link quality estimation metrics and provide the pros and cons of each. This thesis provides a method to estimate the link quality by using multiple link quality metrics: One being the primary and the other being the secondary to better evaluate the channel.

RO3. Design, develop and implement an energy-efficient algorithm to dynamically control the power level

With the design challenges in mind, to start with the control mechanism, first a control algorithm was designed and developed that only changes the power level dynamically during the run time phase at a fixed transmission bit-rate. Various functional blocks were defined during the process that provides novel and effective approaches in adapting the power. The developed algorithm was evaluated using both simulation and experimentation. The second contribution of this thesis is hence the development of a new responsive energy-efficient adaptive control algorithm for transmission power.

RO4. Design, develop and implement an energy-efficient algorithm to dynamically control the transmission power and rate.

As it was observed from the experiment and literature work that, adapting transmission bit-rate further helps to save the energy consumption. Hence, this RO4 aims to extend the design

from the RO3 to support the rate adaptation as well. With some changes in the functional process, a responsive, energy-efficient transmission power and rate control was devised that adapts either the power level or rate level or both as per the link conditions. This proposed design was then evaluated using experimentation.

The research objectives and the contributions from this thesis all tend to assemble to attain the ultimate goal of this thesis which is to provide an energy efficient communication while maintaining similar reliability by dynamically changing the power level and/or rate level.

1.3.2 Structure of Thesis

The remaining part of the thesis is organized as follows. In Chapter 2, we start by looking into the various link quality metrics to estimate the wireless channel conditions along with their pros and cons. This chapter ends with the selection of the link quality metrics for performing the power/rate control. In Chapter 3, we focus on transmission power control mechanism. We study about various impacts of the transmission power on the network, perform literature review on the existing algorithms. As a first step, this chapter presents a new design and concept for energy-efficient algorithm that performs an adaptive control of the power level only at a fixed bit-rate and highlights the novelty. The proposed algorithm is then evaluated using simulation and experimentation. Chapter 4 presents the study of the impact of transmission rate on the network metrics along with the literature review on the existing rate control mechanisms. This chapter shows some experiments at different bit-rates as well. In Chapter 5, we will see how the design idea from Chapter 3 is upgraded to take the transmission bit-rate into account to provide higher energy efficiency. Various experimentations were performed, and their results were shown in this chapter. Chapter 6 concludes the thesis work and indicates the future work in this area.

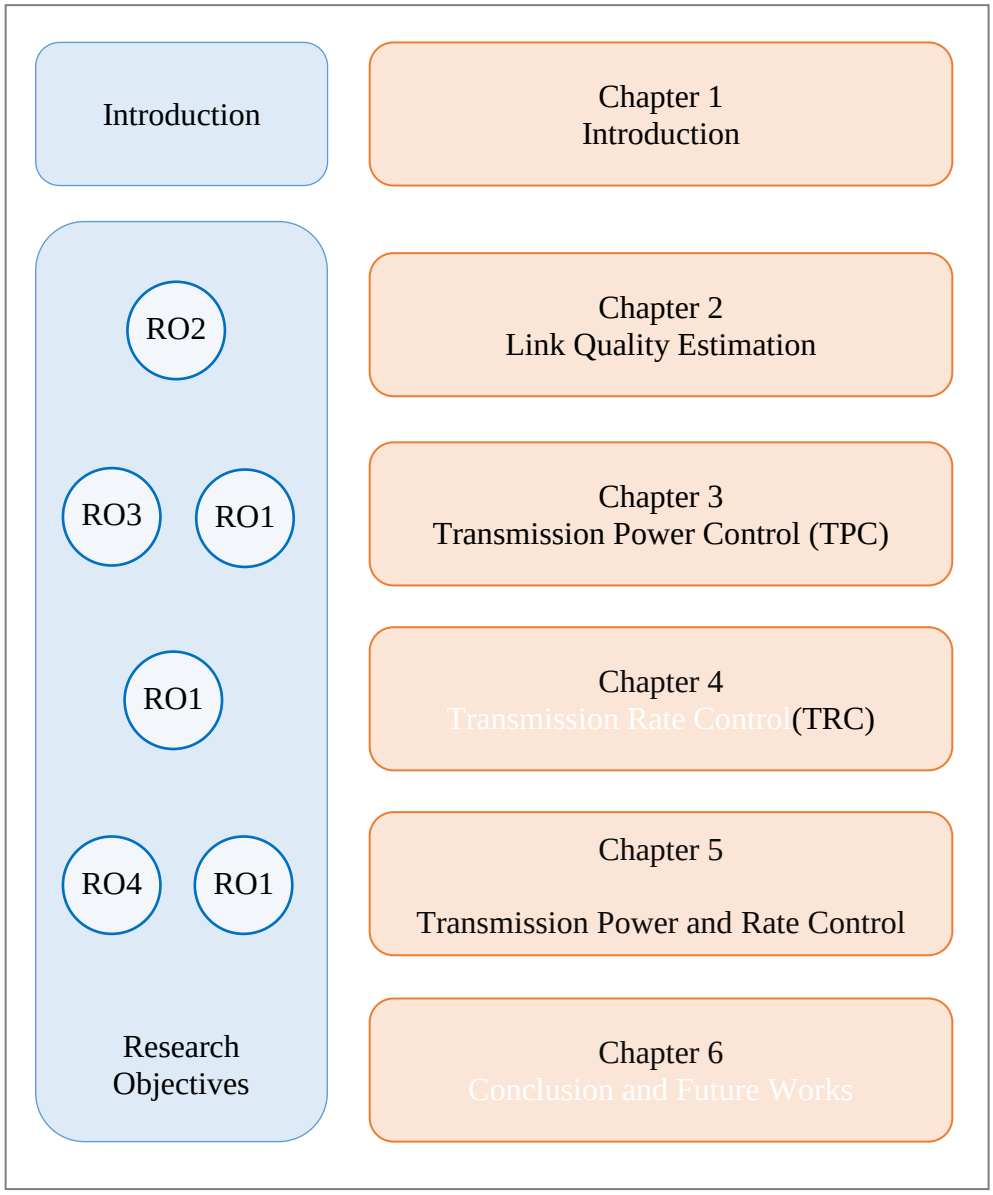

Figure 1-11: Research objectives addressed in each chapters

2. Link Quality Estimation

2.1 Radio Link Quality 27
2.2 Signal-Based 28
2.3 Statistics Based 30
2.4 State of art and Review on signal and statistics-based metrics 32
2.5 Choice of Link Quality Metric 34
2.6 Conclusion 35

2.1 Radio Link Quality

Wireless mediums are highly volatile in nature even for immobile nodes because of several reasons such as single or multi-path signal fading or attenuation, shadowing, collisions, interferences, noises, motion of foreign objects, dense vegetation, orientation of the antenna, remaining battery lifetime, etc. [39]–[42]. The real world wireless network exhibit rich channel dynamics including random channel errors, mobility-induced channel variation and contention from the hidden stations [43]. These transmission quality variations can be classified as either transient short-term modification to the wireless medium or durable long-term modification. Typically, if someone walks around, closes the door, turns on microwave devices or moves big objects around, these will influence the transmission medium but not for long time whereas moving to a new area or change of the weather can have longer enduring impact.

Distance is not the only metric to consider while choosing the optimal power or rate [44]. Radio communication quality between low power sensor devices is affected by spatial and temporal factors i.e. they depend on the space and time and the individual hardware. The spatial factors include the surrounding environment, such as terrain type (such as grassy, indoor, outdoors, parking etc.) and the separation between the transmitter and the receiver. Temporal factors are the dynamic factors that include environmental changes such as weather conditions including temperature and humidity, background noise and the movement of foreign objects [40]–[42]. Because of these random environmental dynamics, the electromagnetic phenomenon such as degree of reflection, refraction, scattering and/or fading of the radio waves will also change resulting in the change of the radio quality.

Adapting to such link conditions and predicting its future state is a thorny problem and requires an efficient link quality estimation (LQE). Choosing a proper link quality metric and making an accurate estimation is crucial for the design of a transmission power and rate control as it has a direct impact on the efficiency and the stability of the entire algorithm and the system. A link estimator should be accurate, reactive, efficient and stable while minimizing both memory requirements and traffic overhead [39], [45], [46]. To elaborate, LQE should be energy efficient as energy is the major concern in WSN/IoT, LQE should minimize the communication overheads, LQE should be accurate. The last one is an obvious one as any false estimation would lead to unstable system. LQE should be reactive. It is necessary to react quickly to the persistent changes in the link conditions. LQE should be

stable which refers to the capability to tolerate the short-term variations in the link quality to prevent from unnecessary changes. Reactivity and stability are often at odds with each other. A good link quality estimator is the one that can provide a good tradeoff between reactivity and stability [39].

Hence, to design a proper transmission power and rate control algorithm, it is necessary to correctly set the TX power level and the rate level considering these various factors into account. Figure 2-1 shows some of the popular available radio link quality metrics used in most of the existing power/rate control mechanisms. They can be broadly categorized into signal-based and statistics-based metrics. They are explained in the next few sections.

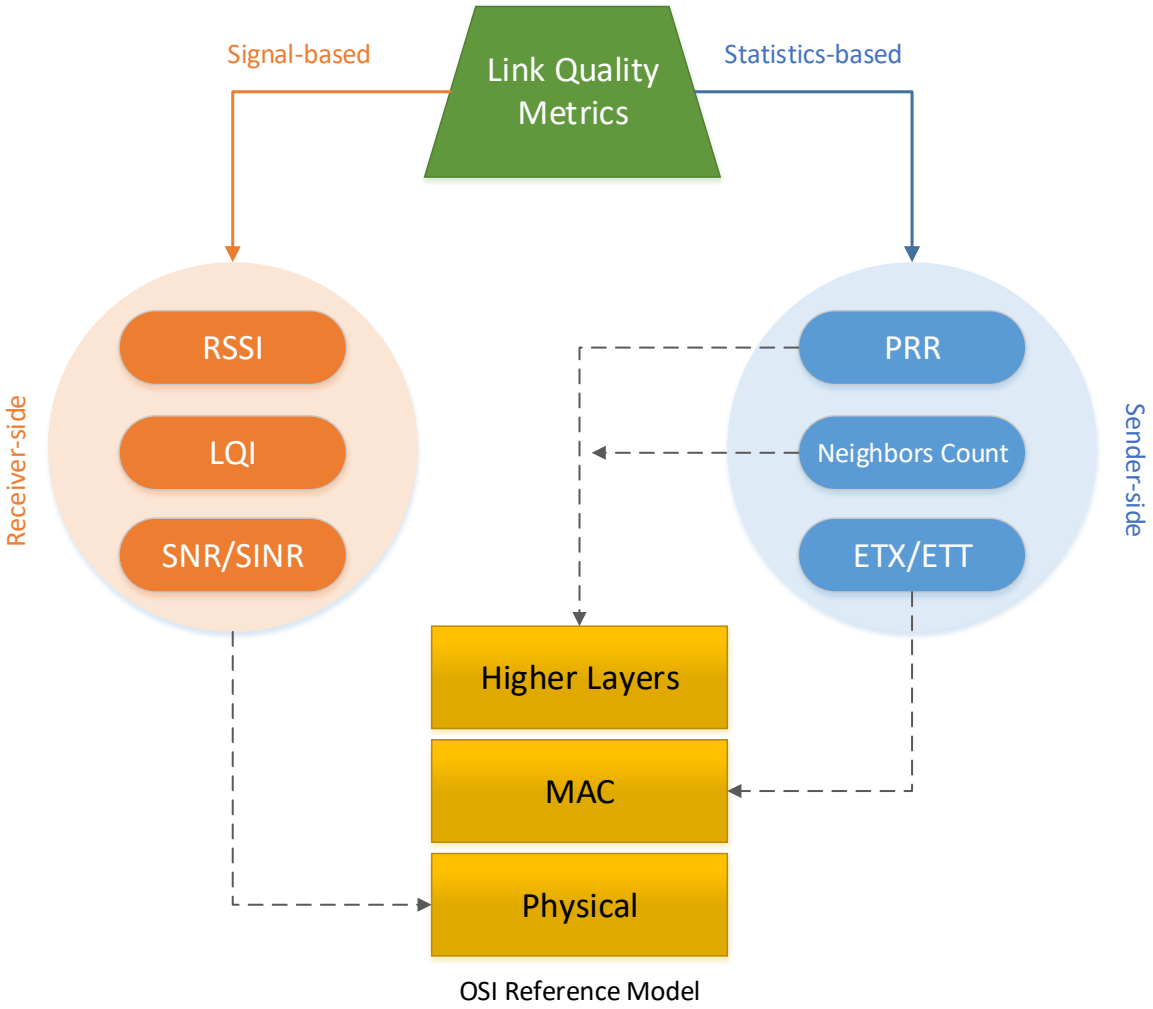

Figure 2-1: Various link quality metrics from various OSI layers

2.2 Signal-Based

The RSSI (Received Signal Strength Indicator), the LQI (Link Quality Indicator), the SNR or SINR (Signal to interference/noise Ratio) are the signal-based metrics used in most

transmission power and/or rate control algorithms. As the name suggests, these metrics are signal based. Radio transceiver chips measure the signal level during the reception of a frame and instantly provide these metric values from the physical layer- hence they are also categorized as hardware-based metrics. As the signal level is greatly affected by the time varying interference, fading and noise floor present, it may not provide the exact information. Being hardware-based, any mis-calibration may also lead to provide wrong estimates of the link quality. It has been stated that 802.15.4 compliant radios such as CC2420 [47] and Atmel AT86RF215 [48] introduce systematic errors and inaccuracy in their measurements.

Sender-based transmission control algorithms using signal-based metrics require a feedback mechanism to send back these direct or processed metric values to adjust the power/rate level at the sender. These metrics do not consider the collisions or retries that have been performed at the sender side. They provide the link quality information when a frame has been successfully decoded at the receiver side. Moreover, these metrics can only be obtained when the frame is received successfully at the receiver and acknowledged back to the sender. So, the signal-based metric alone may not be able to provide efficient estimates about the radio link quality when used alone. However, with signal-based metrics, direct control techniques can be applied using some approximation, mapping, formula or predictive models to converge to the appropriate level of rate and/or power quickly. Brief descriptions of some signal-based metrics are provided in the following sub-sections.

2.2.1 RSSI

The RSSI, Received Signal Strength Indicator, is a signal-based link quality metric and is simply the measure of signal power at the incoming frame. It is the signal strength of last 8 symbols of the incoming 802.15.4 frame. It is measured in dBm and may range from -120dBm to 0dBm. The pure received signal and the noise floor at the receiver sums up to give the RSSI value. It is correlated with PRR (Packet Reception Ratio) except when operating at the edge of receiver sensitivity. This information is obtained only when the frame has been successfully received. Same is true for the LQI.

2.2.2 LQI

The Link Quality Indicator (LQI) represents the quality of the wireless link. Usually this value results from the correlation of multiple symbols within the received frame and

indicates the error performance directly and shows how easily the received signal can be demodulated. The LQI values may range between 110 and 50. Although different vendors calculate the LQI in different ways (for example, AT86RF215 provided by Atmel correlated with the packet error rate, while CC2420 provides an indicator correlated with the chip error rate), it is believed that the LQI is more accurate and reliable than the SNR in representing the link quality. However, the LQI has been challenged by some problems [49]. First, the LQI is related to the error performance and yet only obtainable within the transition zone, i.e. successful receiving ratio is less than 100%, which means it fails to present the broader link margin. Second, the instantaneous raw LQI is known to vary over a wide range. As a result, many algorithms depend on the average of LQI over several frames to achieve reasonable accuracy and thus fail to capture the values in a rapid-changing channel.

2.2.3 SNR and SINR

The Signal to Noise Ratio (SNR) or Signal to Interference plus Noise Ratio (SINR) is a very good metric as this ratio gives a clear information about how much is the signal strength and how much is the noise level. It is measured in decibels (dB). The RSSI is the sum of the pure received signal and the noise floor at the receiver whereas SNR shows how strong the pure signal is with respect to the receiver noise floor and thus is a better link quality estimator than RSSI. However, the SNR value is very difficult to obtain. First, it is difficult to differentiate the actual signal strength with the noise level practically as these two signals may mix randomly either in a constructive way or destructive way. Second, complex mechanism and expensive hardware are required to obtain them, which are not suitable for the constrained devices with battery power and low computation processor. So, accurate calculation of SNR is very difficult and complex. Generally, an estimated SNR is obtained using the RSSI information.

2.3 Statistics Based

The PRR (Packet Reception Ratio), the ETX (Expected Transmission Count), the ETT (Expected Transmission Time) and the number of neighbors are some popular examples of statistics-based metrics. These metrics are software-based. Thus, they require additional computation to be derived by using some statistics. PRR, number of neighbors are the metrics that take time to prepare whereas, ETX and ETT provide the metric values almost instantly. These metric values are locally available, so, no feedback is required. However, while this metric information classifies link conditions as either good or bad, it cannot be

used to distinguish between good and very good links. For example, PRR may be 1 for both cases when the link is good and very good. This binary information provides some notion about the direction in which to adapt the power/rate settings but does not suffice to select the appropriate power/rate directly. As a result, only stepwise-control mechanism may be used. Consequently, the convergence time to the appropriate level may be longer. Because these metrics use only statistics to construct the metric value, there is no complex or expensive channel estimation techniques. Brief descriptions of some statistics-based metrics are provided in the following sub-sections.

2.3.1 Number of Neighbors

This is a node level metric and does not provide enough information about the link conditions. It is the count of the number of neighbors a node can hear.

2.3.2 PRR

Packet Reception Ratio (PRR), also known as Packet Delivery Ratio (PDR) is the ratio of the total number of packets received to the total number of packets sent at the higher layer in the OSI protocol stack. The value of PRR ranges from zero to one or zero to hundred in terms of percentage. This is the most direct form of a link quality and it reflects the actual capability of the channel to deliver a packet. However, it is considered as an expensive metric in the sense that it takes a long time to build this metric value. Some other variants of PRR are Packet Error Rate (PER) and Packet Acknowledgement Rate (PARR) which is the number of acknowledgements received per transmitted packets.

2.3.3 ETX

The ETX stands for Expected Transmission Count which is defined as the expected number of link layer transmissions required to make a successful transmission. ETX ranges from 1 to infinity depending on the application. A single higher layer packet may require multiple frames transmission at the link layer. When ETX is used as a metric, both lossy and long routes have larger weights, so it considers path length (number of hops), packet loss ratio and the energy consumption. Link layer transmissions are the actual number of frame transmissions that take place to send a packet successfully. This provides the information about the number of retransmissions performed which have direct impact on energy consumption.

It is like PRR, except that, this metric value is obtained at the link layer and provides the metric information almost instantly.

2.3.4 ETT

The ETT stands for Expected Transmission Time and is defined as the amount of time a data packet needs to be sent successfully. Mathematically, it is expressed as:

$$ETT = ETX * \frac{S}{R} \ (in\ time\ units) \quad (1)$$

where, *S* is the data frame size and *R* is the transmission bit-rate. In other words, [50] defines *ETT* as a "Bandwidth-adjusted ETX". The ETT is especially used for multi-bitrate networks.

2.4 State of art and Review on signal and statistics-based metrics

Several papers suggest that the RSSI and the LQI are not reliable values and should be avoided [39], [43], [45], [51], [52]. The signal level is greatly affected by time varying interference, fading and the noise floor. These values can be a good estimator when they are above the sensitivity threshold, but they do not have a good correlation with the PRR at the edge of this threshold [52]. Also, hardware mis-calibration may lead to incorrect estimates of these signal-based quality metrics. It has been stated that, 802.15.4 compliant radios such as CC2420 [47] and Atmel AT86RF215 [48] introduce systematic errors and inaccuracy in their measurements. Even for a fixed range between the transmitter and the receiver, the RSSI may fluctuate especially because of the following three reasons as mentioned by [53]: First is the multipath fading that causes the signal variation. Second is the background noise and third is because the radio hardware itself if it does not provide strict stable functionality.

RSSI or LQI is not considered as a robust indicator of link quality as:

- Retransmissions/collisions are not considered.
- Estimations are done only when the frame reaches the RX.
- High RSSI does not imply high PRR
    - RSSI may be higher because of noise and/or interference in the signal as well.
    - A small variation of around 2 or 3 dBm in RSSI may lead to PRR drop from 1 to 0 [54].

- LQI should be averaged over many samples before it can really estimate the link quality [39].
- Hardware mis-calibration may result in faulty values of RSSI/LQI.
- Feedback mechanism required to notify the sender.
- There is a threshold above which the estimation is consistently good. However, this threshold depends on the environment. A priori knowledge of the environment is necessary when choosing the RSSI as a link quality estimator [45], which is not practical in real implementation.

As it is discussed before, pure SNR is difficult to obtain, and only estimated SNR can be obtained. The possibility of data corruption and frame retransmission is higher if the received signal is closer to the noise level [55]. Researches like [39], [49], [56] show how an estimated SNR may be obtained. It involves the nodes listening to an empty channel to measure the noise floor which is not energy-friendly for battery operated devices. Additionally, the estimated SNR is obtained from the RSSI and hence suffers with the same limitations of RSSI as mentioned above.

On the other hand, the statistics-based metrics like number of neighbors, PRR are considered as expensive metric. They require larger time-window to estimate properly the link conditions [57]. Thus, they cannot be used for fast-changing channels [39]. Also, they provide only the binary information about the link quality telling either the link is good or bad.

2.4.1 Comparing Signal-based and Statistics based Metrics

Each of the above-mentioned link quality metrics have their own strengths and weaknesses which are differentiated in Table 2-1.

Table 2-1: Comparison table between Signal-based and Statistics-based link quality metrics

Signal Based	Statistics Based
Examples: RSSI, LQI, SNR or SINR	Examples: PRR, ETX, ETT, neighbors count
Hardware-based technique.	Software-based technique.

Channel quality is obtained instantaneously once the frame is successfully received.	The PRR, neighbors count take time to prepare the metric whereas, the ETX and ETT provide almost instantly.
Control algorithm using this type requires a feedback mechanism to convey these metric values back to the sender.	No feedback required as statistics are locally available.
Direct power control technique is possible by using this type of metrics, so it converges quickly.	Stepwise control is only possible as a result it converges slowly.
It does not consider the retransmissions performed at the sender.	ETX or ETT takes retransmissions in to account.

With these differences, it can be derived that signal-based metrics or statistics-based metrics when used alone cannot provide reliable estimates of link quality. Therefore, some mapping between RSSI and PRR, SNR and PRR, LQI and PRR is performed. However, the correlation between them is still much of a debate [39], [44], [54].

2.5 Choice of Link Quality Metric

After describing various available metrics, their advantages and drawbacks, this section mentions which link metric is used for the proposed scheme in this research. As mentioned in the previous section, each of the signal-based and statistics-based metrics have their own flaws, but they offer a better estimation when combined. Several studies have shown that, combining multiple metrics helps to reduce the flaws of the individual metrics [49], [58]–[60].

Hence, in the proposed scheme, a combination of two metrics is used. The ETX/ETT is used as the primary metric to distinguish the link quality as good or bad. The ETX has all the benefits of PRR which is the most direct form of the link quality but provides the link information almost instantly. In other words, it has lower response time. It can represent the actual capability of a channel to deliver a frame. Being statistics-based metric, there are no hardware dependencies and the metric values are obtained locally, so no feedback is required. Most importantly, it considers the re-transmissions into account that occur at the link layer which has a major impact in the energy consumption. However, being statistics-based metric, it cannot be used to obtain the rate or power level directly by use of approximation or formula so only step-wise control technique is applicable. So, the

convergence time to the near appropriate level may be time consuming. Additionally, this metric value does not provide any information about the link conditions on the receiver (RX) side. In practice, links are not symmetrical.

So, in order to overcome these deficiencies of the primary ETX/ETT metric, a local and temporal attribute from the receiver side, RSSI, is used. This RSSI is used as an auxiliary/secondary metric to improve the link estimation. This value from the receiver is sent back to the sender by using closed-loop feedback. It aids to safeguard the decision made based on primary metric and is used for quick convergence to the appropriate level. More details on the section 3.3.1. As it has been discussed before that RSSI has several weaknesses, namely being unable to provide the metric information during unsuccessful frame delivery. In this research, since it is only used as a secondary metric, in the absence of this metric information, the primary metric will come into play.

In this way, in the proposed algorithm, two metric information are used: one from the sender side, ETX/ETT as a primary metric and the other from the receiver side, RSSI, as a secondary/auxiliary metric to estimate the link quality efficiently.

2.6 Conclusion

This section presented the dynamic and random behavior of the radio environment and the link quality estimation. Various signal-based and statistics-based link quality metrics, their individual pros and cons were also presented with the supporting literatures. This chapter ended with the selection of the link quality metric for the proposed algorithm for this research. In this regard, multiple link information is considered to perform efficient link quality estimation. It uses the local metric ETX as the primary metric from the sender-side and RSSI from the receiver side as the auxiliary metric.

3. Transmission Power Control (TPC)

3.1 Introduction 39
3.2 Literature Review 44
3.3 Proposed Algorithm: REACT-P 46
3.4 Implementation 56
3.5 Performance Metrics 61
3.6 Simulation 62
3.7 Experimentation 71
3.8 Conclusion 82

3.1 Introduction

Radio communication is one of the most energy-consuming events that causes sensor node battery depletion. Among the various states of the transceiver, transmission state is one of the dominant consumers. Hence, one way to save the energy consumption is to reduce the transmission power level at the edge to a minimum level that maintains a desirable reliability.

Transmission Power Control (TPC) basically is a technique to dynamically change the power level of the node depending on the various spatio-temporal factors while ensuring a good communication link quality. The following sub-section presents the impacts of the transmission power and describes the different power control levels at which power control can be performed. Finally, the types of the control mechanism are presented.

3.1.1 Impacts of Transmission Power

Transmission Power has a several impacts on the followings:

i. The coverage or radio's footprint or the range of communication.
ii. Connectivity and the reliability of a link.
iii. Energy consumption of the node and hence the node or the network lifetime.
iv. Interference imposed on the neighbor: collision and overhearing.
v. Channel re-use factor or spectral efficiency.
vi. Near-far problem or fairness to the network.

Transmitting at a high power on a link may improve the link quality, reliability and the throughput on that link but escalates the interference level on other links. The surrounding nodes around the vicinity of the ongoing transmission will suffer from overhearing. This limits the bandwidth re-use. Spectrum efficiency leads to higher performance in the real world. Spectrum efficiency later translates to efficiency, scalability and capacity of a network. The most evident impact of high power transmission is the over-consumption of the energy if the same reliability can be attained at a lower power level [61].

On the other hand, if transmissions are done at a very low power level, the interference can be reduced, and the channel re-use factor can be increased. It may also reduce energy consumption, both directly, by requiring less power to transmit, and indirectly, by reducing contention with other transmitting nodes. However, the links become weak and unreliable.

Transmitting at lower power may not always lead to decrease in the energy consumption. Indeed, if the transmission power is too low, there will be higher BER prompting to retransmissions, which in turn increase the energy consumption together with the latency.

Moreover, transmitting at a constant high/low power leads to the inefficient use of the energy. More importantly, if a constant power level is used by every one of the nodes in the network, they may suffer from near-far problem. For example, if two nodes: one far and one near are attempting to communicate with a receiver at the same time with the same power level, there is a high probability that the signal from the farther node never reaches the receiver or it is attenuated by the other strong one from the nearer node. This brings injustice to the system.

Therefore, in order to eliminate the shortcomings and combine the strengths of the above cases, it is necessary to find an appropriate transmission power level which is neither too low nor too high but is sufficient enough to assure a successful transmission for a given PDR. The optimal power level chosen for one condition at one time is different than that of the other time and condition, so the power level should change dynamically to adapt with the time varying radio link. However, determining the optimal transmission power level is difficult due to variability, instability and unpredictability of random wireless channels as discussed in Section 2.

3.1.2 Key Concept of TPC

Observing the behavior of a wireless link using proper link quality estimation, then utilizing the results to derive predictions about the future link quality and adjusting protocols and radio parameters to satisfy the communication requirements in an energy-efficient fashion is a key concept for creating a dynamic transmission power control that provides a minimal and environment adaptive transmission power [59].

Figure 3-1: Key concept of transmission power control (TPC)

TPC enhances the performance of the network in several aspects. To begin with, it improves the link reliability and aids in converting weak links into reliable ones. When the link reliability falls below certain threshold, the protocol may increase the power level. Second, it provides efficient utilization of the energy. It helps to choose a minimum power level required for a successful delivery of the packet. Third, it decreases the interference and/or collision. TPC helps to choose the power level just enough for communication and therefore the channel outside the range becomes available. This reduces the exposed terminal problem and increases the channel re-use factor. Fourth, by using a higher transmission power, the physical layer can use modulation and coding schemes with a higher bit/baud rate [62] to increase the bandwidth for delay-sensitive application or during heavy workloads, or decreasing the power to maximize energy savings. Moreover, it helps to reduce retransmissions or increase concurrent transmissions thereby reducing the latency. A well designed TPC algorithm can reduce energy consumption, interference and improve channel capacity and reliability by choosing a minimal and environment-adapting transmission power level that ensures an adequate link quality at the same time. It should not overreact during a stable condition and underreact during fast changing condition. There are numerous parameter values that can influence the performance of transmission power control algorithm, such as: choice of the link quality metric and traffic rate, granularity of change of power level, maximum transmission power, threshold values. There are trade-offs for these parameter value selections.

3.1.3 Different Levels of TPC

There are various levels at which a Transmission power control algorithm can operate. They can be broadly categorized into the followings:

a. **Network Level**: All nodes in the network have the same transmission power and it is specified by the network administrator. This does not fully utilize the configurable transmission power provided by the radio hardware. This requires a priori knowledge about the nodes in the network to have full coverage. This is quite not practical.

b. **Node Level**: Each node in the network may use different transmission power but all packets sent to different neighbors from a particular node will use the same power.

c. Neighbor level: Node uses different TX Power for different neighbors. But it remains the same for a particular pair.

d. **Packet Level**: Each node may send data packets with different transmission power for each packet. With proper pair-wise adjustments, more energy saving with finer tuning capability with online control can be achieved at this level [44].

This research focuses on the TPC at packet level. The optimum power level for a pair at any time is the minimum TX power level that supports a good link quality.

3.1.4 Fundamental Blocks of TPC

Any TPC mechanism consists of two fundamental elements namely the link quality estimation and the control mechanism as shown in Figure 3-2. They are described in the next two sections.

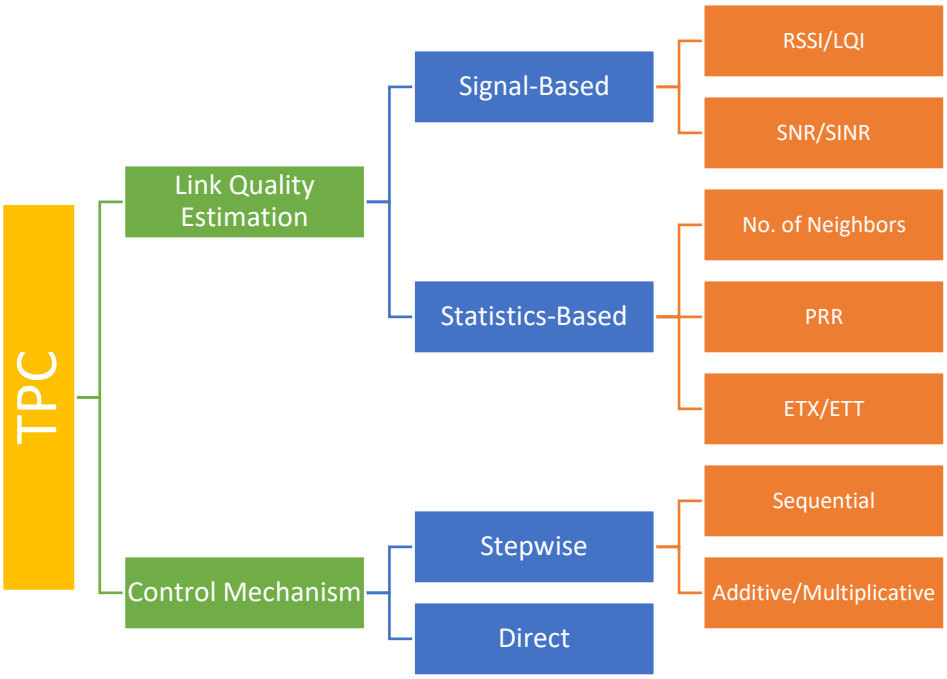

Figure 3-2: Fundamental blocks of TPC

3.1.5 Link Quality Estimation (LQE)

The decision to scale the power up or down by the TPC algorithms is governed by the LQE. LQE is the driver and provides an input for an eventual power level adaptation based on the link conditions. Link Quality Estimation has been described before. More details on Section 2.

3.1.6 Control Mechanism

There are basically two methods of control: Step-wise Control and Direct Control.

3.1.6.1 Direct Control

TPC algorithms using signal-based metrics can use direct control. In direct control technique, certain formula, approximation technique, mapping or predictive model are used to find the appropriate power level directly. Hence, the response time to the optimal level should be quick.

3.1.6.2 Step-wise Control

TPC algorithms using statistics-based metrics can use step-wise control as such metrics provide only binary information. TPC algorithms using step-wise control converge slowly to the appropriate power level. The power can be controlled by using the combination of additive and/or multiplicative control. For example, Additive Increase Additive Decrease (AIAD), Additive Increase Multiplicative Decrease (AIMD) and other combinations.

The remainder of this chapter is as follows. There are lots of research work on transmission power control technique. Section 3.2 mentions some of the popular techniques and their review. Section 3.3 introduces the proposed algorithm. Section 3.4 presents the necessary items for implementing the proposed algorithm. Section 3.5 describes various performance metrics used for evaluation. Sections 3.6 and 3.7 shows the simulation and the experimentation performed respectively.

3.1.7 General Drawbacks of TPC Algorithms

Although TPC has several advantages, some of its recognized downsides are the possibility of an increase in the number of hidden terminals, delay and power control runaway. Because the power is reduced to a level to be sufficient enough to assure a successful transmission, the radio footprint reduces, as a result, the number of hidden nodes tend to increase. Hence, re-transmissions are required due to collisions, increasing the latency as well. On the other hand, with TPC there is a possibility of power control runaway: A situation where the nodes in a network react to each other's power settings and they keep on increasing the power. As an example, let us imagine that a person is going out in a crowded place like a club with his friend. Because the noise level is high, he raises his voice to make a communication. Others will react to this rising noise floor and increase their level as well. Hence, at the end all people will be shouting. In the same manner, if multiple nodes are transmitting at the same time, there is a probability that each of them raises their power level as an action to combat the frame losses. As a consequence, every node will be at their maximum power level. This is the power control runaway.

These problems particularly arise when the nodes are transmitting at the same time and can be reduced by using a proper medium access technique which is a subject out of the scope of this research.

3.2 Literature Review

There exist various Transmission Power control algorithms in the literature. Some of the packet-level control mechanisms are shown in Table 3-1.

Table 3-1: Existing packet level TPC algorithms

Algorithm	Link quality metric	Control Method	Initial phase	Feedback Mechanism
PCBL [61]	PRR	Stepwise	Yes	Open
ATPC [44]	RSSI/LQI	Direct	Yes	Closed
ART [51]	PRR	Stepwise	Yes	Open
I-TPC [63]	RSS	Stepwise	Short	Closed
ODTPC [64]	RSSI	Direct	Short	Closed
MODTPC [65]	RSSI	Direct	Short	Closed
AODTPC [66]	RSSI	Direct	Short	Closed
EAST [67]	RSSI	Direct	Yes	Open + closed
AM-TPC [68]	SNR + Noise	Direct	Short	Closed
DA-TPC [69]	Data driven	Direct	Yes	Open

The reviews on the existing algorithms are discussed further in four aspects as follows:

A. Initial Phase

Among these TPC algorithms, some have a long initial phase [44], [51], [61], [67], [69] and some use frames other than the data in the initialization phase to build up a metric or a model [44], [61]. They all utilize beaconing messages that are sent to all neighboring nodes at all power levels, an effort that is simply an overhead and a waste of energy. With the ever-increasing number of active nodes in networks, it will take more and more time to converge to the optimal level. The algorithms in [63]–[66], [68] reduce the initial phase and do not use any extra overhead. They tend to use DATA-ACK (data- acknowledgement) exchanges to estimate the link conditions. In the proposed algorithm, we tend to use the Data frame with the minimum initial phase to reduce overheads.

B. Approximation Technique:

Some algorithms [44], [66] use techniques like approximations (e.g. least square approximation), predicting models and partial mapping techniques which may be complex and have a higher memory footprint. which may not be suitable for constrained devices like sensors. Some energy is wasted by sending some probe packets in order to initialize such models.

C. Choice of LQE Metric

Regarding the link quality estimators, first, these existing algorithms use either PRR, RSSI, LQI or SNR as a metric to estimate the link conditions. Most of them use signal-based metrics and hence require a feedback mechanism. Signal-based metrics are highly sensitive to the environmental disturbances. On the contrary, PCBL [61], ART [51] use PRR that makes them less responsive to the changes in the environment. It has already been discussed above (Section 2.4) the pros and cons of each of these metrics. None of existing TPC algorithms account for re-transmissions performed at the link-layer that may occur because of collisions or interference. They have an impact on the energy consumption. Also, during losses, when using signal-based metrics, the actual metric value is not obtained, rather an estimate is used to make changes in the power level. This may not provide an accurate information. Secondly, the existing algorithms only make use of a single metric for estimating the link quality, and as indicated earlier, using multiple metrics helps to better estimate the link conditions. DA-TPC [69] does not use any link quality indicators, rather it uses data priority as a metric to change the power level. However, it has an initial phase with higher energy consumption than ODTPC [64]. Moreover, it needs the distance between the neighboring nodes beforehand, so it will not work with randomly distributed nodes which is not practical.

D. Versatility

The current algorithms [44], [63]–[68] using signal-based metrics have defined static thresholds on the signal level. However, these thresholds vary according to the different environmental conditions. As a result, the thresholds defined for one type of environment may not be the same for another, which may have a noticeable impact on the efficiency of the algorithm. This drawback limits the algorithms using signal-based metrics, making them less versatile when exposed to different channel conditions.

3.3 Proposed Algorithm: REACT-P

After considering these rich literatures in the previous section regarding the link quality metrics and existing TPC algorithms, a new REACT-P: Responsive Energy-efficient Adaptive Control of Transmission Power is proposed to satisfy the design challenges as mentioned in 1.3.1 in order to provide better energy efficiency while maintaining similar reliability. The REACT-P is the first to use multiple link quality metrics for link quality estimation as a way to dynamically control the power. It considers both TX-side and RX-side link information to properly estimate the link quality. It is the first to use the ETX as the primary metric to differentiate link quality. Additionally, it uses RSSI from the receiver side as a secondary metric. Unlike the existing algorithms, it defines a dynamic threshold on the signal level and provides adaptive window sizes, making it versatile, self-learning and responsive to different environmental conditions.

We started with the design and development of a new transmission power control at a fixed rate. However, it is designed in such a way that it can later be extended to embrace the dynamic transmission bit-rate as well together with the power level.

3.3.1 Working Principle

REACT-P has two phases: A bootstrap phase and a runtime phase. It uses direct power control technique during the bootstrap phase and a step-wise power control (AIAD) during the runtime phase, thereby offering a “hybrid” control mechanism.

3.3.1.1 Bootstrap Phase

The algorithm starts with a short bootstrap phase with no overhead and lasts for one successful DATA-ACK exchange. The node triggers the bootstrap phase once, when the node is booted. When the node is turned on, it is unaware of the current link condition; therefore, the node transmits at the maximum usable TX power level. For every data frame received, the receiver obtains the RSSI information and then piggybacks this value along with the link-layer ACK message, forming a closed loop feedback. The sender, on receiving this ACK, will perform a loss analysis by using a simple path loss model (6) utilizing the current transmission power and the secondary metric (RSSI) obtained from the ACK. With this link loss, REACT-P roughly estimates the next transmission power directly. This process helps to quickly converge to the closest appropriate power level, thereby providing

a short initial phase without any overheads. The estimate of the next transmission power is found using the following equation:

$$P_{TX}^{NEXT} = linkLOSS + P_{RX}^{SEN}(r) + M\ (in\ dBm) \quad (2)$$

where, $P_{RX}^{SEN}(r)$ is the receiver sensitivity for the bit-rate r, i.e. the minimum signal strength required at the receiver to successfully decode the frame. The receiver sensitivity would be different for different hardware type. *M* is a certain level of margin for a safety purpose respectively. An example of different sensitivities for different bit-rates for Atmel RF215 chip is shown in Table 4-1.

Margin *M* is necessary because it is proved by the researches in the literature and the experiment performed in this research (Figure 3-22) that the RSSI may vary even when the power level remains the same. Second, in the bootstrap phase, the loss is calculated based on a single DATA-ACK exchange i.e. it is calculated on the single value of the RSSI metric which may not be reliable. That is why, a certain margin needs to be added such that the algorithm can converge to the near appropriate power level. Then, it is up to the run-time phase that performs step-wise control to further tune to the proper level.

This phase also involves initializing the various parameters of the TPC algorithms. The window (W) is set to the minimum value i.e. 1. Initial *avgETX*/*EWMA_ETX* and *EWMA_LOSS* are set to the current *ETX* and current *linkLOSS* respectively.

3.3.1.2 Run-time Phase

The runtime phase implies a step-wise control technique (additive increase and additive decrease) and starts with the power level estimated from the bootstrap phase (P_{TX}^{NEXT}). This phase further tunes the power level closer to the optimum value. After each power adjustment, it is necessary to re-evaluate the link conditions. REACT-P uses ETX as the primary metric to determine the link condition as good or bad. Here, ETX is used instead of ETT, as the bit rate and the frame size are considered constant over an application. As discussed in the Link Quality Estimator in sub-section 3.3.2.1, instead of using a single value of ETX, average ETX using EWMA is used to estimate the link quality (4).

The runtime phase consists of BEW Module (Section 3.3.2.2.1) which acts as a learning algorithm to provide variable-sized windows depending on the link quality. This in turn provides the dynamic redundancy constant (*kTX*) as in (5). There is a transmission counter (*nTX*) which is increased after each upper layer (above link layer) transmission attempt that

may further involve more link layer transmissions (ETX). In other words, *nTX* is increased only after a callback from a lower layer to an upper layer. At each power level, the TPC keeps track of the average link loss, (*EWMA_LOSS*), with the help of the current transmission power and the RSSI obtained by using the EWMA as in (7). The finite state transition diagram in Figure 3-3 further illustrates the process during a runtime phase. It consists of one Steady State and three transient states: Increase Power, Decrease Power and Safe2Decrease.

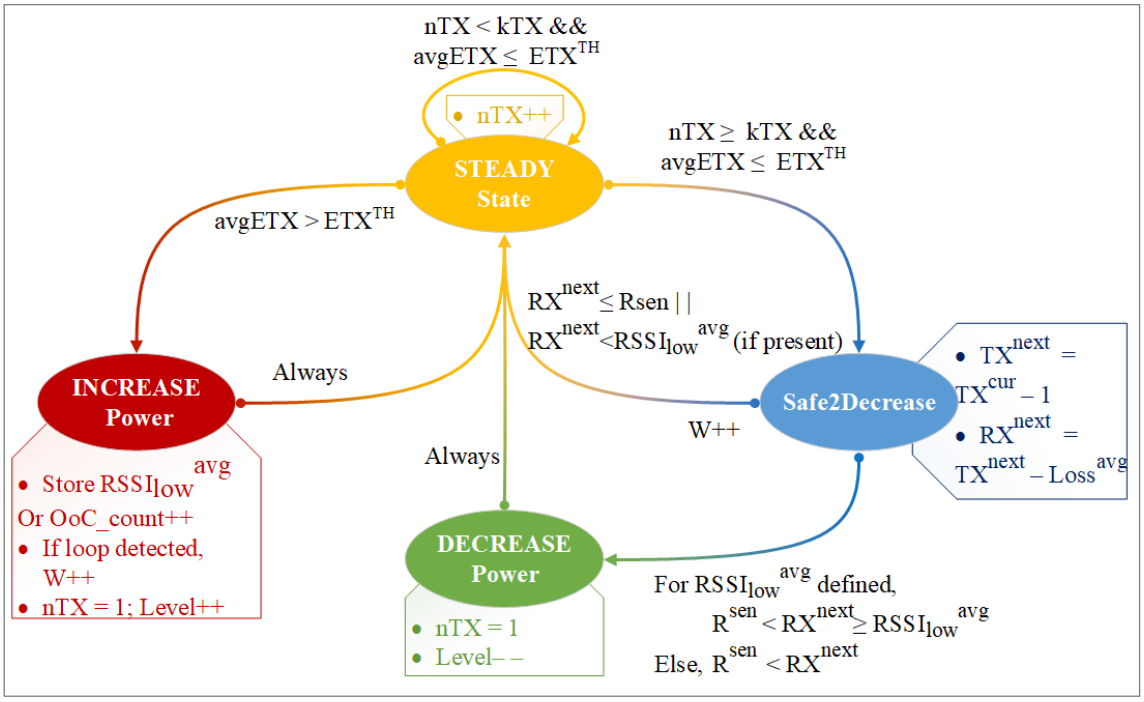

Figure 3-3: Finite state transition diagram for REACT-P in run-time phase

A node tends to make transmissions in the same power level as long as the link conditions are good, and the window has not expired. The window is said to be expired when $nTX \geq kTX$. In other words, a node stays at the same power level in the STEADY state if number of higher layer transmission attempts does not exceed the redundancy counter and the average ETX (*avgETX*) is within the threshold (ETX^{TH}). Here, *avgETX* is the *EWMA_ETX*.

As a first scenario, whenever the *avgETX* crosses the threshold or the LQE module estimates that the link is deteriorating, the power level is increased by one. It does this without waiting for the current window to expire. Upon a power level increase, two tasks are performed. First, it stores the average RSSI, $RSSI_{low}^{avg}$, in the last power level if there was at least one successful TX before. If not, it increases the *out_of_coverage* counter. Second, window size (*W*) is increased by one. More details on how the *out_of_coverage* count/limit is calculated

is explained in Section 3.3.2.2.5. $RSSI_{low}^{avg}$ is calculated by using the current transmission power and the calculated average link loss as shown in (3). It is used later by Safe2Decrease module to check if the link has improved or not.

$$RSSI_{low}^{avg} = P_{TX}^{NEXT} + EWMA\_LOSS\ (in\ dBm) \quad (3)$$

In the second scenario, if the link conditions are estimated to be good throughout the window period then at the end of the window, i.e. when $nTX \geq kTX$, the node will decrease the power level to examine if the node can save some energy by reducing the TX power. When the sender reduces the TX power, there are two possible cases. First, the radio link condition may still be acceptable. In this case, the process follows as before. Second, the radio link condition deteriorates, as the transmission power level may not be enough to overcome the link losses. Hence, the TPC will increase the TX power as per the algorithm. Here is the formation of a loop. This algorithm can detect such loop, so it increases the value of the Window size so that it can stay in the last stable state for a longer time and the process continues till it reaches the maximum window size. The algorithm is learning from the environment and tries to maintain the last stable power level. However, if this process continues, there are two potential risks: First, there is a risk of oscillation during a stable condition between two adjacent power levels at the end of the different window sizes. Second, there is a risk of loss of packet every time the power level is reduced corresponding to the decision of the BEW module.

To reduce the risk of packet loss every time a node tries to reduce the power level when the window expires, it passes through an intermediate state, Safe2Decrease. In this state, REACT-P estimates the next lower transmission power level and the next lower received power level with the help of *EWMA_LOSS* by using (8) and (9). This estimated next lower received power must be higher than the receiver sensitivity for a defined bit-rate. If this next lower transmission power level was not visited before, then, only this condition needs to be satisfied to decrease the power level. If this next transmission power level was visited before with at least one successful transmission, there would be a $RSSI_{low}^{avg}$ value at that power level as well. The presence of this $RSSI_{low}^{avg}$ value indicates that the lower power level was not stable when the average received signal strength was $RSSI_{low}^{avg}$. Hence, the predicted next received power must be higher than $RSSI_{low}^{avg}$ also. If both conditions are satisfied, then the node is allowed to decrease the power level, otherwise it instructs the node to stay at the same power level and increase the window size. Also, in case *out_of_coverage* state is

detected at the next lower power level, the otherwise action is taken as well. These mechanisms help to safeguard the decision made by the BEW mechanism preventing unnecessary losses in the network.

In this way, REACT-P self-learns from the environment by dynamically changing the window size and the lower unstable RSSI threshold, thereby providing a stable and optimal power level for a successful transmission.

In REACT-P, whenever the node goes to states other than the steady state, the counter needs to be restarted so *nTX* is reset to 1. The metric values calculated by using the EWMA are reset upon a change in the power level. This step is necessary because, with the change in the power level, the link conditions would be different, so the averaging needs to be restarted.

3.3.2 REACT-P Block Diagram

A general block diagram of the invented algorithm is shown in Figure 3-4. It is a sender based TPC where the transmission power control is at the sender side. On the receiver, the only change required is that it needs to piggyback the RSSI information along with the ACK message thereby forming a closed loop feedback. For each frame received, the receiver sends the RSSI of the incoming frame back to the sender. As any other TPC, it has two basic modules. The first is the link quality estimator and second is the Power control mechanism. The novelty in this algorithm is in the choice of metric for the link quality estimation and the techniques applied to perform a smarter and stable transmission power control.

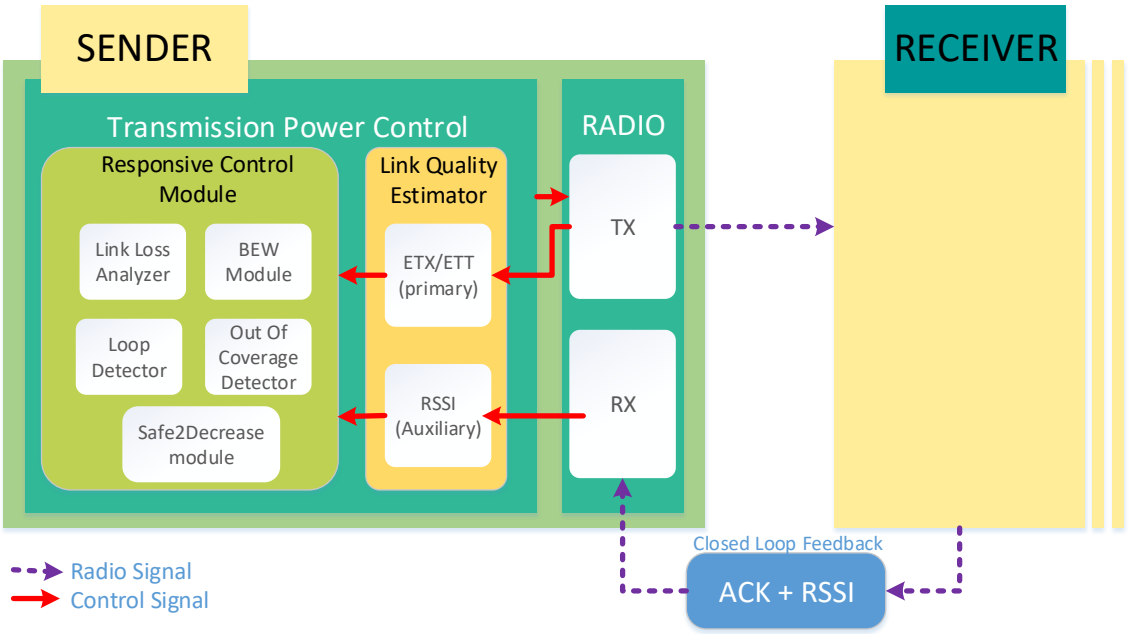

Figure 3-4: REACT-P block diagram

The following explains the modules and sub-modules of the proposed TPC:

3.3.2.1 Link Quality Estimator

Link quality estimation is a thorny problem. Choosing a proper link quality metric and performing a proper link quality estimation is very crucial to a design of any TPC algorithm as it directly impacts the stability and efficiency of the algorithm and hence the system.

The algorithm uses ETX as the primary metric that has all the benefits of PRR but has lower response time. In other words, it can provide the metric value almost instantly. The ETX or Expected Transmission Count is the number of link layer transmissions required to make a successful transmission. It can represent the actual capability of a channel to deliver a frame. Unlike other metrics, this metric considers the collisions that occur, or re-transmissions performed as well. This is a software-based metric so there are no hardware dependencies unlike other link quality metrics like RSSI or LQI. Transmission Control algorithm that uses ETX as a metric does not require a feedback mechanism as these metric values are locally available. However, this metric has some negative aspects. Firstly, ETX can only provide a binary information about the channel i.e. either the link is good or bad and can aid the algorithm to head in a proper direction, but its value is not sufficient enough to obtain the appropriate power directly. Therefore, only stepwise power control technique is possible because of which the algorithm may converge slowly to the appropriate power level.

Secondly, as the TPC (Transmission Power Control) is done at the TX side, it does not have any information about the RX side.

In order to improve these deficiencies, the REACT-P takes the local metric from the Tx side and the temporal attribute/metric from the Rx side into account, which is the RSSI whose value is sent back to the sender via a closed loop feedback mechanism. This provides information on the link quality at RX side to the sender. In this algorithm, RSSI from the receiver is used as an auxiliary metric as a safeguard. RSSI is also used in the initial/bootstrap phase for the fast convergence to the optimal power (More details explained in Section 3.3.1). Using multiple metrics would help in determining the link quality more efficiently and perform a better control over the transmission power.

A single value of ETX is not used to distinguish the radio link conditions. Rather, an averaging technique called Exponential Weighted Moving Average (EWMA) is used as shown in (4). This is an inexpensive way of keeping an average value (*EWMA_ETX*) as it requires only one variable to store the result.

$$EWMA\_ETX^{k} = \begin{cases} ETX^{k}, for\ k = 0 \\ \alpha EWMA\_ETX^{k-1} + (1-\alpha)ETX^{k},\ otherwise \end{cases} \quad (4)$$

where, $0 < \alpha < 1$ is the weighing factor, $EWMA\_ETX^{k-1}$ and ETX^{k} *are* the old average and new instantaneous values of ETX. Higher α indicates that more priority is given to the history values. For the first time, $EWMA\_ETX^{k}$ is the ETX^{k} itself. This averaging technique helps to smoothen the link quality value that prevent triggering unnecessary changes in the power level due to abrupt minor variations in the link conditions. This can also be viewed in the experimental result in Figure 3-23.

3.3.2.2 Responsive Control Module

The power control module is intelligent, self-learning and environment-adaptive. It has various sub-modules which are described in the next sub-sections.

3.3.2.2.1 BEW Module

The Binary Exponential Window (BEW) module is responsible for providing variable-sized windows depending on the averaged primary metric *EWMA_ETX*. It acts as a learning algorithm that stabilizes the selected TX power level and prevents minor oscillations during a stable condition. The name comes from the fact that it uses the formula (5) that uses an

exponent of two. The BEW provides a dynamic redundancy constant (kTX) that changes for different window sizes as follows:

$$kTX = W^{MAX} * 2^{(W-1)} \quad (5)$$

Here, *kTX* gives the upper limit for the number of transmissions recurring at the same power level. W^{MAX} is the maximum window size and *W* is and integer value starting from 1 that represents the current window size (1 to W^{MAX}).

BEW provides different window sizes (W) and hence different redundancy constant (kTX) depending on the stability of the environment. When the environment is unstable, the window size is reset to the minimum value so that the power level can be changed more frequently. On the contrary, when the environment is stable, the window size is increased so that the last stable optimal power is maintained for a longer duration. Increasing the window size(W) by one means doubling the redundancy constant (kTX). The increase in the window size means that, the node will try to stay at the last stable power level for a longer time in terms of the number of transmissions. A larger window size also increases the number of samples in the average of the primary link quality metric ETX, thereby providing a better link estimation. In this way, the BEW helps to prevent both overreacting during rapid changes and underreacting during slow changes of the link conditions and thus aids in better stabilizing the transmission power. The control flow diagram is also shown in Figure 9-10.

3.3.2.2.2 Link Loss Analyzer

The Link Loss Analyzer keeps track of the losses in the link by using the RSSI value that is piggy-bagged along the link-layer ACK message. The Link loss is the attenuation in the signal strength when a frame travels from a source to a destination. This sub-module uses a simple path loss model to calculation the link loss as follows:

$$linkLOSS = P_{TX} - P_{RX}\ (in\ dB) \quad (6)$$

Where, P_{TX} and P_{RX} are the transmission power used at the sender and received power at the receiver (RSSI) in dBm respectively for a DATA-ACK exchange. Similar to the ETX, this calculated loss in the link is also averaged by using EWMA as follows:

$$EWMA\_LOSS^k = \begin{cases} linkLOSS^k\ , for\ k = 0 \\ \beta\ EWMA\_LOSS^{(k-1)}\ + (1-\beta) linkLOSS^k,\ otherwise \end{cases} \quad (7)$$

Where, $0 < \beta < 1$ is a weighing factor and $EWMA\_LOSS^{k-1}$ and $linkLOSS^{k}$ are the history and the new link loss respectively. Equation (6) is used in the bootstrap phase and equation (7) is later used by the Safe2Decrease Module.

Being based on the RSSI value in the obtained acknowledgement, this sub-module cannot provide the actual path loss if the frame never reaches its destination or fails to receive an ACK. However, in such situation, there is no impact on the algorithm, as it will take necessary actions by using the ETX, which is the primary metric.

3.3.2.2.3 Loop Detector

Loop Detector helps the TPC to detect the back and forth oscillation between adjacent power levels during a stable condition. It directs the BEW module to increment the window size whenever such loop is detected so that the node can remain in the last stable power level for longer duration.

It is necessary to reset the window size (W) to a minimum value when the link undergoes fast-fading. This is done by using the variable *last_stable_level (LSL)*. This variable is updated when the power level changes and specifically when its value is different than the next estimated power level. The window size is then reset if the LSL is beyond the next estimation. Following is the pseudo code to explain the process.

Pseudo Code:

```
If current_level != previous_level{
        If LSL != next_estimated_level{
                If (next_estimated_level+1) < LSL || LSL < next_estimated_level
                        W = 1
                If current_level > previous_level
                        LSL = current_level
                Else
                        LSL = previous_level
        }
}
```

3.3.2.2.4 Safe2Decrease Module

This sub-module is invoked each time before decreasing the power level to ensure that it is safe to decrease. It provides an estimation of the next received power level (P_{RX}^{NEXT}) to decide whether to reduce the power or not:

$$P_{TX}^{NEXT} = P_{TX}^{CUR} - 1\ (in\ levels) \tag{8}$$

$$P_{RX}^{NEXT}(dBm) = P_{TX}^{NEXT}(dBm) - EWMA\_LOSS(dB) \quad (9)$$

where, P_{TX}^{CUR} and P_{TX}^{NEXT} are the current and next lower transmission power levels, respectively. *EWMA_LOSS* is the averaged link loss in dB. Being step-wise control (AIAD), P_{TX}^{NEXT} is exactly one level lower than P_{TX}^{CUR}. This module safeguards the decision of the BEW module (More details on Section 3.3.1). The control flow diagram is also shown in Figure 9-14.

3.3.2.2.5 Out of Coverage Detector

REACT-P employs out of coverage detection mechanism. Whenever the power level is decreased, if no ACKs are received consecutively after the expiration of three window sizes, it declares that the receiver is out of coverage at this lower power level. When an out of coverage state is detected, the node will not reduce the transmission power until and unless the maximum window size has been reached. This reduces packet losses during the expiration of the intermediate window sizes. If a node becomes successful again at lower power level, the out of coverage counter is reset. This mechanism is also shown via flowchart in Figure 9-15.

3.3.3 Novelty

REACT-P is designed with the goal to overcome the flaws of the existing algorithms and hence has some novel methods applied. They are categorized as follows:

3.3.3.1 Multiple Link Quality Metrics

REACT-P is the first TPC algorithm to use combination of multiple metrics to adapt the power level. It is also the first one to use the ETX as a primary metric to distinguish and predict the future link conditions. It uses environment-dependent signal-based metric, RSSI as a secondary metric as a safeguard. It uses both TX side and RX side link information to perform link quality estimation and adapt the power level. This provides an efficient way of improving the link quality estimation. It neither primarily depends on the environment-varying metric, nor on the expensive PRR that takes time to build its statistics.

3.3.3.2 Responsive Control Mechanism

REACT-P uses direct control method in the bootstrap phase and step-wise control during runtime phase thereby giving a hybrid control. With various sub-modules as defined above

in sub-section 3.3.2.2, the control mechanism is self-learning, responsive and environment-adaptive. It reacts appropriately with the spatio temporal factors.

3.3.3.3 Versatility

Unlike most of the existing TPC algorithms [44], [63]–[68] using signal-based metrics that defines a static- signal threshold, REACT-P has a dynamic signal threshold on the secondary metric, RSSI that varies with the time and space. This threshold is updated during the run-time. This provides the versatility and adaptability of the algorithm in any kind of environment deployed for WSN or IoT. The algorithm does not need to perform any priori tests to get the signal thresholds.

3.3.3.4 Realistic Experiment Scenario

Some of the existing algorithms have been evaluated by simulation only [63], [65], [67] while some of the other have been evaluated by experimentation [44], [51], [64], [68]. However, various assumptions were made in the literature regarding the radio link conditions. Some assume that there are no collisions in a network [67], [68]. Some assume there is no fading [44]. But the real field experiences both of them in a random way. So, it is necessary to perform the tests in an environment experiencing both collision, interference and fading. In this thesis work, tests were performed in simulation as well as in experimentations in both congested and uncongested environment. This provides the information about how the algorithm performs under sparse as well as dense radio conditions.

3.4 Implementation

The transmission control function block is placed between the MAC and the higher layers in 802.15.4 protocol stack (Figure 3-5). The main function of the proposed algorithm is invoked whenever there is a callback from a lower layer to a higher one. The proposed algorithm was developed in C (650 lines, 27KB) using preprocessor conditions to work with both simulation and experiments. One source file and one header file were developed, and a few changes were made on the MAC layer callback. Some of the parameter values used in the algorithm are given in Table 3-2.

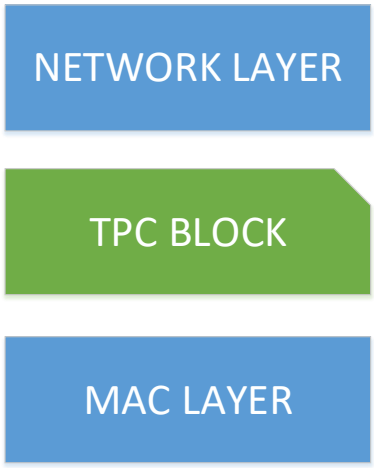

Figure 3-5: Placement of REACT-P block in the IoT netstack

Table 3-2: REACT-P Algorithm Parameters

Parameters	Values
Sensitivity Margin (M)	10 dB (experiment) and 3 dB(simulation)
W^{MAX}	8
α and β	0.85 and 0.40 respectively
ETX_FACTOR and ETX^{TH}	128 and 64 respectively

M is the receiver sensitivity margin which is set to 3dB for simulation and 10dB for experimentation as a safety. The variation in the margin between a simulation and experiment is due to the fact that real environment exhibits higher randomness and variations than the simulated environment. As this margin is only used in the bootstrap phase, so it would not have a big impact on the efficiency of the algorithm. W^{MAX}=8 means the maximum length of the window can be 1024 found by using (5). So, at its maximum, the algorithm performs 1024 transmissions at the same power level. α and β are the weighing factors on the history values of ETX and linkLOSS, respectively, in their EWMA calculation. More priority is given to the new values for path loss, as it was necessary to consider the impact of the latest path loss. On the other hand, more weight is given to the history values of ETX to stabilize the ETX values in case there are abrupt changes in the network. This prevents excessive churn in the power levels. The value of 0.85 for α is chosen in such a way that when there are four consecutive frame transmission failures, the average value reaches above the threshold (ETX^{TH}). The actual ETX value is multiplied by an ETX_FACTOR to account for floating values. So, the ETX threshold of 64 means that when

the deviation of the EWMA_ETX from the optimal value (=1*128) is more than 0.5 times, i.e. 64, then the algorithm considers that the link has deteriorated and takes the necessary actions. The value of these weighing factors and thresholds depends on the traffic rate and type of application deployments. Performing various experiments with different values of the weights and thresholds and choosing the optimal ones are left for future work.

REACT-P at constant rate (w/REACT-P) was compared to constant transmission power and constant rate (w/CPCR) by means of simulation and real experimentation. Data were logged on the sink side and analyzed using JavaScript and Excel.

3.4.1 Assumptions

Some valid assumptions were made while implementing the proposed algorithms. They are listed below:

i. All nodes boot only once i.e. they do not reboot. This assumption has almost no impact on the proposed algorithm. This assumption is only made to keep the counters for number of packets sent, total energy consumption.

ii. All nodes are using the same hardware and flashed with the same firmware.

iii. Only transmitting radio activities are considered to compute the energy consumption.

iv. A fixed sized data frame is used.

3.4.2 Calculation of Transmission Time

The calculation of the transmission time is explained in detail in Section 4.3 as it is more relevant in that section.

3.4.3 Energy Consumption Model

A simple state-based linear software energy estimation model [70] is used to compute the energy consumption, where the energy consumption of a node is calculated as the sum of the energy spent in the various states of the transceiver, basically, Transmission (TX), Reception (RX) and Sleep/Idle state (SLP). The amount of energy consumed in a particular state ‘s’ of the transceiver (E_s) is formulated as:

$$E_s = time\ spent\ (T_s) * current\ drawn\ (I_s) * Voltage\ (V) \quad (10)$$

The total energy consumption of a node is then given by

$$E_{con} = E_{TX} + E_{RX} + E_{SLP} = VI_{TX}T_{TX} + VI_{RX}T_{RX} + VI_{SLP}T_{SLP} \quad (11)$$

In this research, the prime focus is on optimizing the transmission energy therefore the reception state (RX) and idle state (SLP) are ignored and only transmission energy is considered. Hence,

$$E_{con} = E_{TX} = VI_{TX}T_{TX} \quad (12)$$

I_{TX} is given by the different power levels settings and depends on the type of the hardware. Different current consumption at different power levels for two hardware are shown in the Table 3-5 and Figure 3-20.

3.4.4 Live Tool

The sink logs all the data incoming from various nodes in a network and they are sent to a PC connected via a serial output. In order to view the logged data in a graphical way, a live web-based tool was developed using HTML, jQuery, canvasJS [71] during this thesis. This tool filters the various metrics that is sent in the payload from the data logged at the sink. It then shows these metrics in the form of line chart, bar chart, stacked column. It basically categorizes the metrics into two parts namely the Network (Figure 3-6) and the Power related (Figure 3-7).

There is a control tool bar at the top of the page that can be used to automate the collection. It can start, stop the collection at any time. Interval of collection, maximum limit of reception can be also set.

The payload of the data contains the following application data.

```
struct my_data_msg {
  uint16_t len;
  uint32_t clock;
  uint8_t node_id;
  uint16_t seq_id;
  uint8_t cur_power;
  uint16_t etx;
  uint16_t ewma_etx;
  uint16_t total_sent;
  uint32_t total_tx_energy;
  uint16_t cca;
  uint8_t modulation;
  uint8_t path_loss;
```

```
  uint8_t avg_path_loss;
  uint16_t neighbors;
  int8_t rssi;
  char data_msg [40];
}
```

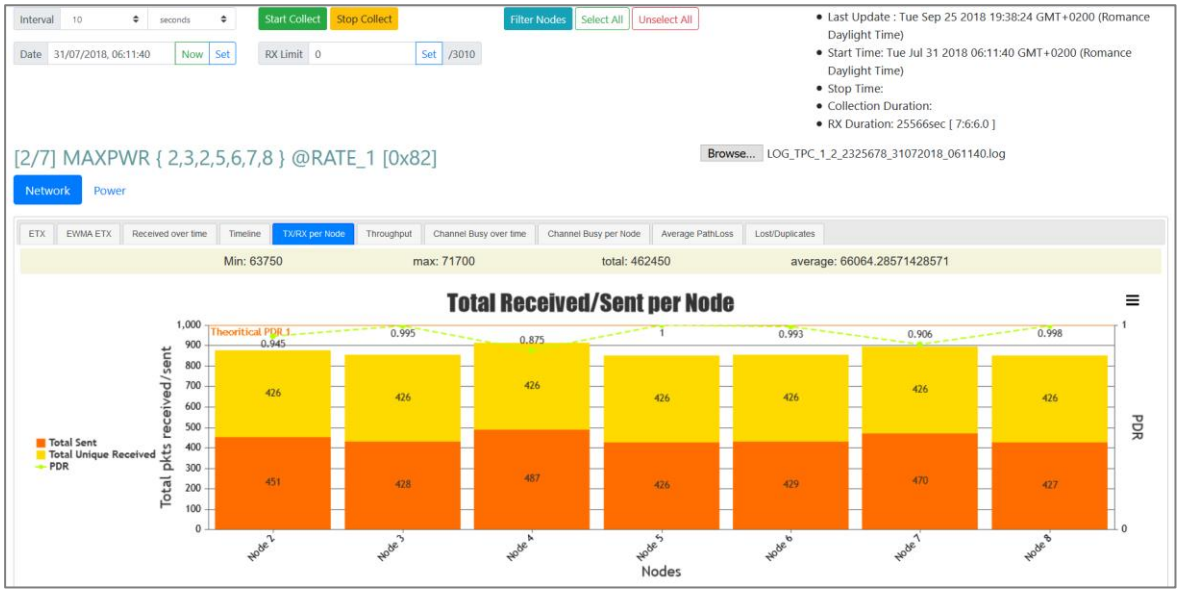

Figure 3-6: Live tool showing network metrics

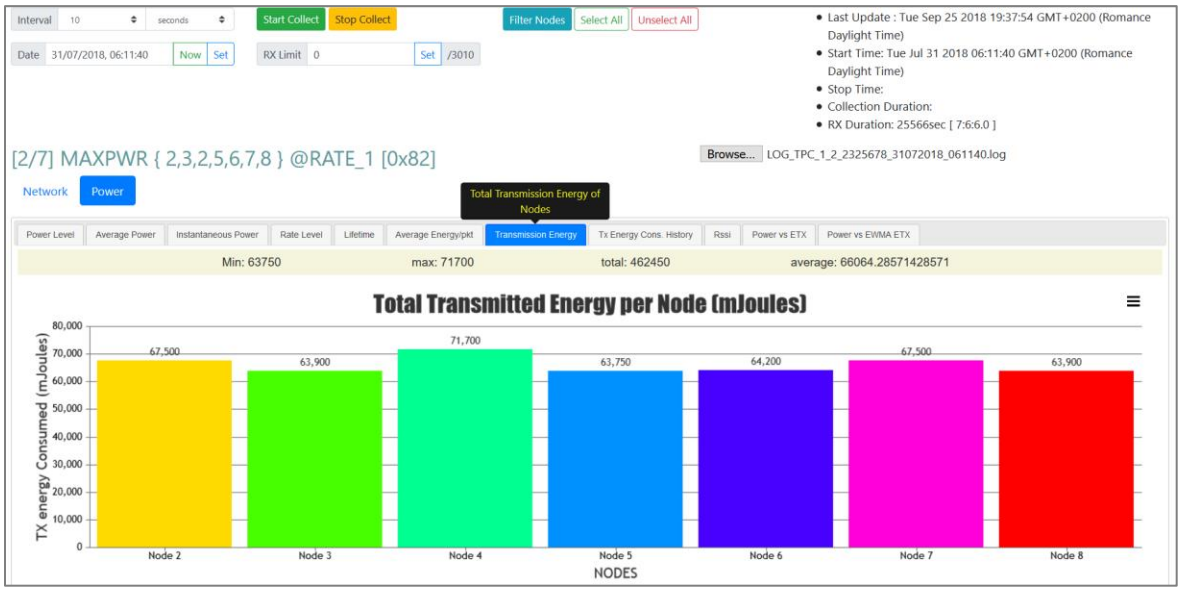

Figure 3-7: Live tool showing power related metrics

3.5 Performance Metrics

To execute the performance evaluation of the proposed algorithm, three parameters were used in this chapter. They are: Network Energy Consumption, Average energy consumption and PDR. Brief descriptions on these parameters are explained as follows:

3.5.1 Network TX Energy Consumption

It is defined as the total transmission energy consumed by all the nodes in the network at the end of the simulation/experimentation time.

$$Network\ Energy\ Consmuption = \sum_{i} E_{con}^{i}\ ;\ \forall i \in BPD\ clients$$

3.5.2 PDR

When the nodes transmit packets, not all packets reach the sink in a single try, so there may be frame re-transmissions involved. Re-transmission may happen due to any of the followings:

- Frame is lost on the way due to fading.
- Frame is corrupted and fails at the various layers of the stack at the receiver.
- Frame successfully reaches the receiver, but the acknowledgement fails to reach back to sender.

Hence, the actual value is in the unique frame received. The lost and the duplicate frames are wasted. PDR is the Packet Delivery Ratio and is also called Packet Reception Rate (PRR) which is defined as the ratio of the total number of unique frames received to the total number of frames sent by all nodes in the network.

$$PDR = \frac{Total\ number\ of\ unique\ frames\ received}{Total\ number\ of\ frames\ sent}$$

3.5.3 Average TX Energy Consumption per Frame

It is the average amount of transmission energy spent per unique frame received. In other words, this represents the amount of transmission energy on average to send a frame successfully.

$$ENERGY_{AVG} = \frac{Total\ transmission\ energy\ consumed}{Total\ number\ of\ unique\ frames\ received}$$

3.6 Simulation

The proposed algorithm was implemented in ContikiOS and simulated with COOJA [72]. COOJA (COntiki Os JAva) is a Java-based simulator that is designed for the wireless sensor networks to run ContikiOS [72]. Contiki is an open source, lightweight, multi-threading OS developed for the Wireless sensors having constrained characteristics. Contiki fully supports IPv6, IPv4, 6LoWPAN, RPL, and CoAP standards. The development of programs is easy and fast as the applications can be written in standard C programming language and therefore making it portable. Today, the latest version available is Contiki 3.0. The main feature of COOJA simulator is the different motes such as TelosB can be emulated.

Cooja supports various radio mediums:

a. No Radio Traffic

This model does not allow radio communication and thus not suitable for the simulations requiring radio activity.

b. UDGM-Constant Loss

Unit Disk Graph Medium-Constant loss is a radio model where the transmission range is modeled as a disk and the nodes lying outside this disk do not receive any frame whereas the nodes lying inside the disk receive the frames.

c. UDGM-Distance Loss

It is the extension of UDGM-Constant Loss where first, a simple interference model is added. In case any interference is detected, the frame is lost. Second, transmission and reception success probabilities are added. If there is unsuccessful transmission, no devices receive the frame, and if there is unsuccessful reception, only the particular destination does not receive the frame. The successful frame reception probability at a node within a distance D from another node can be calculated as:

$$Probability\ of\ success\ (PSR) = 1 - \frac{D^2}{R^2} * (1 - RX)$$

where, D is the distance between two nodes and $D \leq R$, R is the reception range and $R > 0$ and RX specifies the success ratio. This means the probability of successful packet reception decreases as the node is farther from the transmitter node. This radio model is used in this research.

d. DGRM

DGRM (Directed Graph Radio medium) is model that builds the graph through the edges and is mainly used for specifying the transmission success ratio for asymmetric links. In addition, propagation delay to the links can also be defined.

In addition to the radio medium, Cooja supports various interactive plugins. Some of them are described as:

a. Simulation Visualizer

It aids in configuring the topology. It allows drag and drop of the nodes, changing the radio medium (transmission and reception radio ranges and success ratios). It can show information related to nodes as: types, IDs, radio traffics, addresses, log outputs, positions and LED states.

b. Timeline

It displays the state of the radio of each node at each instant through different colors: on (grey), off (no color), packet reception (green), packet transmission (blue) and packet interference (red).

c. Event Listener

This plugin can be used for debugging purpose. It provides break points on various activities like radio, LEDs, log outputs, radio medium event, simulation event etc.

d. Mote Output

This displays the output of the nodes created by the printf function in the C. It allows node specific coloring and provides the filter option. It also permits to save the logs.

e. Power Profiler

It can be used to measure the energy consumption. It provides the total time spent by the node in different states in terms of percentage.

3.6.1 Setup

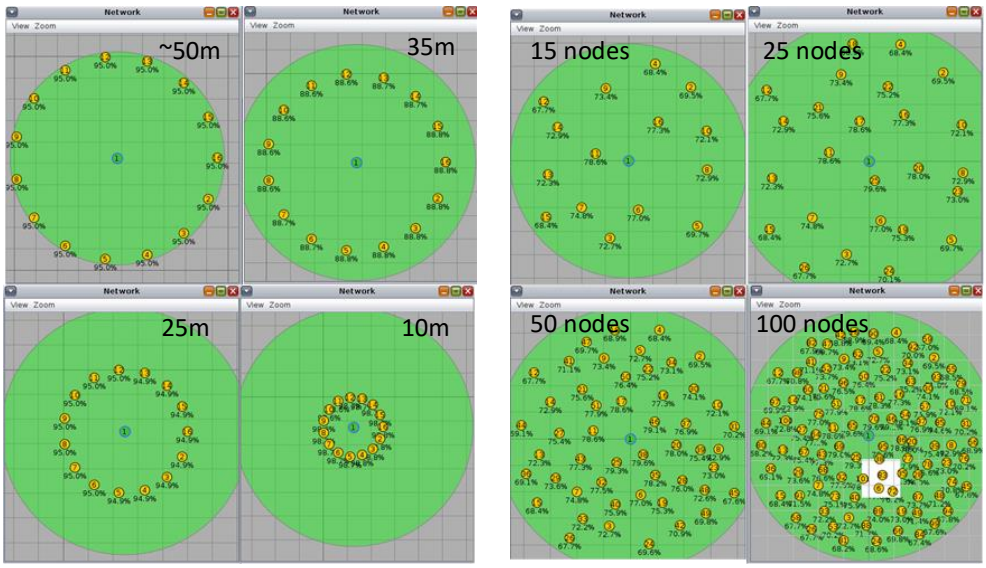

Figure a Figure b

Figure 3-8: Two simulation test networks

3.6.2 Parameters

Table 3-3: Algorithm parameters for Simulation

Parameters	Value
Sensitivity Margin (M)	3 dB
W^{max}	8
β and α	0.40 and 0.85 respectively
ETX_FACTOR and ETXTH	128 and 64 respectively

Table 3-4: REACT-P Simulation Parameters

Parameters	**Value**
Simulator	Cooja with ContikiOS [72]
Device Model	TMote Sky Node [73] with CC2420 Transceiver
Network	Star Topology with 1 sink
Number of Nodes	15, 25, 50, 100
Position	10m, 25m, 35m, ~50m (max), random
Radio Medium	UDGM - Distance Loss
TX Power	8 levels: Table 3-5
Link Quality	PSR: 20%, 40%, 60%, 80%, 100%
Total Packets sent	300 per node
Data Size and Rate	100B and 250Kbps, respectively
Data Traffic	2 packets/min
Algorithms	REACT-P Vs CPCR *
Repetitions	Three with different random seeds. The same seed is maintained when comparing using and not using TPC.

*Here CPCR is the maximum constant power (power level 31) at constant rate of 250Kbps and REACT-P is the proposed transmission power control algorithm at constant rate of 250Kbps.

Table 3-5: CC2420 Output power settings and typical current consumption @ 2.45GHz [47]

Power Level	**Output Power (dBm)**	**Current (mA)**
31	0	17.40
27	-1	16.50
23	-3	15.20
19	-7	12.50
15	-10	11.20
11	-10	11.20
7	-15	9.90

3	-25	8.50

Simulations were performed to compare the proposed algorithm REACT-P (w/REACT-P) with the maximum constant transmission power at constant bit-rate (w/CPCR) using COOJA simulator. At high level, two test simulations were performed to validate the efficiency of the proposed algorithm. One with different constant distances and the other with different number of nodes at random positions. These are illustrated in Figure 3-8 (a) and (b), using the parameters shown in the Table 3-4. In each of the scenario, simulations were performed for different link qualities, i.e. Packet Reception Success Ratio (PSR). For example, a PSR of 60% means the packets are received successfully with 60% probability. Each simulation was run until the sink received 300 packets from each node. Each test was repeated three times with different random seeds to increase the confidence. However, same random seed was maintained while comparing the proposed algorithm with CPCR in order to compare the result in the same environment situation of the network.

Data were logged on the sink side and were analyzed by using jQuery, canvasJS [71] and Excel.

3.6.3 Results and Discussions

3.6.3.1 Test Scenario I

The first test simulation was performed with 15 nodes at different distances for different link quality levels as shown in Figure 3-8.a to observe the impact of distance on REACT-P. Figure 3-9 shows the % improvement in the total transmission (TX) energy consumed when REACT-P is used compared to using CPCR for different packet success ratios at different distances. Figure 3-10 shows the network throughput and the PDR at different distance at a particular PSR of 60%.

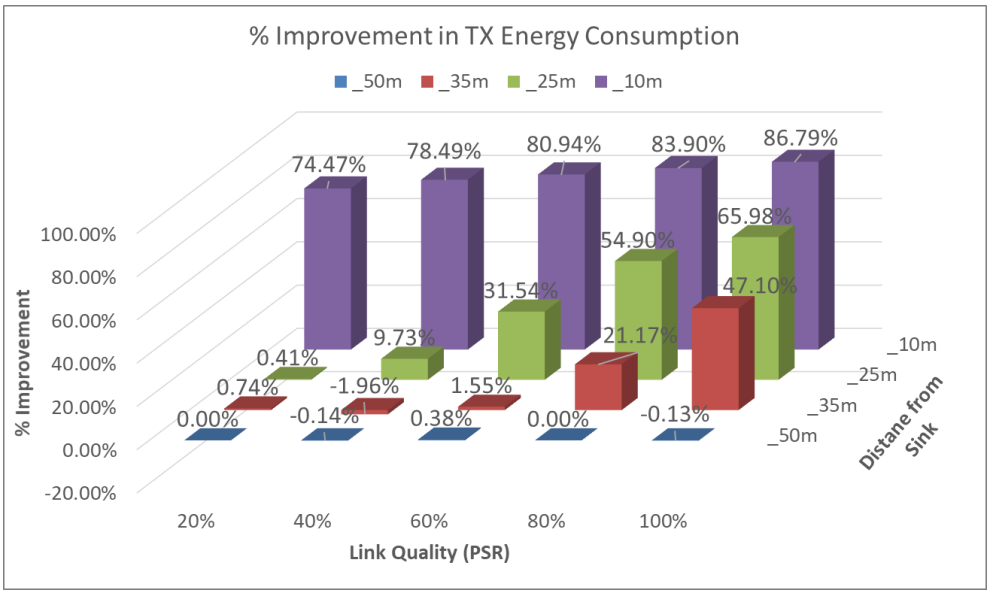

Figure 3-9: The % improvement in TX energy consumption at different distances and PSR

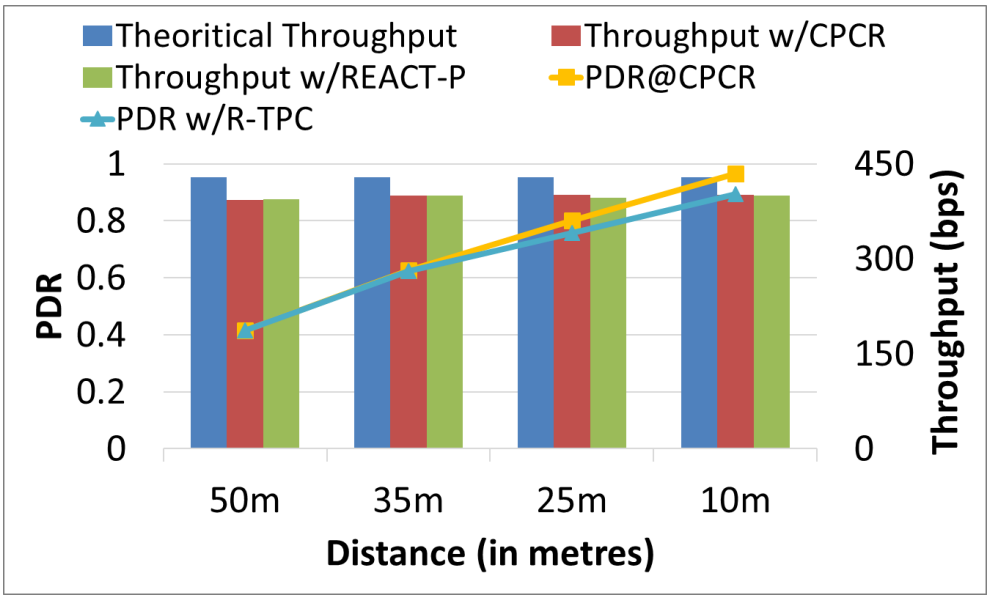

Figure 3-10: Throughput and PDR at different distances at 60% PSR

The above results show that nodes closer to the sink gain maximally when REACT-P is used. Up to 87% improvement in the TX energy consumption was observed during the simulation. The improvements were observed with low compromise on the throughput and PDR as shown in Figure 3-10. Also, it can be clearly observed that the improvement in the energy consumption decreases as the link quality decreases.

3.6.3.2 Test Scenario II

A more realistic test was performed with different numbers of nodes at random positions/distances from the sink for different link quality levels as shown in Figure 3-8.b

The graph in Figure 3-11 shows an improvement of up to 45% in the TX energy consumption with low compromise in the throughput and Packet Delivery Ratio (PDR) (Figure 3-12). This also shows that the REACT-P offers satisfactory energy savings with a higher number of nodes, proving the algorithm's scalability. It can also be perceived from Figure 3-12 that, at a good link quality, there is minor gap between the PDRs when REACT-P is used and when CPCR is used. This is expected because without any loss in the simulated network (for example, 100% PSR), the maximum powered nodes have higher PDR. The losses experienced are only due to collision of frames between multiple nodes and not due to environmental factors. Since in the REACT-P, occasionally the nodes attempt to reduce the transmission power to check if the node can improve the energy consumption, so some losses are inevitable. However, the gain in the PDR with CPCR comes at a huge price in the energy consumption. As seen in the graphs, with the decrease in the link quality or PSR, two PDR lines tend to have similar values.

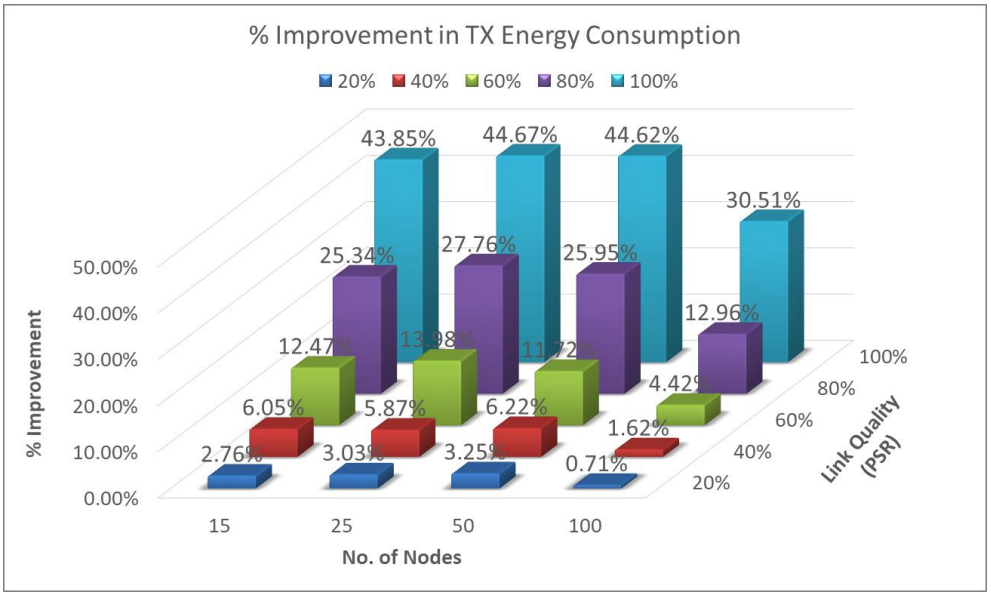

Figure 3-11: The % improvement in TX energy consumption for different numbers of nodes and link quality levels

Figure 3-13 shows energy consumption history and the average transmission energy per frame of Node 6. Node 6 is around the center of the sink's coverage in a 25-node environment in Figure 3-8(a). It can be observed that Node 6 has 50% less energy

consumption on average when using REACT-P than when using CPCR thereby doubling the node lifetime.

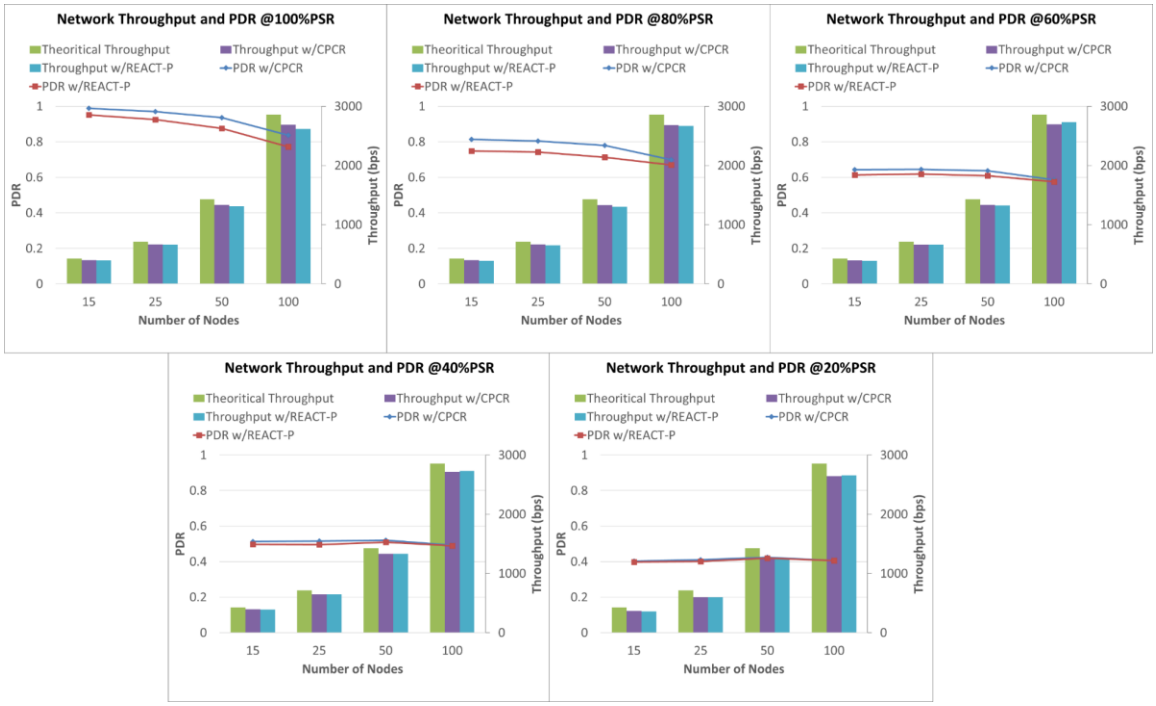

Figure 3-12: Network Throughput and PDR at different PSR

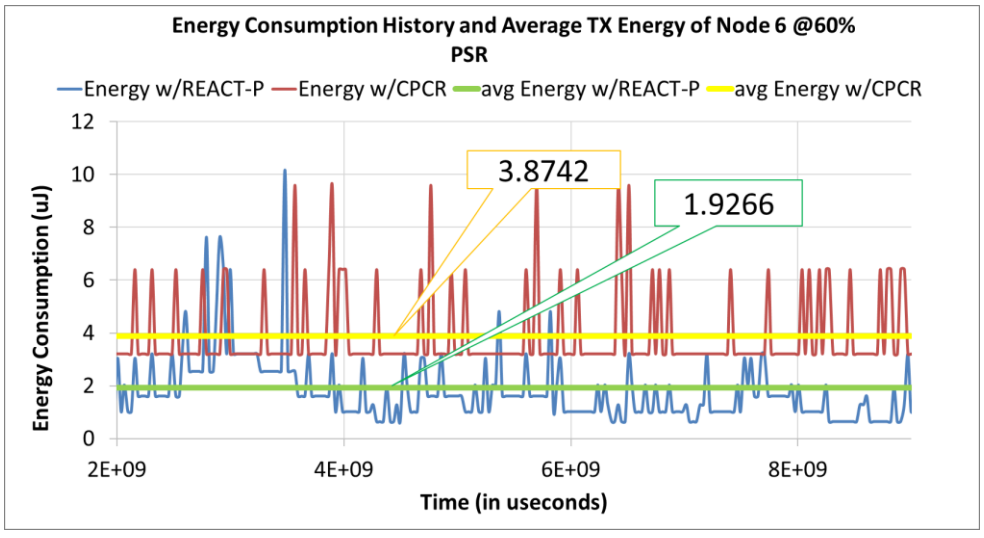

Figure 3-13: Node 6's TX Energy consumption history and its average for a 25-node environment at 60% PSR

3.6.3.3 Comparison with ODTPC

In order to compare the efficiency of the proposed algorithm with one of the existing ones, ODTPC (On Demand Transmission Power Control) is chosen as a reference as it showed superior results than previous existing ones such as PCBL [61] or ATPC [44]. There were

some extended versions of ODTPC but with marginal improvements only. Following is a short description of how ODTPC works.

On Demand Transmission Power Control (ODTPC) [64] is an on-demand scheme that uses RSSI as a metric, which is piggy bagged along with the ACK message. Link quality between the pair of the nodes is estimated only after the exchange of data ack messages. This reduces the additional overheads. ODTPC has two phases: large-scale phase and small-scale phase. In the first one, nodes firstly roughly approximate the transmission power level with the help of RSSI obtained from the ACK frame after the data-ack exchange. And in the small-scale phase, it sends the data with the appropriate power level in the neighbor table (max power if empty) and the receiver sends back the RSSI information with the ACK. If the corresponding RSSI values exceed or fall below a given threshold boundary, the sender will change its transmission power accordingly. ODTPC does not utilize any initialization stage. However, as the link quality changes its state quickly due to the multi path fading, ODTPC cannot respond fast enough [19].

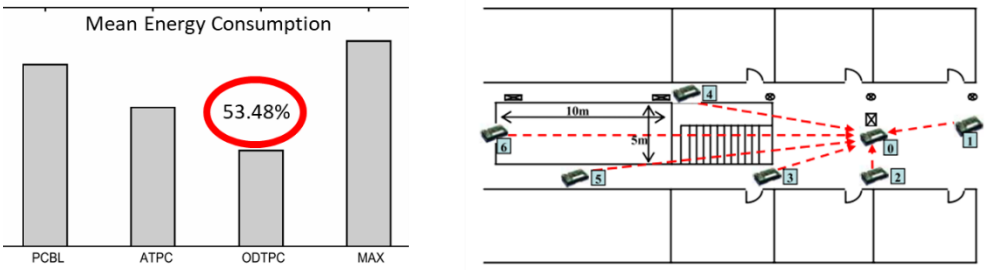

Figure 3-14: Mean energy consumption of ODTPC (left) and experimental setup (right) [64]

The bar graph in the Figure 3-14 showed that ODTPC consumed less energy than previous transmission power control algorithms (PCBL [61] and ATPC [44]).

We have mimicked the setup in the COOJA simulation with similar parameters such as (6 nodes, 500 pkt transmissions from each node, data packet of size 30 bytes every 30 seconds). Compared to the maximum power used for CPCR, 53.48% improvement in mean energy consumption was observed with ODTPC (Figure 3-14) while 76.44% improvement was observed with REACT-P (Figure 3-15) proving the higher energy efficiency of the REACT-P than ODTPC.

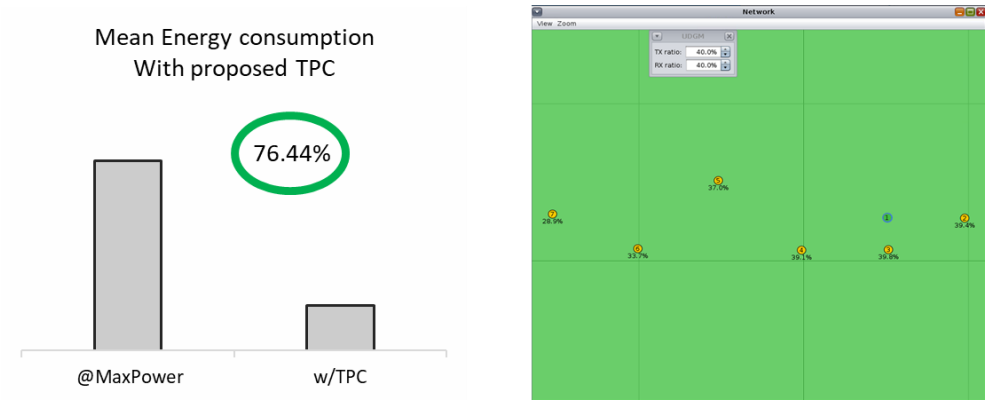

Figure 3-15: Mean energy consumption of REACT-P (left) and mimicked simulated setup

3.7 Experimentation

The real environment exhibits rich dynamics and randomness. Therefore, it is absolutely necessary to validate the proposed algorithm in a real case scenario. Itron IoT module uses low-power, 32-bit ARM cortex-M4 RISC as a microcontroller [74]. It has AT86RF215 [48] as a fully integrated radio transceiver compatible for IEEE Std 802.15.4g™-2012 [30]. For this research, experiments were done in the sub-GHz band.

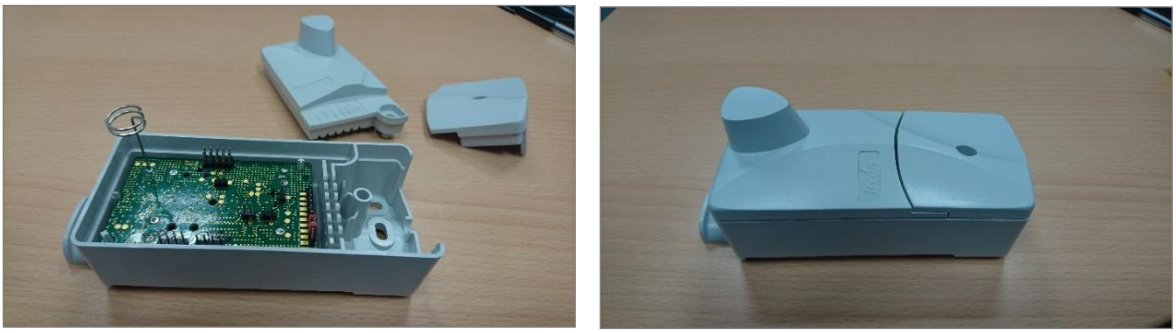

Figure 3-16: Itron wireless IoT Module

3.7.1 Setup

One sink and seven client nodes were deployed in various locations of the Itron office floor as shown in Figure 3-17. The experiments were performed with the parameters listed in Table 3-7.

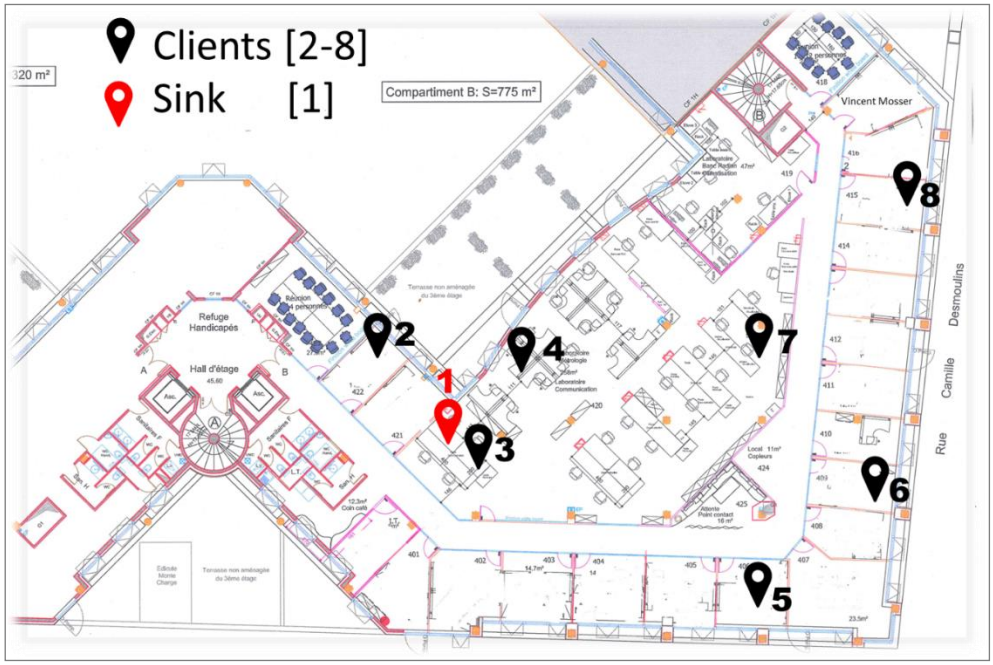

Figure 3-17: Experimentation floor deployment plan I

3.7.2 Parameters

Table 3-6: Algorithm parmeters for experimentation

Parameters	Value
Sensitivity Margin (M)	10 dB
W^{MAX}	8
β and α	0.40 and 0.85 respectively
ETX_FACTOR and ETX^{TH}	128 and 64 respectively

Table 3-7: REACT-P Experimentation Parameters

Parameters	Value
Device Model	Itron Module with ATRF215 [75]
MAC Re-Transmissions	3 attempts at link layer
CCA Attempts	3 attempts
Network	Star Topology with 1 sink
Number of Nodes	7 clients and 1 sink
Position	Immobile positions in the floor (Figure 3-17.b)
TX Power	-13 to 0 dBm with step-size 1 dB

Attenuation at Receiver(sink)	22dB
TX Bit Rate	12.50 Kbps
Modulation	DSSS MR-OQPSK @100Kchips/second
Total Received	9000 packets at sink per experiment
Average Experiment duration	21 hours 43 mins and 13 seconds
Data Size and Traffic Rate	180B (MPDU 142B) and 1 packet/min
Algorithms	CPCR Vs REACT-P*
Frequency	920.4MHz, single channel
MAC and PHY Protocol	802.15.4 e/g [29][30]
Battery Rating	3V, 3AH x 2

*Here CPCR is the maximum usable constant power (power level 13, 0dBm) at constant rate of 12.50Kbps @100Kchips/second and REACT-P is the proposed transmission power control algorithm at constant rate of 12.50Kbps @100Kchips/sec.

ATRF215 allows to program the output power level during the run-time. A register-Transmission Power Amplifier Control is used to change the power level whose format is shown in the Figure 3-18.

7	6	5	4	3	2	1	0
-	PACUR		TXPWR				

Figure 3-18: Transmission Power Amplifier Control Register for ATRF215 Tranceiver

where, PACUR is a 2 bit-field sub-register that configures the power amplifier DC current as shown in Table 3-8. In this research this sub-register value is kept constant to 0x0.

TXPWR is a 5-bit sub-register that controls the transmit output power as shown in Table 3-8 ; maximum being 31 and minimum being 0, giving a total of 32 configurable power levels. In this research, out of 32 power levels available for the transceiver, only 14 power levels (0 to 13) were used.

Table 3-8: Different settings for controlling the output power in ATRF215 transceiver

Sub-register	Value	Description
PACUR	0x0	Power amplifier current reduction by 22mA
	0x1	Power amplifier current reduction by 18mA

	0x2	Power amplifier current reduction by 11mA.
	0x3	No Power amplifier current reduction.
TXPWR	0x00	Minimum output power
	...	About 1dB steps
	0x1F	Maximum output power

An experiment was performed on the Itron module to measure the amount of current consumed at different power levels (PACUR 0x0, TXPWR 0 to 13) by the use of multimeter. The circuit diagram is shown in Figure 3-19. Figure 3-20 shows the average value over five measurements of the current consumed by a node at different power levels. These current consumption values are later used to calculate the energy consumption in section 3.4.3.

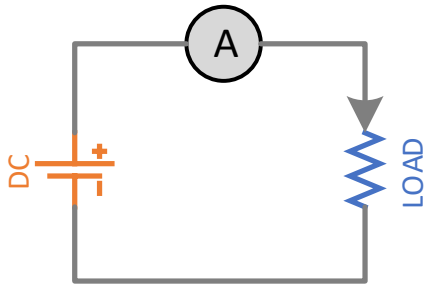

Figure 3-19: Circuit connection to measure the current

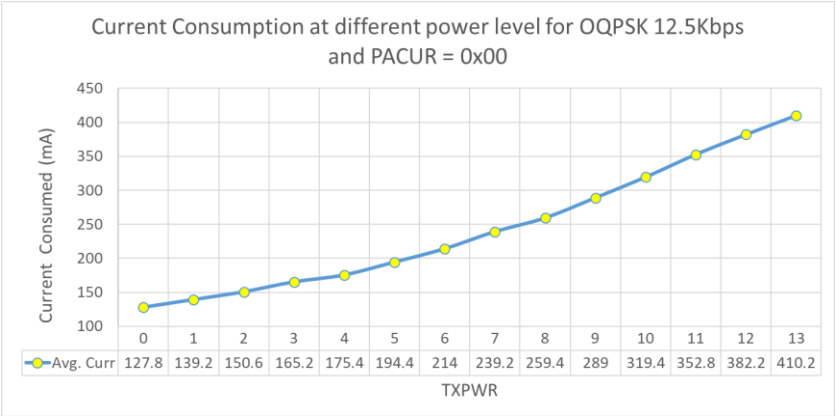

Figure 3-20: Current consumption at different power levels for ATRF215

3.7.3 Results and Discussions

Different experiments were performed with different numbers of clients competing to transmit on the same channel at the same time, a situation that generates collisions in the network. This is shown in Table 3-9. In this experiment, the REACT-P (at constant rate of

12.50Kbps) is compared with constant power level (0dBm) and rate (12.50Kbps). Several graphs were plotted. They are shown and explained next.

Table 3-9: Client IDs involved with different setup for REACT-P Test

Competing clients	Clients involved to compete for channel
0/7	0; All clients transmit in different timeslot.
2/7	Client 2 and 3
5/7	Clients 2, 3, 4, 5, 6
7/7	All clients compete for the channel at the same time.

The four pictures with the cases, described in Table 3-9, are shown in Figure 3-21. These pictures have illustrated that for different cases, the client nodes have transmitted in same or different time slots. For example, in case 2/7, out of 7 clients that were transmitting packets to the sink, 2 of them i.e. clients 2 and 3 transmitted at the same time slot and thus they compete for the channel using CSMA/CA. The others transmitted at different time slots. In other words, there are 2 concurrent transmissions every minute. However, in most of the cases, even when transmitted at the same time slot, the contending nodes may succeed because of re-transmissions.

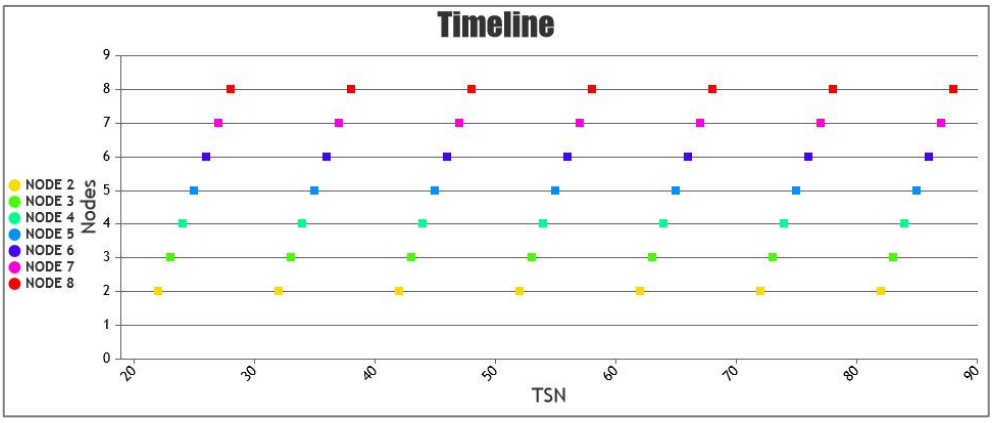

(Case 0/7)

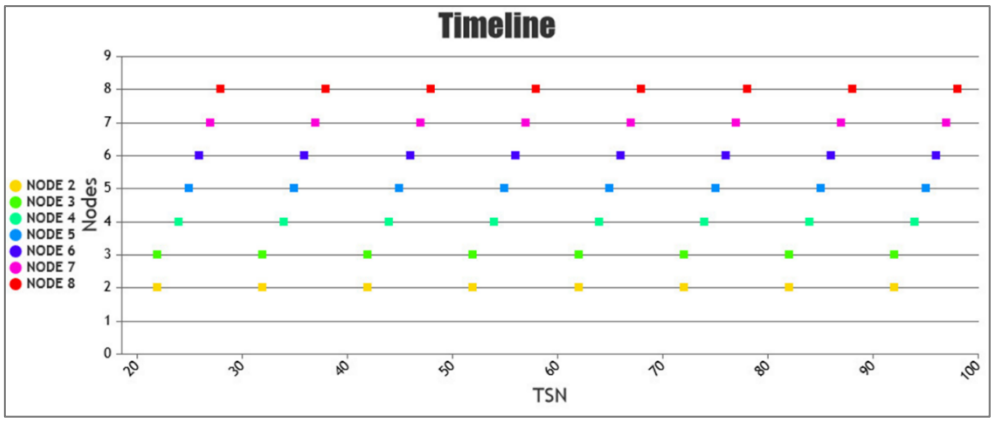

Case 2/7

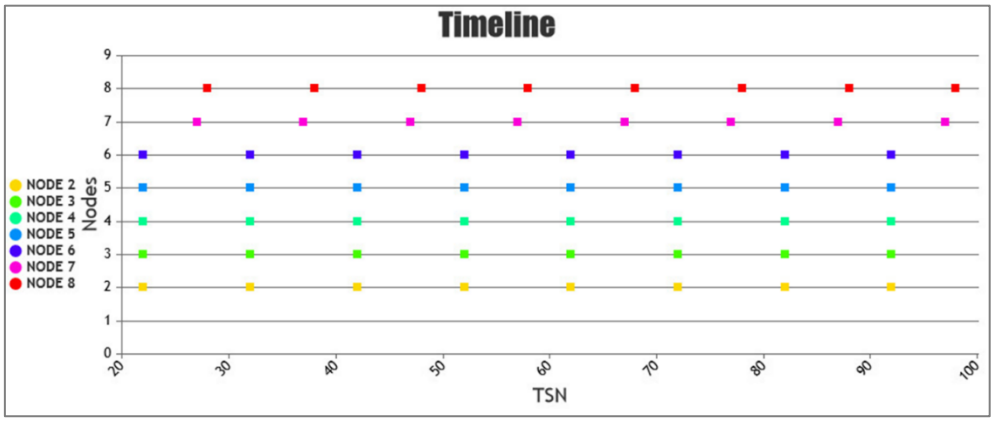

Case 5/7

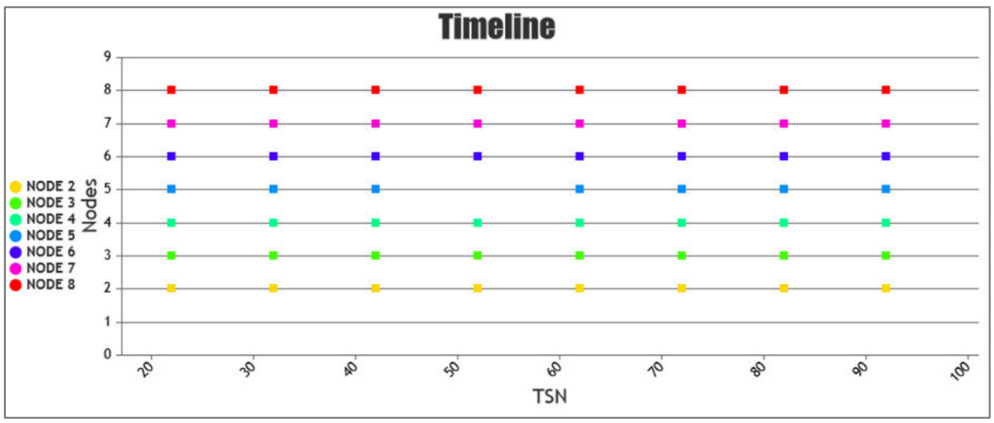

Case 7/7

Figure 3-21: Timeline showing transmitting in different time slots (TSN)

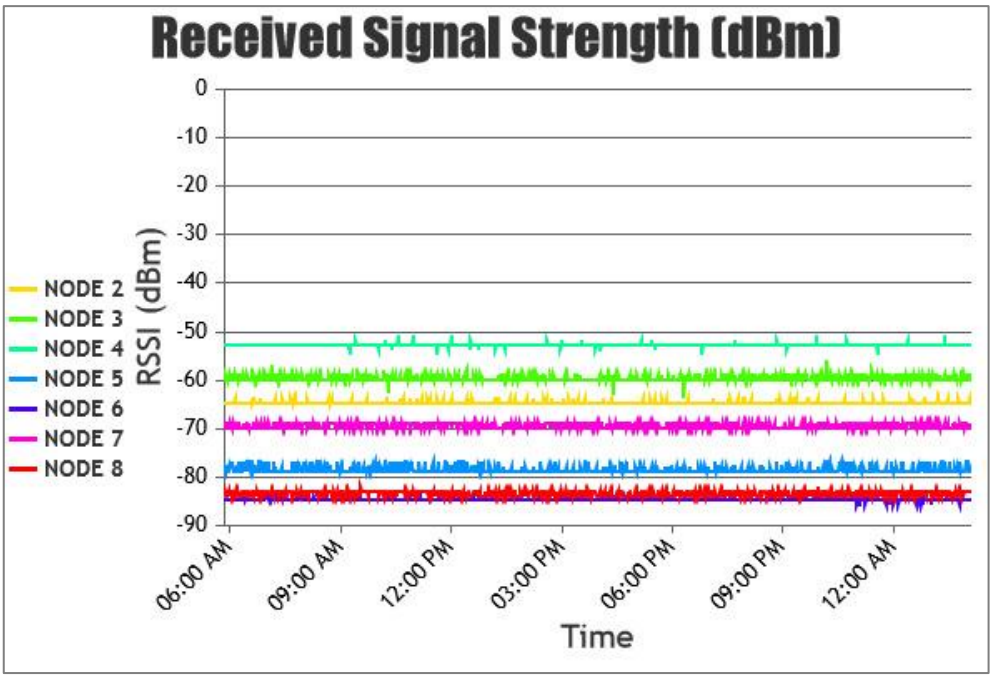

(a) On a holiday

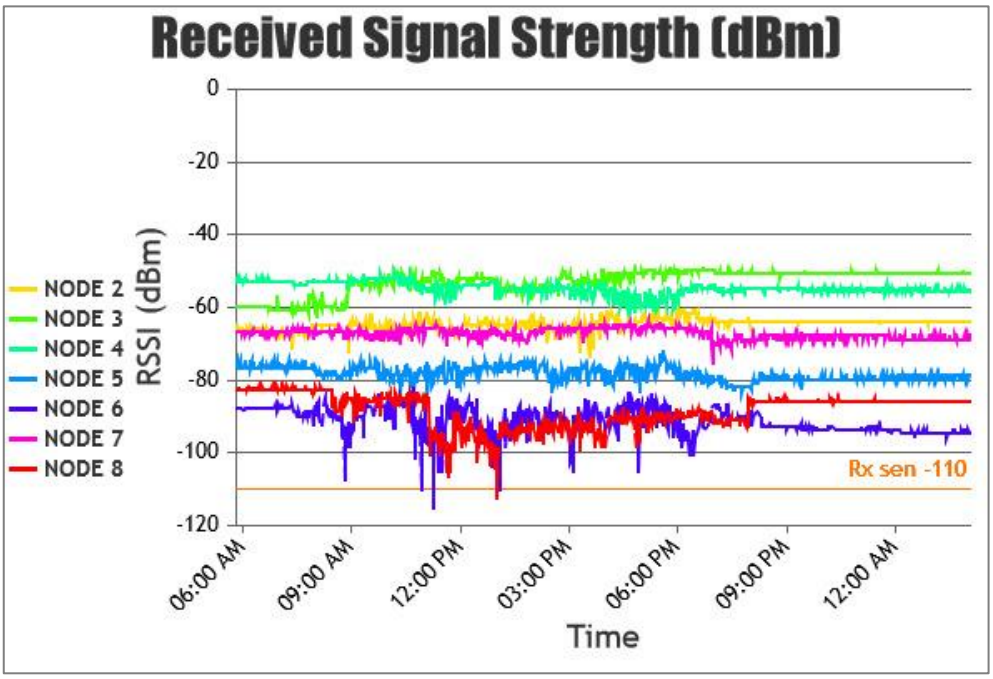

(b) On a Working day

Figure 3-22: Received Signal Strength (RSSI) of all clients over time

Figure 3-22 portrays the RSSI of the seven client nodes over 18 hours for 0/7 case when a constant power and rate were used during a holiday (Figure 3-22.a) and a working day (Figure 3-22.b). The graphs clearly showed huge variances in the RSSI during a working

day, especially throughout the working hours (8 a.m. to 8 p.m.). For example, the difference between the lowest and the highest RSSI for client 8 was found to be 34 dB. On the other hand, the variance was low during a holiday. This shows that the received signal strength is greatly affected by noise, the motion of people and interference from other sources. This result also justifies the research conducted in [43], [45], [52], [76] indicating the RSSI/LQI are not robust link quality indicators.

Figure 3-23 shows the variation of ETX and EWMA_ETX with time for all the nodes for a case 2/7. It can be perceived that, the EWMA filter helps to stabilize the fast changes in the link quality. With the ETX_THRESHOLD of 1.5, there were 128 cross-overs with ETX whereas there were around 17 cross-overs with EWMA_ETX. So, the algorithm prevents from abrupt changes in the power or rate level.

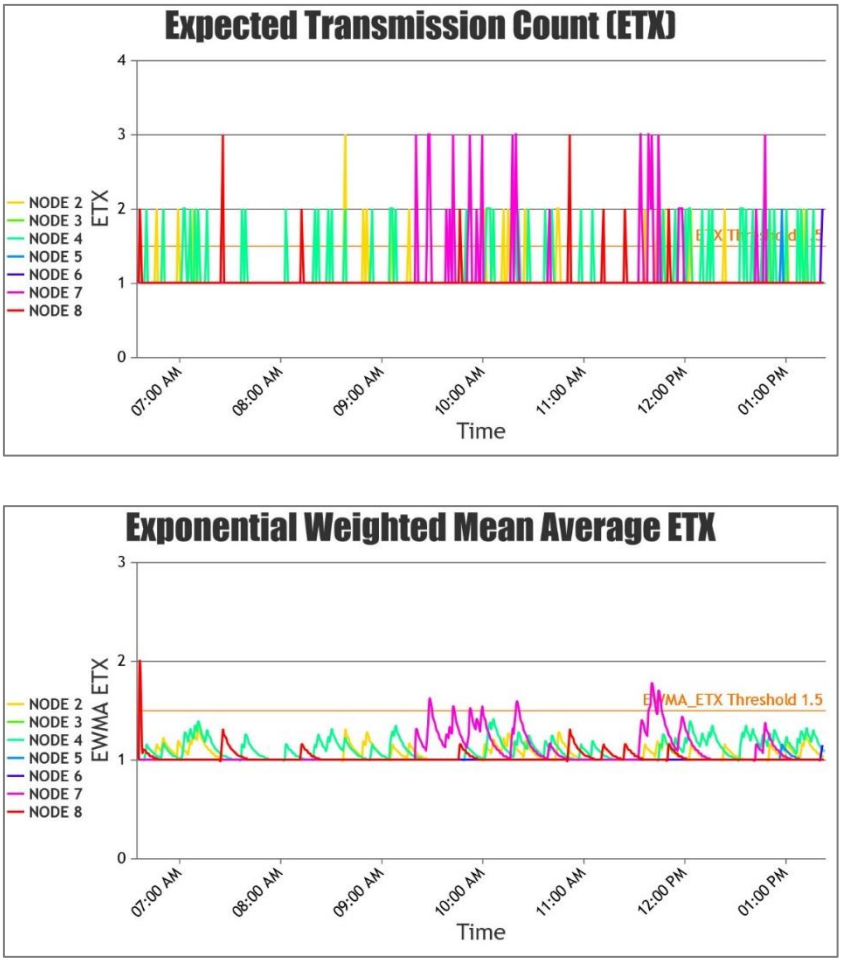

Figure 3-23: ETX and EWMA_ETX for a case of 2/7 at CPCR

The further results obtained are classified into Network Behavior and Node Behavior.

3.7.3.1 Network Behavior

Figure 3-24 shows a plot of the average transmission energy consumption per unique frame received at CPCR against the proposed REACT-P algorithm. It also presents the percentage improvement while using REACT-P in the total transmission energy consumption with respect to the different number of clients competing at the same time on the x-axis. The experimental results reveal that, with REACT-P, up to 68% improvement is achievable as compared to using CPCR, and with insignificant compromise in PDR and frame losses (Figure 3-25). Here in Figure 3-25, PDR (Packet Delivery Ratio) is the ratio of the unique number of frames received to the total number of transmission attempts at the link layer. Figure 3-24 also indicates that the energy consumption improvement decreases as the number of competing nodes for the same channel increases. This means that, with a proper channel access technique, REACT-P can reduce the energy consumption to more than half, thereby doubling the lifetime of the nodes.

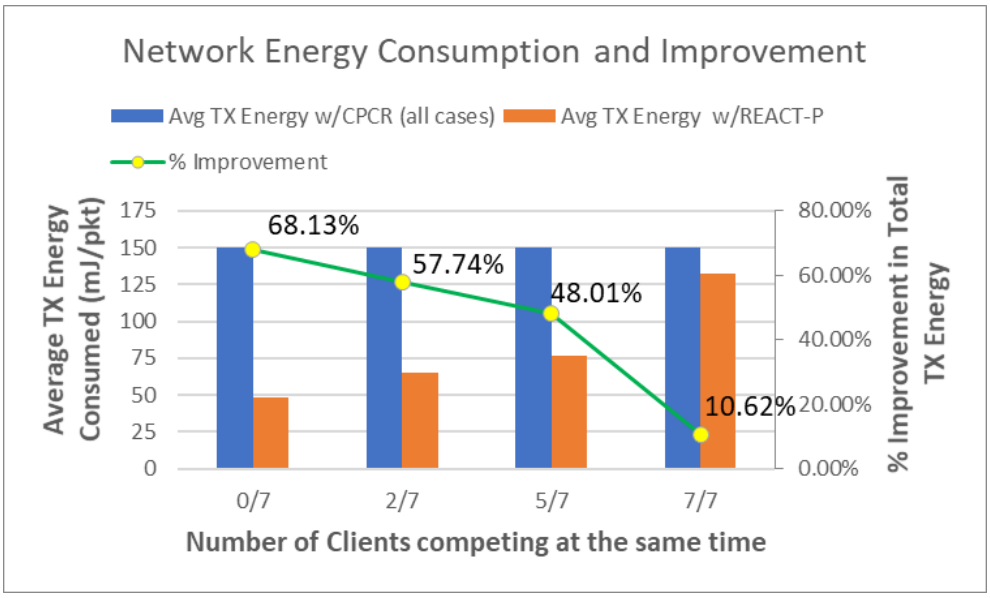

Figure 3-24: Average energy consumed per frame and % Improvement in Total TX Energy

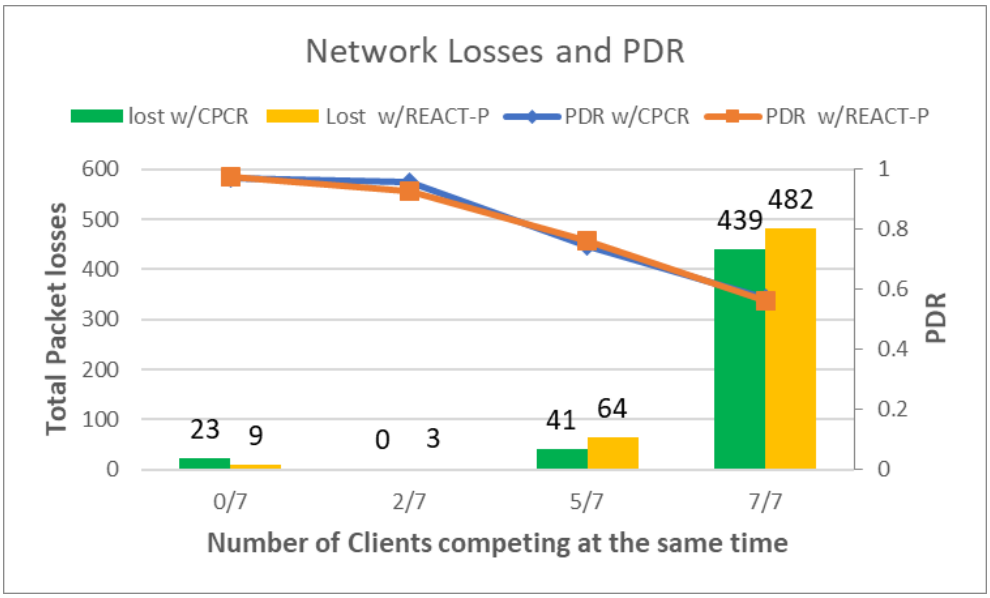

Figure 3-25: Total frame losses and PDR in a network

3.7.3.2 Node Behavior

Figure 3-26 shows that in all cases, all clients consume less energy per transmission on average with REACT-P than when using CPCR. The average energy per frame is constant (=150mJ/pkt for the case of 12.50Kbps and power level 13) when constant power is used for all cases. The following shows the details of computing the transmission energy for a packet.

$rate\ (r) = RM1 = 12.50kbps$
$power(p) = MAX = 13$
$current(I) = \ 410.2mA\ from$ Figure 3-20
$transmission\ time(TT) = 121.9msec\ for\ 142\ Bytes\ PPDU\ from$ Table 4-3
$Energy\ (E) = Voltage * I * TT\ using\ (12)$
$E = 3 * 410.2mA * 121.9msec\ \cong 150\ mJoules$

Figure 3-27 shows the total TX energy consumed by the clients for different cases. For example, in 5/7 case, where 5 out of 7 clients (2, 3, 4, 5 and 6) compete at the same time. The results show that for each of the nodes, the total TX energy consumption is lower when REACT-P is used than when using CPCR. The energy consumption of clients 7 and 8 are relatively lower than the others because there are fewer failures/retries for those nodes as they do not take part in the competition for the channel at the same time for 5/7 case.

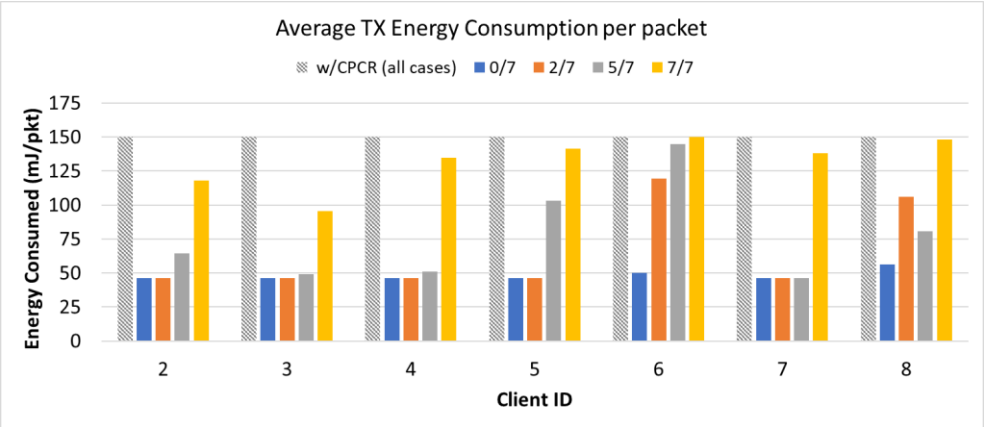

Figure 3-26: Average TX Energy consumed per client

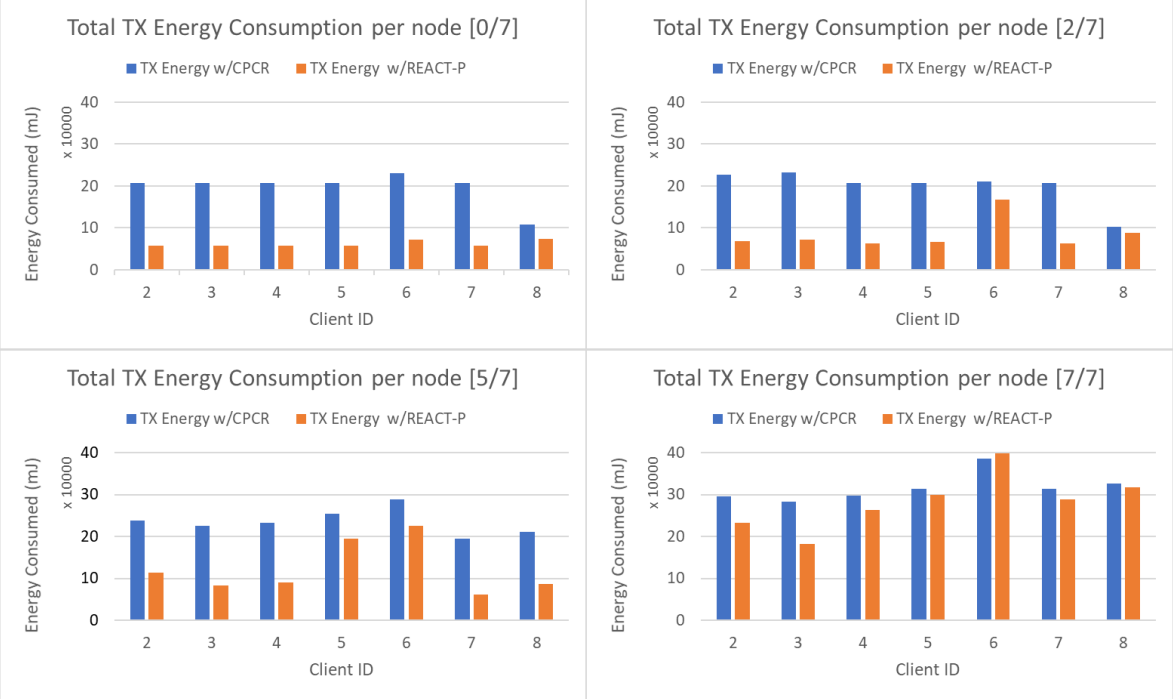

Figure 3-27: Total TX Energy consumption of the clients

Figure 3-28 shows a plot of how the REACT-P adapts the transmission power level in Client 8 with respect to the change in the EWMA ETX for 0/7 case. The node changes the power level only when the EWMA_ETX crosses the threshold preventing excessive churn in the power level.

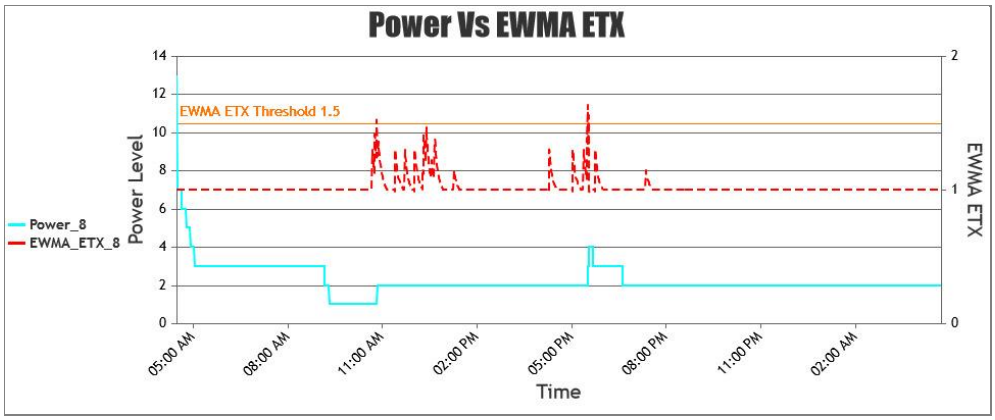

Figure 3-28: Client 8 adapting power over time with EWMA ETX with REACT-P

3.8 Conclusion

In this chapter, the impacts of the transmission power on various aspects have been discussed. The key concept and design for any transmission power control technique have been portrayed in this chapter. A thorough study of the existing TPCs in the literature was needed to understand their flaws and positive aspects, which was provided in this chapter. Then this chapter has introduced the proposed algorithm, which has novel approaches in performing the link quality estimation and controlling mechanism of the transmission power. Various building blocks of the algorithm and their functionalities were also presented. It has described the working principle of the REACT-P together with a block diagram and state transition diagram. It can be realized that the implementation complexity is low. This chapter has also provided some valid assumption made while performing the simulation and experimentation and performance metrics used to evaluate the algorithm. The performance of the proposed algorithm was assessed using simulation with the COOJA and experimentation with the Itron IoT modules. It was compared with when using maximum power level at constant rate. The results have shown that more than 50% improvement can be attained in terms of TX energy consumption with a low compromise in the packet delivery ratio. This chapter has also shown the comparison of the proposed algorithm with one of the existing algorithms in a similar simulated environment. The comparison results have shown that there was an improvement of around 23% when REACT-P was used.

4. Transmission Rate Control

4.1 Introduction 85
4.2 Literature Review 88
4.3 Calculation of Transmission Time 90
4.4 Experimentation 90
4.5 Conclusion 93

4.1 Introduction

Today's hardware provides the flexibility to dynamically change the rate level for low-powered and lossy network. For instance, MR-O-QPSK PHY specification supports multiple PSDU bit-rates for different frequency band in the standard IEEE 802.15.4g [30]. The following is a typical IEEE 802.15.4g PPDU format for MR-OQPSK.

<table>
<tr><td colspan="2"></td><td colspan="2">Octets</td></tr>
<tr><td colspan="2"></td><td>3</td><td>Variable</td></tr>
<tr><td>Preamble</td><td>SFD</td><td></td><td>PSDU</td></tr>
<tr><td colspan="2">SHR</td><td>PHR</td><td>PHY payload</td></tr>
</table>

Figure 4-1 : Format of the MR-O-QPSK PHY PPDU

<table>
<tr><td>0</td><td>1</td><td>2</td><td>3</td><td>4</td><td>5 - 15</td><td>16 - 23</td></tr>
<tr><td>Spreading Mode</td><td colspan="2">Rate Mode</td><td>Reserved</td><td></td><td>Frame Length</td><td>HCS</td></tr>
</table>

Figure 4-2: Format of the PHR for MR-O-QPSK

Rate Mode	Data Bit Rate(kbps)	PSDU/MPDU (Bytes)	Frame length(msec)
RM0	6.25	250	362.90
RM1	12.50	250	191.70
RM2	25	250	105.90
RM3	50	250	63.10

Figure 4-3: Rate Mode mapping for MR-OQPSK @100Kchips/sec

The preamble and Start of Frame Delimiter (SFD) form the Synchronization Header (SHR). MR-OQPSK supports up to four different PSDU rate modes for each frequency bands. And the data rate selection was determined by the 2-bit Rate Mode field as shown in Figure 4-2.

It is important to understand that even though the bit rate is doubled or halved among the adjacent rate levels, the transmission time is not exactly halved or doubled respectively. This is due to the fact that a portion of a frame namely PHY header and SHR header are modulated at the same basic rate. A fixed spreading parameter was used for the PHR and SHR depending on the frequency, and thus require same duration. The PHY header consists of a field that tells the receiver at which rate the following bits are modulated. The receiver then

tunes to this rate and can demodulate/decode the frame. For a frequency band of 920MHz, 100Kchips/sec, it resulted in the following values of PHR and SHR duration.

$$PHR\_dur = 4.80\ msec\ and\ SHR\_dur = 15.36\ msec \tag{13}$$

The chip rate for each of the RF transceiver is always the same. The only change is symbol to chip ratio. This makes the changes in the final bit rate. This makes it possible for a node to change the bit rate allowing dynamic rate adaptation. For an Atmel Transceiver ATRF215, four rate levels are achievable at 100KChips/sec. as shown in the Figure 4-3.

The following is a reference modulation diagram for MR-OQPSK.

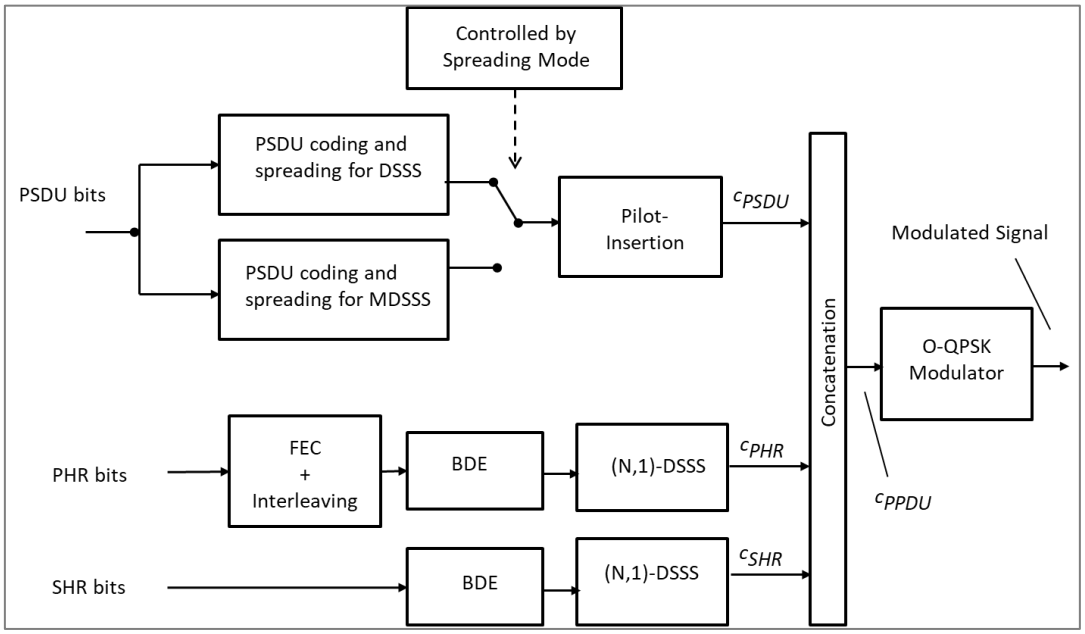

Figure 4-4: Reference Modulator diagram for MR-OQPSK [30]

4.1.1 Impacts of Transmission Bit Rate

Transmission bit-rate has a huge impact on the various factors. Most important being the throughput, energy consumption, latency, channel occupancy and the radio coverage.

- Energy Consumption: Bit-rate is directly related to the energy consumption as the transmit time will change. Additionally, rate adaptation has impact on the receiver side as well as the reception time will also change accordingly. Hence, for a frame transmission, transmitting at a higher rate would consume less energy than transmitting at lower rate.

- Radio Coverage: Rate is inversely related to the radio footprint. For example, with higher data rate, the BER increases as a result, they have lower range. When considering the transmission bitrate, it is also necessary to keep track of the receiver sensitivity. It is because, there exists a tradeoff between the data-rate and the BER: The higher the data-rate, the higher the BER. To maintain same BER, higher SNR is required. Figure 4-5 from [77] shows this tradeoff as well. In other words, the receiver sensitivity decreases with increase in the bit-rate. An example of an ATRF215 transceiver is shown in Table 4-1.

Table 4-1: Different receiver sensitivities at different rate modes for MR-OQPSK

Rate Mode	Data rate	Sensitivity
0	6.25 kbps	-123 dBm
1	12.50 kbps	-121 dBm
2	25 kbps	-119 dBm
3	50 kbps	-117 dBm

- Fragmentation: Depending on the size of the packet used and the rate level, the packet may undergo fragmentation. Adapting the packet size to the link quality is another possibility for improving the performance. This involves partitioning the packets to smaller packets called fragmentation. As sending smaller frames improves the probability of successful transmission however, it has been shown in [78] that fragmentation yields only marginal improvement and is always better to switch the bit rate.
- Throughput or Goodput: As the transmission and reception time changes with the change in the rate level, the coding/decoding rate changes hence a node will be able to transmit and receive a data faster or slower which will impact the throughput of the network together with the latency.
- Channel occupancy: As the transmission time changes, the air time changes as well. For example, a frame may occupy the channel for a longer duration if transmitted at lower rate. This can further impact the interference and collision on the neighboring nodes.

The problem with the fixed rate and fixed power is that they are not taking advantage of higher data rate when the channel is good. Comparing to the power control, transmission bit-

rate control has higher potential to reduce the energy consumption and channel allocation time [79].

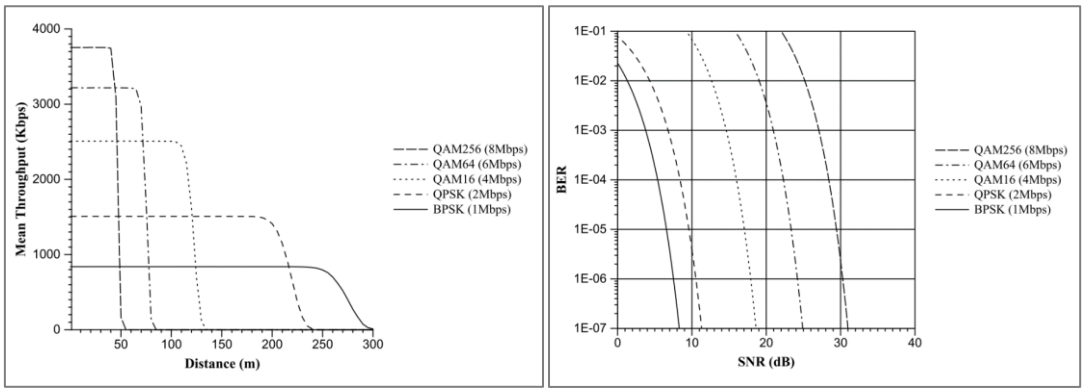

Figure 4-5: Trade off between data rate, distance, SNR, and range [77]

4.2 Literature Review

Many existing rate control algorithms proposed have been simulated and experimented for IEEE 802.11 WLAN network but few for LLNs or LPWANs. While designed to improve the throughput and the delay, most of them does not takes the energy efficiency into consideration. The following are some of the existing algorithms.

Table 4-2: Existing transmission rate control algorithms

Scheme	Metric	Loss diagnosis	Based on	RTS/CTS	Open/closed Loop
ARF [80]	Frame loss	No	Sender	No	Open
AARF [80]	Frame loss	No	Sender	No	Open
Onoe	Frame loss	No	Sender	No	Open
SampleRate	Frame loss	No	Sender	No	Open
RBAR [77]	SNR	No	Receiver	Yes	Closed
CARA [81]	Loss ratio	Yes	Sender	Yes	-
RRAA [82]	Loss ratio	Yes	Sender	Yes	-
ERA [83]	Loss ratio	Yes	Sender	No	Open
Smart Sender [53]	Goodput + RSSI	No	Sender	No	Open

[80], [53], [77], [81]–[84] are some of the researches on the rate control techniques which are designed for IEEE 802.11. [80] discusses about ARF (Auto Rate Fallback) and AARF

(Adaptive ARF) which are the primitive algorithms to perform rate control. AARF is more suitable than ARF for slow channel quality variation but for quick channel quality variation, both are not suitable enough. [81] shows that with the increase in the contending stations, the performance of ARF decreases. [77], [81], [82] utilize RTS/CTS whereas [83] utilizes fragmentation to perform the loss diagnosis. RTS/CTS mechanism helps to combat the well-known hidden terminal problem. A sender sends a short RTS (Request-To-Send) before sending the actual data frame. The receiver upon reception, replies with a CTS (Clear-To-Send) frame. The sender then continues to transmit the actual data. Other unintended nodes upon receiving CTS will defer their transmission attempts until the end of the current transmission. Although RTS/CTS sounds promising, they are simply overhead and may lead to the waste of energy consumption [85], [86]. This energy waste further increases with the increase in the number of nodes. Also, RTS/CTS mechanism cannot guarantee the complete elimination of all the hidden nodes [87]. [77], [84] are based on priori channel model, so they need some parameters like number of contending stations, collision probability, etc. in advance which is not quite practical in real life. [81], [82], [84] further considers a non-fading channel where all the losses are due to collision. [88] provides a mechanism to select the optimal combination of the PHY mode and the fragment size, depending on the wireless channel condition. It assumes that no interfering stations nearby, only one node is transmitting, and its queue is never empty, i.e. there are no collisions on the wireless medium, there is no retry limit for each frame. In the real environment, losses are due to both fading and collision. The ERA approach using fragmentation technique [83] clearly outperforms the other algorithms. However, [78] shows that it is more appropriate to switch to a lower rate than to fragment a packet. Fragmentation also adds extra overhead and may not be suitable for energy constrained nodes.

Papers [81]–[83] suggest that loss diagnosis is important while performing rate adaptation. Loss diagnosis helps not only to protect from the frame losses due to collisions but also avoid the link quality estimation being poisoned by the collision losses [82]. It is often a wrong idea to make changes in the rate level or power level during a collision. Collisions happen due to timing issues rather than the radio signal itself. Hence a proper diagnosis of the loss is necessary to distinguish whether the frame loss is due to the fading or collision. Once determined, then the algorithm should act accordingly. However, performing a loss diagnosis is difficult. Some algorithms use RTS/CTS, some use fragmentation to perform the diagnosis which are overheads and may not be suitable for constrained devices. A

successful probe packet or RTS/CTS exchange may be misleading and trigger incorrect rate changes [82]. The diagnosis methods used cannot guarantee the 100% diagnosis of the losses and hence needs further research. A low-energy cost diagnosis mechanism is required which is out of the scope of this research work and left for future work.

4.3 Calculation of Transmission Time

As discussed before in section 4.1, for a particular frequency range and modulation, SHR and PHR duration are fixed whereas PSDU duration is variable depending on the rate mode and frame size. Additionally, some padding bits and pilot overheads are added. This is the reason why the transmission time is not exactly halved when doubling the bit-rate or vice-versa. PHR duration, SHR duration and PPDU duration are calculated as described in the IEEE 802.15.4g standard [30]. Basically, for a particular rate *r* and PSDU size *S*, total frame transmission duration is given by

$$PPDU\ Duration\ (r, S) = SHR\_overhead + PHR\_overhead + tail\_and\_pad\_bits\_overhead + pilot\_overhead\_\_DSSS + LR\_mod\_overhead + S / r \quad (14)$$

Frame duration for 142B PSDU length for different rate modes is shown in Table 4-3.

This way of calculating the transmission time is used in the proposed algorithm to compute the amount of time spent in the transmission state which is later used to compute the transmission energy consumption using (12).

4.4 Experimentation

4.4.1 Transmission Time

An experiment was performed in order to check the correctness of the calculated transmission time with the actual transmission time for a frame at different rate levels. MR-OQPSK at 100Kchips/sec modulation was used. A node was programmed to transmit a data frame of size 142B MPDU every 30 seconds changing the rate in a sequential cyclic fashion such as RM0, RM1, RM2, RM3, RM0, RM1, … The output of the radio was fed to a signal analyzer (EXA N9010A Signal Analyzer) which was tuned to the operating frequency of the node, i.e. 920.4MHz to capture the frames (Figure 4-7). Table 4-3 shows the calculated frame duration using the formula *(14)* and the experimental value obtained from the Signal Analyzer for frame size of 142B MPDU for MR-OQPSK at 100Kchips per second at 920.4MHz. The differences between experimental and the calculated values were minimal.

Table 4-3: Calculated and Experimental frame duration at different rates

		PPDU duration	
Rate Mode	**Data rate**	**Calculated**	**Experimental**
0	6.25 Kbps	223.9 msec	223.916 msec
1	12.50 Kbps	122.0 msec	122.073 msec
2	25 Kbps	71.3 msec	71.314 msec
3	50 Kbps	45.7 msec	45.774 msec

The following snaps were obtained from the signal analyzer.

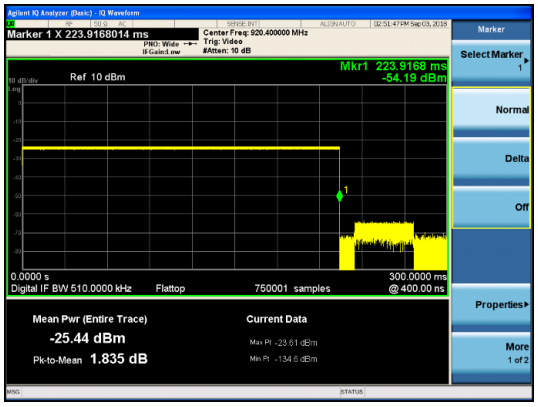

(a) 6.25Kbps

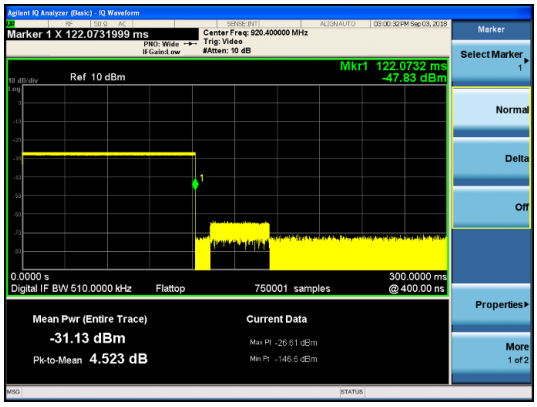

(b) 12.50Kbps

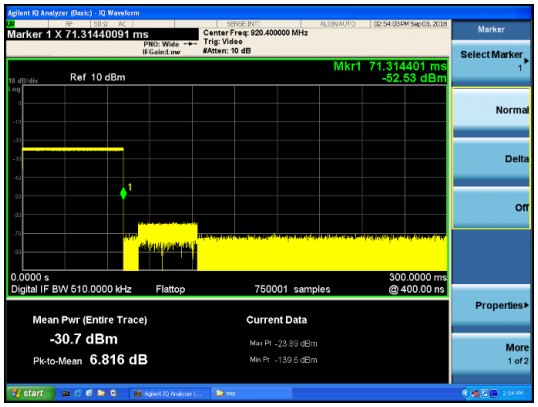

(c) 25Kbps

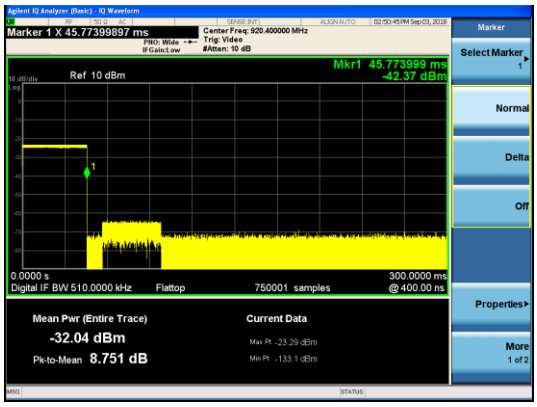

(d) 50Kbps

Figure 4-6: Experimental PPDU frame duration for 142B MPDU frame at different rate modes

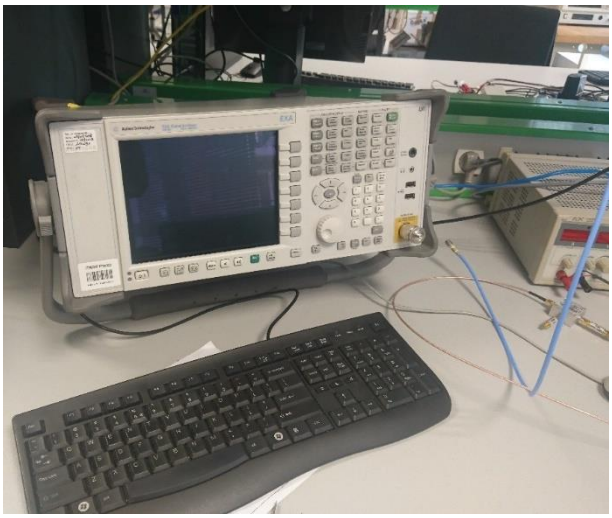

Figure 4-7: Agilent EXA Signal Analyzer in lab

4.4.2 Experimentation at different TX Bit-Rates

Two experiments were performed to see the energy consumption when using different rate levels for 2/7 and 4/7 case. Figure 4-8 shows the average network consumption and total CCA busy experienced by all the nodes in a network for the case of 2/7 and 4/7. It shows the results when CPCR is used and when REACT-P is used for different bit-rates. The results portray that, with the increase in the rate, the energy consumption decreases along with decrease in the CCA busy counts. It means changing the rate level not only decreases the energy consumption but also the interference that it imposes on the other nodes. As the rate increases, channel is less busy because the transmission time is lower. The graphs also depict the percentage improvement in the total energy consumption when the proposed algorithm is used instead of the maximum power. Now that it has been observed that with the increase in bit-rate, both transmission energy consumption and interferences can be reduced, so it is necessary that the rate level changes dynamically with the spatio temporal factors. The next chapter 5 explains how the REACT-P algorithms is extended to take the bit-rate into account for better energy efficiency.

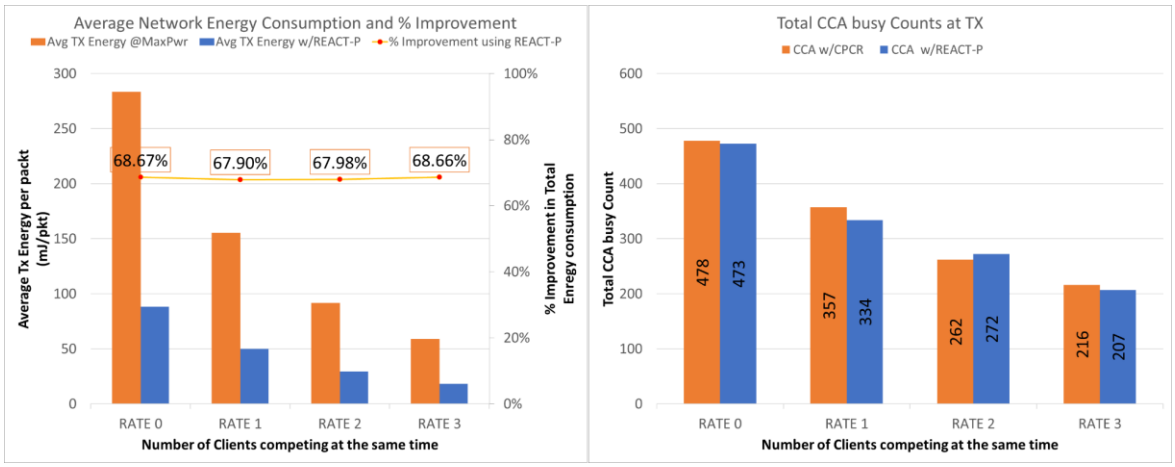

(a)

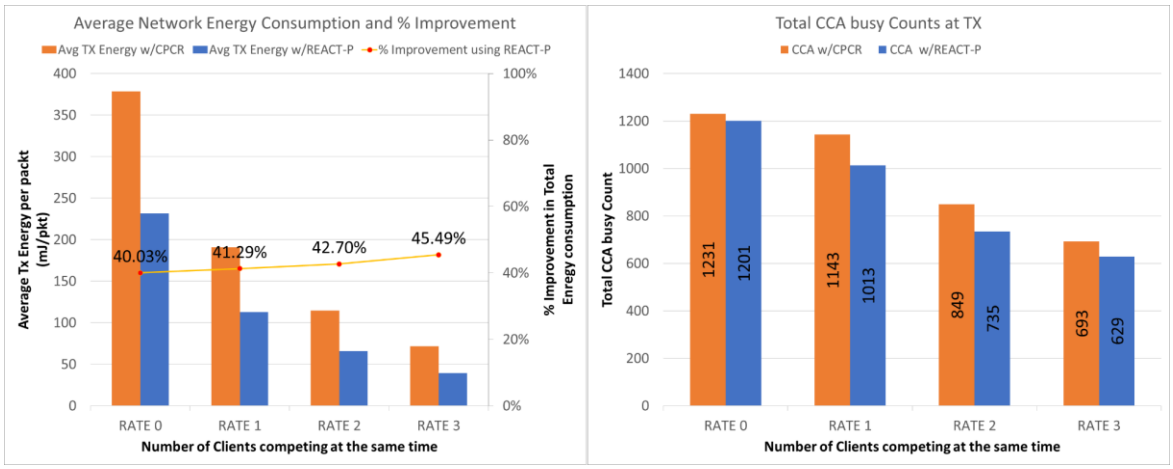

(b)

Figure 4-8: Average network energy consumption and Total CCA busy counts at different bit-rates for the case of 2/7(a) and 4/7(b)

4.5 Conclusion

In this chapter, the impacts of the different transmission bit-rate were studied. This chapter also presented some related works on controlling the rate dynamically. The method to calculate the transmission time for different frames was also shown in this chapter, which is used to compute the energy consumption of the nodes. Experiments were performed to see the performance regarding the energy consumption and interference were performed in this chapter. The results obtained showed that higher rates provide lower transmission energy and lower interference on the surrounding nodes.

5. Transmission Power and Rate Control

Contents

5.1 Introduction 96
5.2 Literature Review 97
5.3 Proposed Algorithm: REACT or REACT-PR 98
5.4 Performance Metrics 100
5.5 Implementation 102
5.6 Experimentation 106
5.7 Conclusion 119

5.1 Introduction

As the transmission bit-rate and the power are the two dominant radio parameters that highly impact the energy consumption of a node and as we have seen from Chapter 4, that rate has much higher impact on the energy consumption, therefore it became absolutely necessary to dynamically control the bit-rate of the devices along with the power to achieve the desired goal. It would be more efficient to control both of them to provide higher energy efficiency without significant compromise on other performance aspects. Rate and power are related by a basic physics equation as

$$Energy\ consumed = Power\ used * time\ taken(r)$$

where the time taken depends on the transmission bit-rate, r. Energy consumption is high when both the Power level used, and the amount of time spent at that power level is high and vice-versa. So, in simple words, to reduce the energy consumption, the power level and the transmission time must be reduced. However, these settings should not have a significant compromise on the other performance aspects like latency, PDR, throughput. For this scope of thesis, the parameter latency is relaxed.

In this research's domain of LLNs and LPWANs, there exists a tradeoff between the power, speed or bit-rate and distance. This trade-off can be portrayed by Figure 5-1.

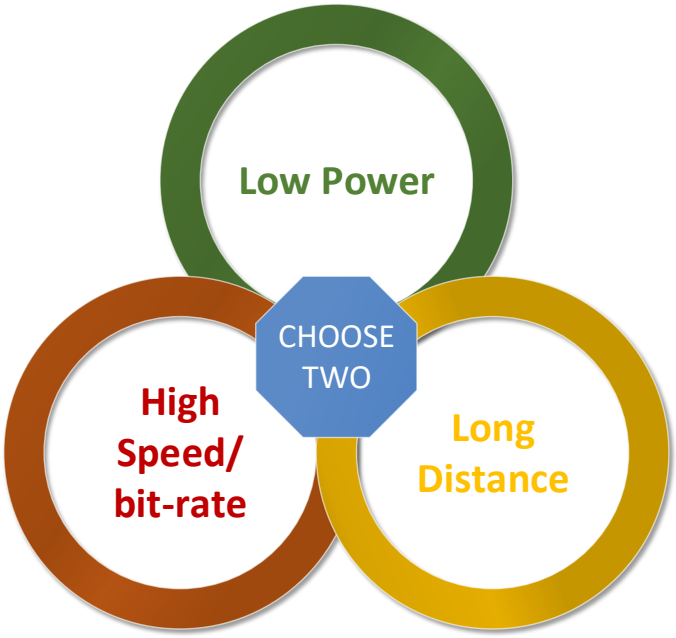

Figure 5-1: Tradeoffs in LLNs or LPWANs

With reference to the Figure 5-1, it is possible to achieve two of the parameters, but the third parameter needs to be compromised. For example, it is possible to have low power and long-distance communication, but this may happen only at a lower bit-rate. Another example, it is possible to have long distance coverage and high-speed rate, but higher power is required. So, the goal is to find a proper balance amongst these three parameters. By choosing a proper power level and proper rate, a satisfactory reliability may be obtained to cover a certain distance.

With this regard, first, this chapter shows the study on some existing algorithms that perform both rate and power control. Then, this chapter explains how the REACT-P algorithm that controls only power level is extended/adapted to take the bit-rate into account as well. Finally, this chapter presents the results of experiments performed to see the efficiency of the final proposed algorithm.

5.2 Literature Review

There are few researches that perform both dynamic transmission power and rate control. All of them are designed for IEEE 802.11 WLAN standard. This is the first research to work on the 802.15.4 compliant modules.

Table 5-1: Existing transmission power and rate control algorithms

Algorithm	Link quality metric	Evaluation	RTS/CTS
PRACT [89]	SINR	Simulation	Yes
TA-ARA [90]	Interference Margin	Simulation	Yes
Link adaptation strategy on [91]	History of consecutive ACKs received and average RSS	Experiment	No
MiSer [87]	Rate-power table	Simulation	Yes

[89], [90], [91], [87] are some researches that perform both power and rate control. They are designed for 802.11 WLAN only. [89], [90], [87] use RTS/CTS exchanges to control the power/rate which are overheads and not suitable for LLNs with constrained devices. Also, they have not evaluated their performance on the real experiment. Some have made unrealistic assumptions for example, [87] requires priori knowledge of number of contending stations, channel model, path loss and probability of collision and ignores error due to background noise on RTS, CTS, ACK, and [89] assumes the links are symmetric.

[78] adapts either transmission rate or power depending on the link condition. Except [89], others focus on the throughput and do not address the energy efficiency in their studies, which is the prime focus of this thesis. Hence, the proposed algorithm in Chapter 3 is further extended to support the rate adaptation as well such that it can be easily implemented to the real IoT hardware and has low overhead wastage.

5.3 Proposed Algorithm: REACT or REACT-PR

The Responsive Energy-efficient Adaptive Control of Transmission Power and Rate (REACT-PR or simply REACT) is an extension to the algorithm developed for REACT-P as explained in Chapter 3. The way the algorithm works is derived from REACT-P. Hence in this section, only the changes are highlighted.

As the main goal of this research was to optimize the energy consumption, so in this section we try to reduce the energy consumption rather than just rate or power level alone. An array of energy levels is created with each element as a unique combination of the power level and rate. This array is sorted in the ascending order such that whenever the energy level is decreased, energy consumption is actually reduced and vice-versa.

In contrast to REACT-P, in REACT, instead of changing the power levels, energy levels are changed. The amount of energy consumed during a transmission is a function of Power level at which the transmission is done and the transmission time. Mathematically,

$$TX\ Energy = Voltage * Current(P) * TX\_time(S, R)$$

Here, Voltage is the potential difference applied which is constant. The amount of current consumed depends on the choice of the power level whereas the amount of time required for a transmission depends on the bit-rate level chosen and the size of a frame.

$$TX\_time(S, R) = \frac{Packet\ Size(S)}{Bit\ Rate(R)}$$

However, as explained in Section 4.3, actual transmission time is not simple as above and involve some other computation as shown in *(14)*.

For a fixed frame size and ETX = 1, different energy levels are formed. Each energy level is a unique combination of the power level and rate.

$$TX\ Energy(e) = Voltage * Current(p) * TX\_time(r) \quad (15)$$

Where,

p = power level: 0, 1, 2, …

r = rate level: 0, 1, 2, …

e = number of energy levels = 0, 1, 2, …

More details on number of energy levels are explained in Section 5.5.2.

5.3.1 Working Principle

The working principle of the REACT is similar to the REACT-P. Therefore, in this section, only the changes are emphasized. As mentioned before, the major difference between the REACT-P and the REACT is that, the latter uses the energy levels instead of the power levels to make the changes in the rate and/or power. The link Quality Estimation technique is similar. As in the REACT-P, this algorithm also has two phases: a bootstrap phase and a run-time phase.

A. Bootstrap Phase

During the bootstrap phase, two changes are amended. First, even before the actual data transmission, each node configures the energy level array in an ascending order of the energy consumption for a fixed sized frame using (12), from the available power levels and rate levels. Hence, the combination of the power and rate level that provides the lowest energy consumption is at energy array index zero. Second, with the first successful DATA-ACK exchange, the client node will try to attain the next transmission power level for different rate that satisfies their corresponding sensitivities for a given link loss and certain margin. It starts with the highest rate as it is better to stay at the higher rate. It calculates the next power level feasible. If this next power level required is higher than the maximum power level, next lower rate is used, and the process continues. If none matches, maximum power level and minimum rate level are chosen. This is also explained via flowchart in Figure 9-6. And, the next energy level is selected corresponding to the chosen rate and power. The chosen power and rate are then written to the radio driver making them ready for the next transmission. The flowcharts in Figure 9-3 and Figure 9-4 show the changes explained to setup the energy level array.

B. Runtime Phase

The run-time phase begins after the bootstrap phase with the energy level chosen from the bootstrap phase. The run-time phase runs like that of REACT-P with additive increase additive decrease technique except that, the energy level is changed instead of power level that takes into account both the power as well as the rate. Secondly, in safe2decrease module, being a step-wise control technique, the next energy level is exactly one level below the current energy level. The transmission power and the transmission rate corresponding the next energy level is then extracted. The next estimated RX power is obtained as before and is compared to the sensitivity level for the extracted rate level corresponding to the next lower energy level. As discussed before in Section 4.1.1, when bit-rate is used, it is necessary to consider the receiver sensitivity as it varies for different rates. Additionally, while calculating the expected transmission time using *(14)*, current bit-rate is used which is dynamic rather than the constant one that is used in REACT-P.

Although REACT implies rate adaptation together with power adaptation, the primary metric used is still ETX. It is due to the fact that the frame size is still considered constant over an application and the average metric values calculated by using the EWMA are reset upon a change in the energy level. So, either ETT or ETX is used, they would have the same impact.

The full flowchart of REACT is shown in the Appendix-C: Flowcharts of the proposed algorithm.

5.4 Performance Metrics

Along with the performance metrics defined in section 3.5, following are two other performance metrics used in the experiment in this chapter.

5.4.1 CCA Busy Count

CCA busy count is specific to the transmitter side and represents the number of channel busy experienced by the nodes when trying to transmit. Within a certain transmission range, the neighboring stations is able to physically sense the channel to know if it is busy or free either by carrier detection or energy detection. When this happens, they defer their own transmission to some later time to avoid collision. This count gives an idea about how much the channel is occupied or how much the neighboring nodes are interfering its own transmission. Although an actual transmission is not made when channel busy is encountered but it can impact the other performance metrics like delay. Transmitting at lower power and

higher bit-rate may reduce this count and vice-versa. At lower power, the radio footprint is reduced thereby reducing the exposed terminal and at higher bit-rate, the transmission air-time is reduced which reduces the probability of collisions.

5.4.2 Network Lifetime

Network life time in this research is the remaining lifetime after the completion of the experiment. More details on how the remaining lifetime is calculated is described in the Section 5.5.3. Network life time can be interpreted in various ways. Some of them are as follows:

i. Network lifetime is the average remaining lifetime amongst all the nodes in a network. This gives the average remaining lifetime of the whole network.

ii. Network lifetime is the time when a first node dies in the network. In this case, the network lifetime is the minimum remaining lifetime amongst the nodes in the network.

iii. Network lifetime is the time until there are no more nodes in a network. In this case, the network lifetime is the maximum remaining lifetime amongst the nodes in the network.

iv. Similarly, there can be other intermediate definitions such as network lifetime is the time until half of the nodes are dead or 70% of the nodes are dead and so on.

5.4.3 Standard Deviation Error

The test performed in this chapter were repeated multiple times to gain confidence in the results. The average values of the performance metrics were displayed in the graphs of this chapter along with their corresponding standard errors. Standard deviation error (σ) was calculated as follows:

$$\sigma = \sqrt{\frac{\sum(x - x_m)^2}{n}}$$

Where, x_m is the sample mean and n is the sample size. In the graphs, both positive and negative errors were plotted.

5.5 Implementation

5.5.1 Initializing the Control Mechanism

Even before starting the bootstrap phase that occurs after a successful DATA-ACK exchange, the control mechanism needs to be initialized. This helps to command the client node to work in a particular control mechanism. Before sending the DATA packet, the client needs to synchronize with the sink. To do so, there is an exchange of DBR-EB (Discovery Beacon Request-Enhanced Beacon) messages. After receiving the EB for the first time, a function init_rc () is invoked which uses some fields in EB to distinguish which test to run on the client regarding the control mechanism. The control mechanism can be one of the following:

i. NO_CONTROL

   This mechanism is the implementation of CPCR (Constant Power and Constant Rate control Mechanism) where the client neither changes the power nor the bit-rate.

ii. POWER_CONTROL

   This mechanism is the implementation of REACT-P where the client dynamically changes the power level at a constant rate.

iii. POWER_RATE_CONTROL

   This mechanism is the implementation of REACT where the client may dynamically change the power as well as the bit-rate.

More details on how the control mechanism is selected by the client node are shown Figure 9-2.

5.5.2 Setting the Energy Level Array

As mentioned in the working principle (Section 5.3.1), a client node sets the energy level array and sorts it before a first DATA-ACK exchange. To account both power level and rate levels, an energy structure of type ENERGY_T of one byte is defined that takes two variables: 5 bits power level and 3 bits rate in order to accommodate the different power levels and rate levels.

```
typedef struct energy_st {
        uint8_t power: 5;
```

```
    uint8_t rate   : 3;
} ENERGY_T ;
```

More details on how the energy level array is setup are explained by the flowchart in Figure 9-3 and Figure 9-4.

As in REACT-P (Section 3.7.2), 14 out of 32 (0 to 13) power levels are used that have different current consumption as shown in Figure 3-20 and four rate levels (0 to 3) for 100Kchips/s MR-OQPSK modulation are used for the Atmel AT86RF215 chip. The sub-registers in AT86RF215 such as: SR_BBC1_PC_PT, SR_BBC1_OQPSKC0_FCHIP and SR_BBC1_OQPSKPHRTX_MOD help to choose the modulation type, chip rate and the mode rate respectively. More details on these registers can be found in [48].

Table 5-2 shows the transmission (TX) energy consumed for different combination of power and rate levels for MR-OQPSK at 100Kchips/sec for 142B MPDU frame size and 3 Volts. The energy array is then formed using (15). A total of 56 energy levels (14 power levels * 4 rate levels) were obtained. This energy level array is then sorted using qsort algorithm with O (nlogn) as shown in Figure 9-4. This resulted to the table in Appendix-B: Sorted Energy level array in the ascending order.

Table 5-2: TX Energy consumed (µJoules) for different combination of power and rate levels

Rate / Power	**RM0 (6.25Kbps)**	**RM1 (12.50Kbps)**	**RM2 (25Kbps)**	**RM3 (50Kbps)**
0	85766.58	46736.46	27259.74	17483.04
1	93417.12	50905.44	29691.36	19042.56
2	101067.66	55074.42	32122.98	20602.08
3	110865.72	60413.64	35237.16	22599.36
4	117710.94	64143.78	37412.82	23994.72
5	130461.84	71092.08	41465.52	26593.92
6	143615.4	78259.8	45646.2	29275.2
7	160527.12	87475.44	51021.36	32722.56
8	174083.34	94862.58	55330.02	35485.92
9	193947.9	105687.3	61643.7	39535.2
10	214349.34	116804.6	68128.02	43693.92
11	236764.08	129019	75252.24	48263.04

12	256494.42	139770.5	81523.26	52284.96
13	275285.22	150010.1	87495.66	56115.36

From this energy array list, the bootstrap phase helps to jump start to the closest appropriate energy level. Then the run-time phase further tunes the energy level to get the optimal values of power and rate that provides satisfactory reliability.

5.5.3 Calculation of Remaining Lifetime of a Node

In this chapter, we would be using the Remaining lifetime as one of the performance metrics. Hence, this section explains how the network life time is calculated. In this calculation, a $LiMnO_2$ battery with rating 3V,3000mAH is used as a reference.

We used two batteries of above ratings with a DC/DC converter. The DC/DC efficiency is 90% in average. Additionally, only 80% of the battery capacity is serviceable. Therefore,

The available capacity will be

$$Available\ Capacity\ (C) = \ 3AH * 2 * 0.90 * 0.80 = 4.32AH$$

For a 3V potential difference, the initial energy is given by

$$Initial\ Energy\ (E^{INIT}) = voltage\ applied * available\ capacity$$
$$E^{INIT} = 3V * 4.32 * 1000 * 3600 = 46656000\ mJoules$$

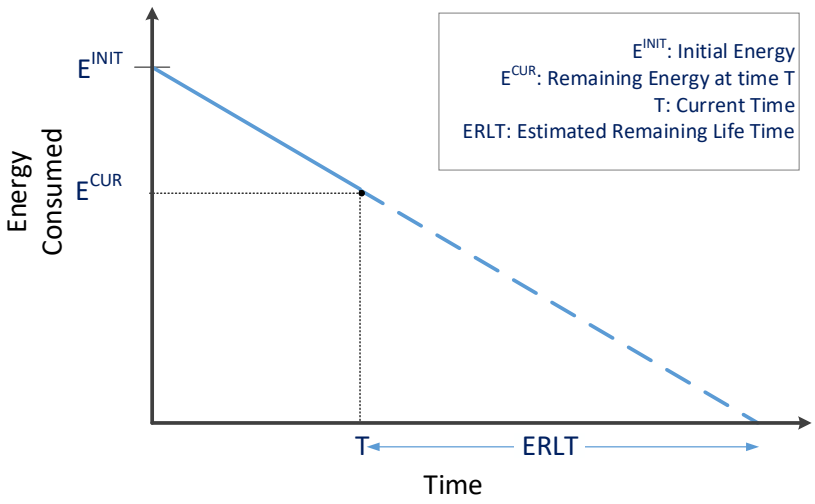

Figure 5-2: Estimated Remaining Life Time (ERLT) calculation

With the E^{INIT}, from Figure 5-2, let E^{CON} be the amount of energy consumed after time T. Then the remaining energy at time T is given by E^{CUR} as

$$E^{CUR} = E^{INIT} - E^{CON}$$

The drain rate (m) is given by

$$m = \frac{E^{CON}}{T}$$

Although the battery discharge curves are typically non-linear in nature but for this thesis, it is considered to be linear. Hence, if a node is projected to continue at this same drain rate (m), then the estimated remaining lifetime of the node ($ERLT$) can be forecasted as

$$ERLT = \frac{E^{CUR}}{m} = \frac{E^{INIT} - E^{CON}}{E^{CON}} * T \ (in\ time\ units) \qquad (16)$$

Let us take an example of the client 7 for the case of 0/7 when the sink has received 400 unique frames from client 7. Then using (16), we get the following remaining lifetime.

Table 5-3: Calculation of Remaining life time of Client 7

Client	Initial Energy (mJ)	Energy Consumed (mJ)	Duration (sec)	Remaining lifetime (hours)
7 w/CPCR	46656000	60600	24102	5147.792
7 w/REACT-P	46656000	18646	23976	16657.98

7 w/REACT	46656000	7563	24270	41582.469

In this thesis, the network lifetime or remaining lifetime is not used as a metric to control the algorithm but used as a performance metric to evaluate the performance of the proposed algorithm. Hence, it is calculated only at the end of the experiment time which gives an approximation of the lifetime of the nodes/network. In equation (16), *T* is experiment duration.

5.6 Experimentation

To evaluate the efficiency of the proposed algorithm: REACT-PR or REACT, it was compared with the REACT-P and the constant power and rate conditions using experimentation. Due to the COOJA's limitation of not being able to support dynamic rate adaptation, only experimentations were performed. Different experiments were performed with different number of contending clients at the same time. Each of the experiment were repeated four times to provide higher confidence on the results. Various graphs were plotted that showed the average of the four repetitions including their corresponding variance.

5.6.1 Parameters

Table 5-4 shows the parameters used for one-sink-one-client setup whereas Table 5-5 highlights the parameters that are changed for all 7 clients to one sink star network setup.

Table 5-4: Experimental parameters for one-sink-one-client setup

Parameters	**Value**
Device Model	Itron Module with ATRF215 [75]
MAC Re-Transmissions	3 attempts at link layer
CCA Attempts	3 attempts
Network	one-to-one
Number of Nodes	One sink and one client (ID 7)
Position	Immobile positions in the floor (Figure 5-3)
TX Power	-13 to 0 dBm with step-size 1 dB
Attenuation at sink	15dB, 20dB, 25dB
TX Bit Rate	6.25Kbps, 12.50 Kbps and 50Kbps
Modulation	DSSS MR-OQPSK @100Kchips/second

Total Received	600 packets at sink per experiment
Average Experiment duration	~1 hour
Data Size and Traffic Rate	180B (MPDU 142B) and 1 packet/6 sec
Algorithms	CPCR Vs REACT-P Vs REACT
Frequency	920.4MHz, single channel
MAC and PHY Protocol	802.15.4 e/g [29][30]
Battery Rating	3V, 3AH x 2

Table 5-5: Experimental parameters for 7 clients star topology setup

Parameters	**Value**
Network	Star Topology with 1 sink
Number of Nodes	7 clients and 1 sink
Position	Immobile positions in the floor (Figure 5-3)
TX Power	-13 to 0 dBm with step-size 1 dB
Attenuation at sink	20dB
TX Bit Rate	12.50 Kbps
Total Received	2900 packets at sink per experiment
Average Experiment duration	6 hours 49 mins and 50 secs
Data Size and Traffic Rate	180B (MPDU 142B) and 1 packet/min
Algorithms	Constant power and rate Vs REACT-P Vs REACT
Repetitions	4

5.6.2 Environment

As the office was shifted to a new location, we had a different floor plan. One sink and seven client nodes were deployed in various locations of the Itron office/lab environment as shown in Figure 5-3.

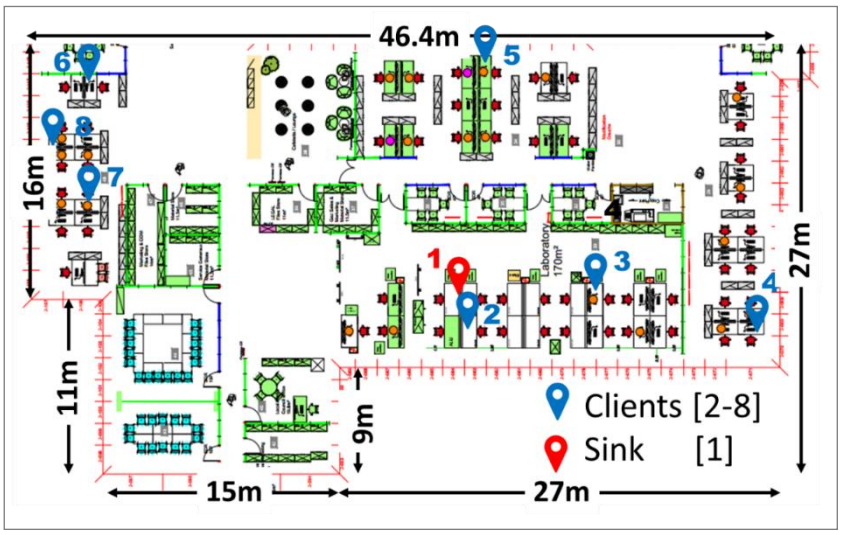

Figure 5-3: REACT deployment plan

The approximate distance and the average link loss experienced by the client nodes from the sink is shown in the Table 5-6. The distance is approximated by the means of map and ruler whereas the link loss was averaged over several test experiments. In order to have some nodes near the sensitivity level, an attenuator of 20dB was used at the sink.

Table 5-6: Approximate distance of clients from sink for REACT deployment plan

Client ID	Distance from Sink (ID:1)	Average path loss
2	1m	34.50 dB
3	8 m	55.33 dB
4	19 m	70.83 dB
5	14.4 m	67.19 dB
6	27 m	97.50 dB
7	24.4 m	94.33 dB
8	27 m	91.67 dB

5.6.3 Results and Discussion

5.6.3.1 Single Sender-Receiver Pair

An experimental test was performed between one sender and one sink at variable attenuation and different constant rates with CPCR, REACT-P and REACT with the parameters using Table 5-4. The attenuation was varied at the sink side by using a variable attenuator.

The results in the Figure 5-4 shows that, with REACT, the average energy consumption per unique frames obtained is quite low as compared to using CPCR or REACT-P for all cases of attenuation and rates. On the other hand, only minor compromise with the PDR was observed with REACT as shown in Figure 5-5. These results show that, REACT helps not only to reduce the energy consumption but also to maintain an acceptable PDR by correctly choosing the power and/or rate for different attenuations.

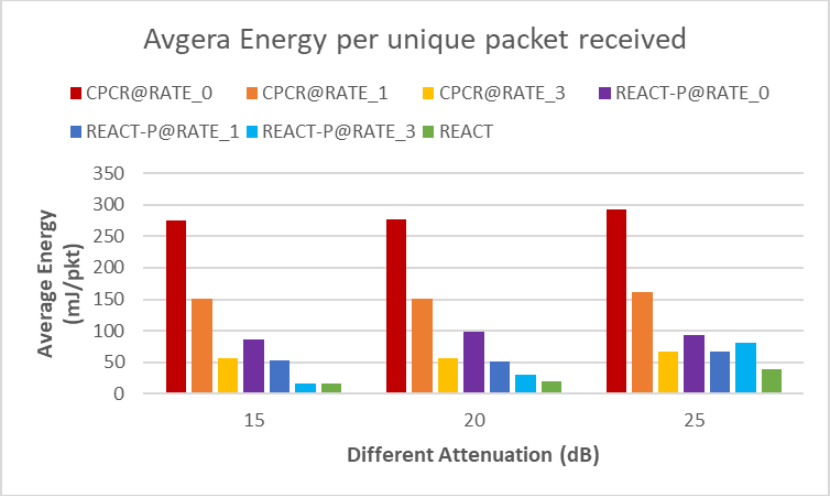

Figure 5-4: Average Energy consumed per unique frame received for CLient 7 at different rates and attenuation

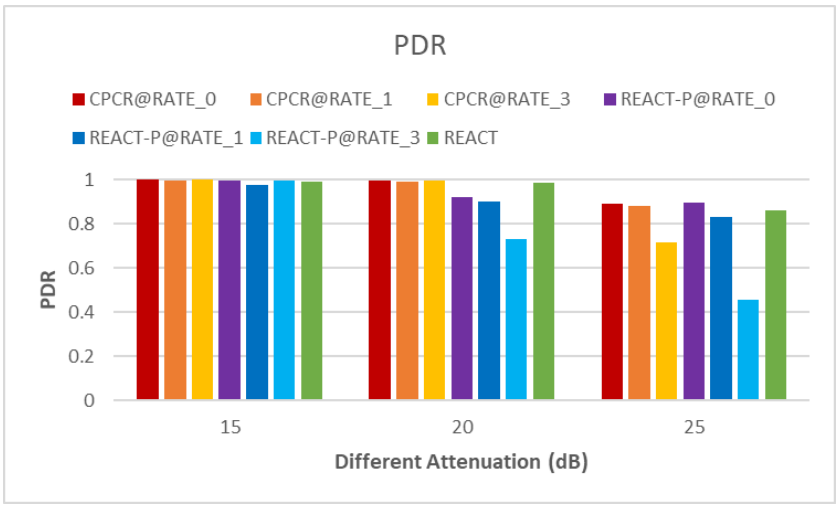

Figure 5-5: PDR of client 7 at defferent rates and attenuation

Now, next work is to show that REACT would perform well in all client environment with different congestion level. As the PDR was low at 25 dB, 20 dB attenuation is used for the next tests. Also, RATE_1 (@12.50Kbps) is chosen as a base rate to continue the test on all 7 clients in a star topology setup. This means, transmission bit-rate of 12.50 Kbps or rate

level 1 is used as a constant rate for REACT-P and CPCR and as a minimum rate level for REACT.

5.6.3.2 Seven Clients – One Sink Star Topology Setup

Seven clients and one sink were deployed in the office floor as shown in Figure 5-3 and experiments were run using the parameters defined in Table 5-5. The performance of the proposed algorithm in this chapter i.e. REACT (w/REACT in graphs) was compared with REACT-P (w/REACT-P) and constant maximum power at constant rate i.e. CPCR (w/CPCR) at 12.50Kbps with different number of nodes competing for the channel at the same time. Different number of contending nodes and the corresponding client IDs involved are shown in Table 5-7. The experimental results obtained were classified as Network Behavior and Node Behavior.

Table 5-7: Client IDs involved with different setup for REACT Test

Competing clients	Clients involved to compete for channel
0/7	0; All clients transmit in different timeslot.
2/7	Client 2 and 4
4/7	Clients 2, 4, 6, 8
7/7	All clients compete for the channel at the same time.

5.6.3.2.1 Network Behavior

In this section the evaluation of the proposed algorithm is observed at the network level to see how the proposed algorithm improves on average.

Figure 5-6 shows a plot of the average transmission energy consumption per unique frame received in the primary vertical axis at maximum power (CPCR) against the proposed algorithms REACT-P and REACT. These values in the graphs are averaged over four repetitions. The graph also shows the positive/negative standard deviation error. It also presents the percentage improvement in the total transmission energy consumption in the secondary vertical axis with respect to the different number of clients competing at the same time on the x-axis. The percentage improvement shown here is with respect to the CPCR. The experimental results reveal that with REACT-P, up to 68% and with REACT, up to 88% improvements are achievable as compared to using CPCR, with insignificant compromise in PDR (Packet Delivery Ratio) and frame losses (Figure 5-7). Even in the worst-case

scenario of [7/7], where all nodes transmit and compete at the same time, the percentage improvement in the total energy consumption is 58% lower with REACT than CPCR. Here in Figure 5-7, PDR is the ratio of the unique number of frames received to the total number of transmission attempts at the link layer. The PDR line for CPCR, REACT and REACT-P are almost overlapping to one another for different cases. Like before, these values were also averaged over 4 repetitions. Figure 5-6 also indicates that the energy consumption improvement decreases with the increased number of competing nodes for the same channel, which is obvious. This means that, with a proper channel access technique, REACT-P or REACT can reduce the energy consumption by more than three quarters.

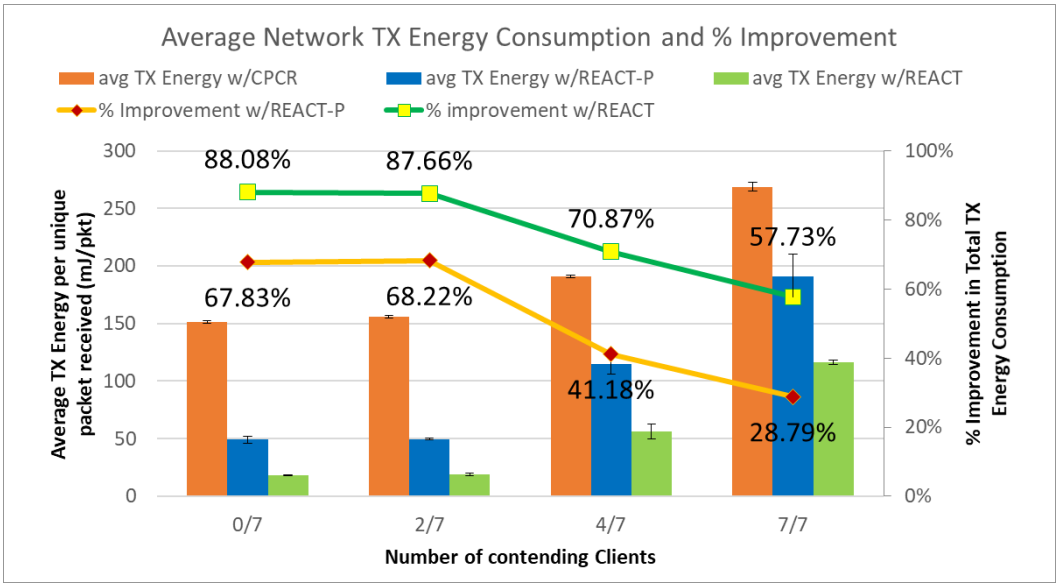

Figure 5-6: Average network energy consumption and % improvement of REACT and REACT-P

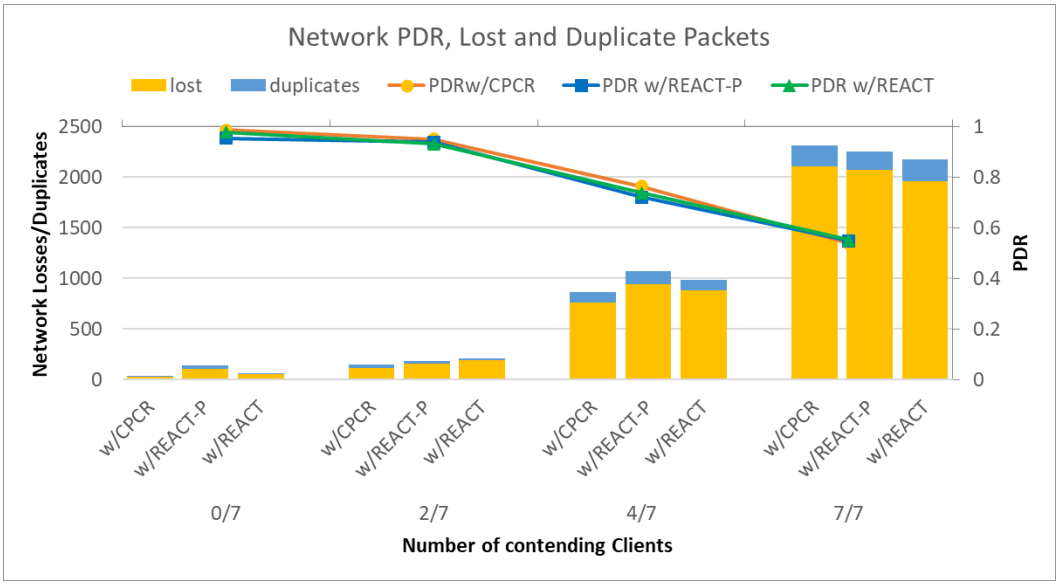

Figure 5-7: Total frame losses and PDR in a network

As discussed in section 5.4.2, there exists various interpretation of the network lifetimes which are shown in the next few graphs.

Figure 5-8 shows the network life time for different numbers of concurrent transmissions. The network life time in this graph is the average remaining lifetime amongst all the nodes in the network over 4 repetitions at the end of the experiment. The graphs in Figure 5-8 reveal that the average network lifetime improves up to 85% and 414% in the worst case whereas it improves up to 213% and 747% in the best case with REACT-P and REACT respectively, as compared to using CPCR at 12.50Kbps rate. For example, in the worst case of 7/7, a node that normally lasts 1 year would last 1.85 years and 5.14 years using REACT-P and REACT, respectively.

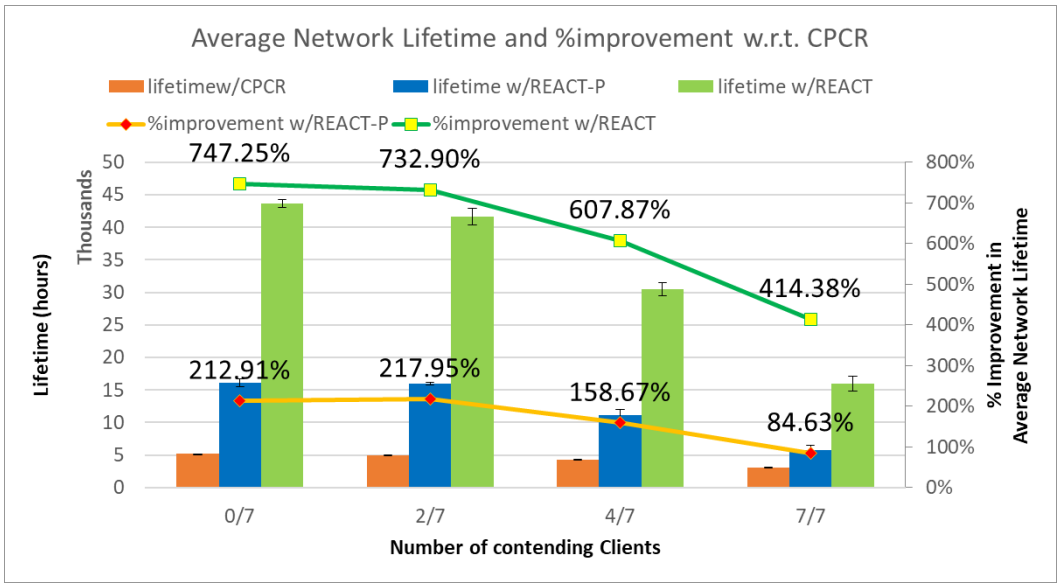

Figure 5-8: Average network lifetime and % improvement

Figure 5-9 shows the network lifetime when different percent of nodes are dead depending on its interpretation. Results were taken for 30%, 50%, 75% and 100% of dead nodes. In the case when the network lifetime is the time when 30% of nodes are dead i.e. when 30% of 7 which is 2 nodes are dead, the network lifetime in the worst scenario (i.e. 7/7) is still higher than that of CPCR or REACT-P. In the case when the network lifetime is the time when the last node is dead. i.e. all nodes are dead, the network lifetime with REACT in the worst scenario i.e. 7/7 is still 759.18% higher than using CPCR and 237.14% higher than REACT-P. With lesser number of contending stations, the improvement is much higher when REACT is used.

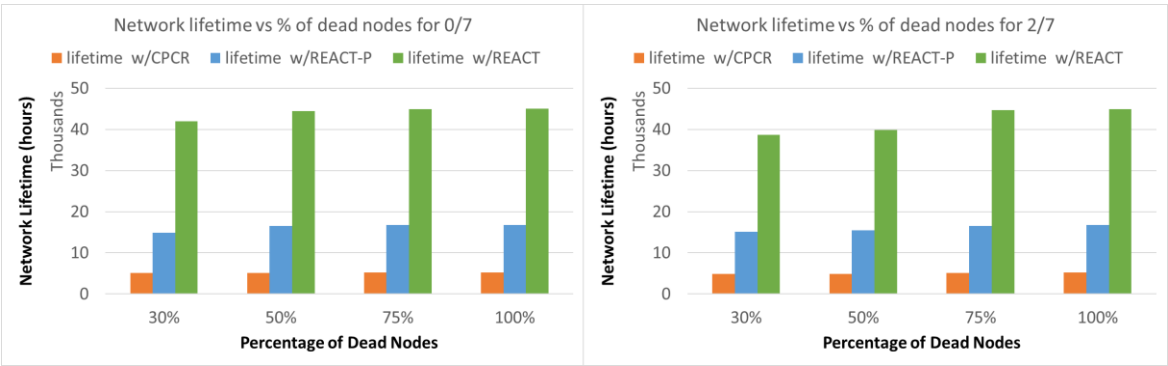

(a) *(b)*

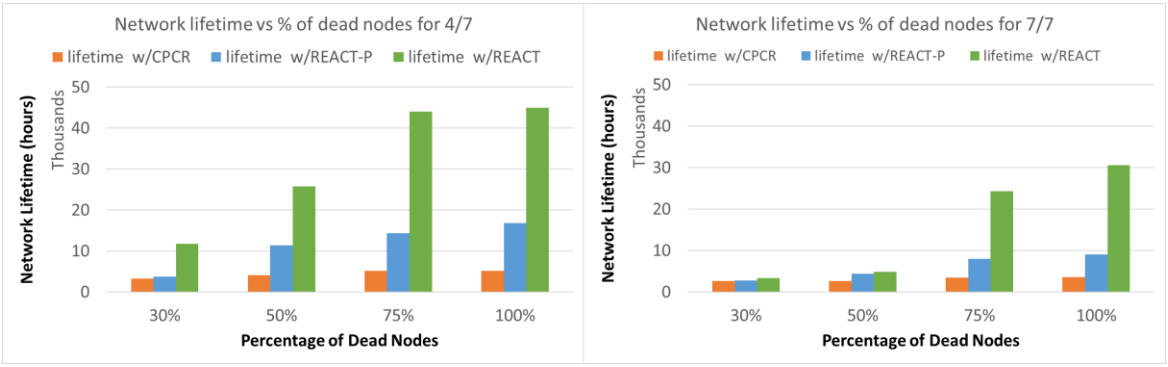

(c) *(d)*

Figure 5-9: Network lifetime when different % of nodes are dead

Figure 5-10 shows the total CCA (Clear channel Assessment) busy count averaged over four repetitions encountered by the nodes in the network for different number of concurrent transmissions. The graph shows that, with the increase in the number of the competing clients at the same time, the CCA busy count increases. It can also be seen that the count is lower in the REACT-P than at CPCR, due to decrease in interference as it optimizes the power level. This count further decreases in the REACT, as it controls both power and rate which reduces the over-hearing as well as the channel occupancy time. This graph shows that REACT not only aids to reduce the transmission energy consumption but also helps to reduce the interference by optimizing the power level and channel occupancy time.

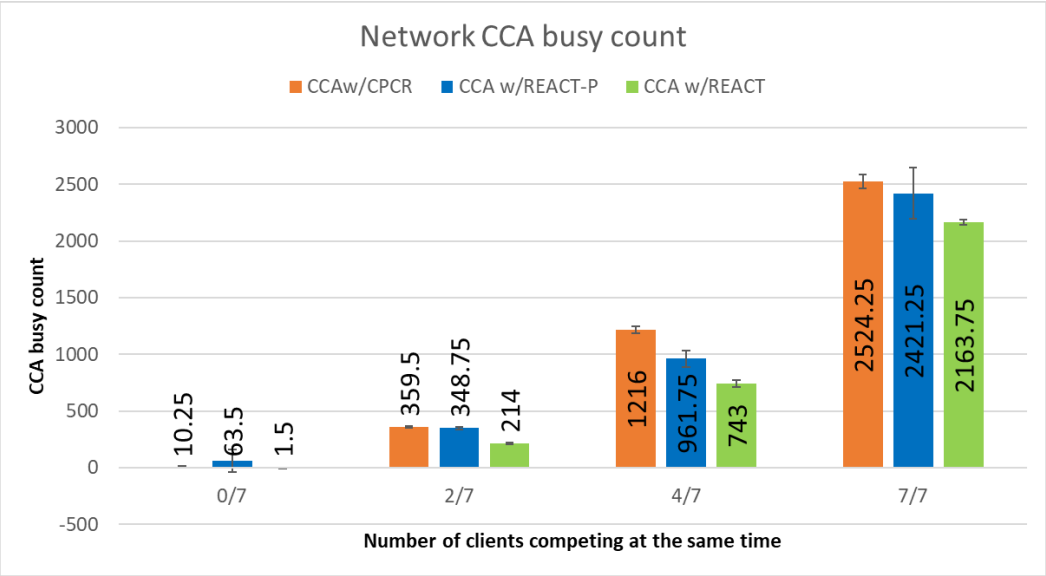

Figure 5-10: Total CCA busy counts in a network

5.6.3.2.2 Node Behavior

In this subsection, detailed per node evaluation are shown. Figure 5-11(a) shows that in all cases, all clients consume less energy per transmission with REACT-P than when using the CPCR. The average energy per frame is constant when CPCR is used for all cases (=150mJ/pkt for the case of 12.50Kbps and power level 13). Section 3.7.3.2 explains the detail of the above result.

Figure 5-11(b) shows the same when REACT is used. All nodes using REACT have lower energy per transmitted frame than CPCR and REACT-P. It can also be observed the error variance is higher for the nodes 6, 7 and 8 whereas they are relatively smaller for the other nodes. It is due to the fact the fact that nodes 6, 7 and 8 are comparatively farther from the sink than the other nodes (Figure 5-3). So, they experience higher variation in the link quality.

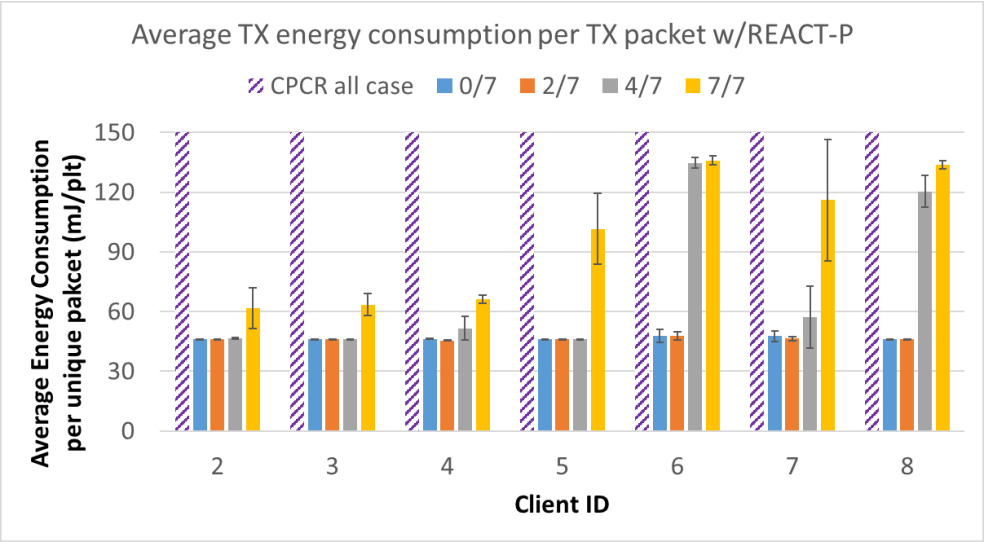

(a) REACT-P

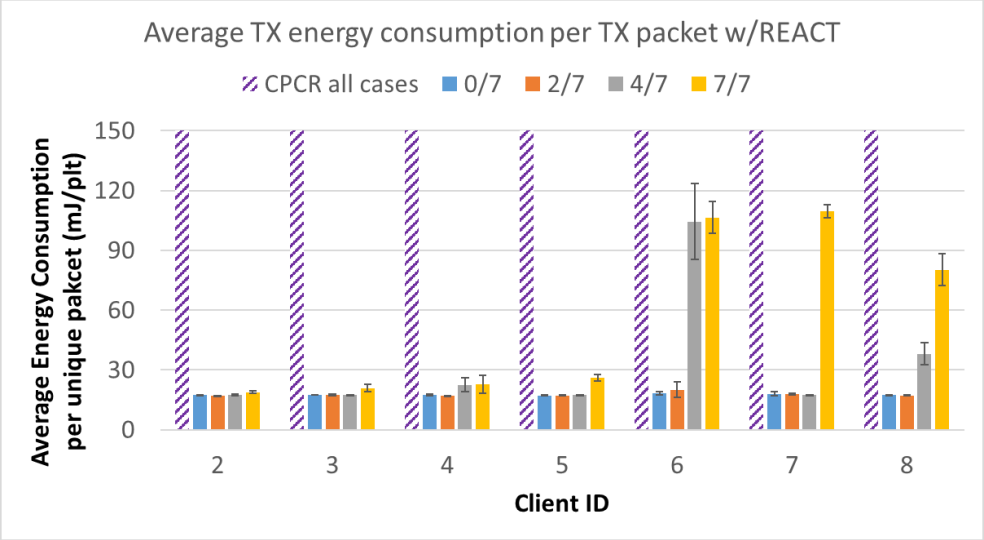

(b) REACT

Figure 5-11: Energy consumed per TX frame for the case of 5/7

Figure 5-12 and Figure 5-13 show the total TX energy consumption and the PDR of each nodes for different cases respectively, averaged over four repetitions. It can be observed that, with similar PDR, the total TX energy consumption is lowest with REACT for all of the nodes in all cases. And as shown before in the network behavior, energy consumption increases as the number of contending nodes increases.

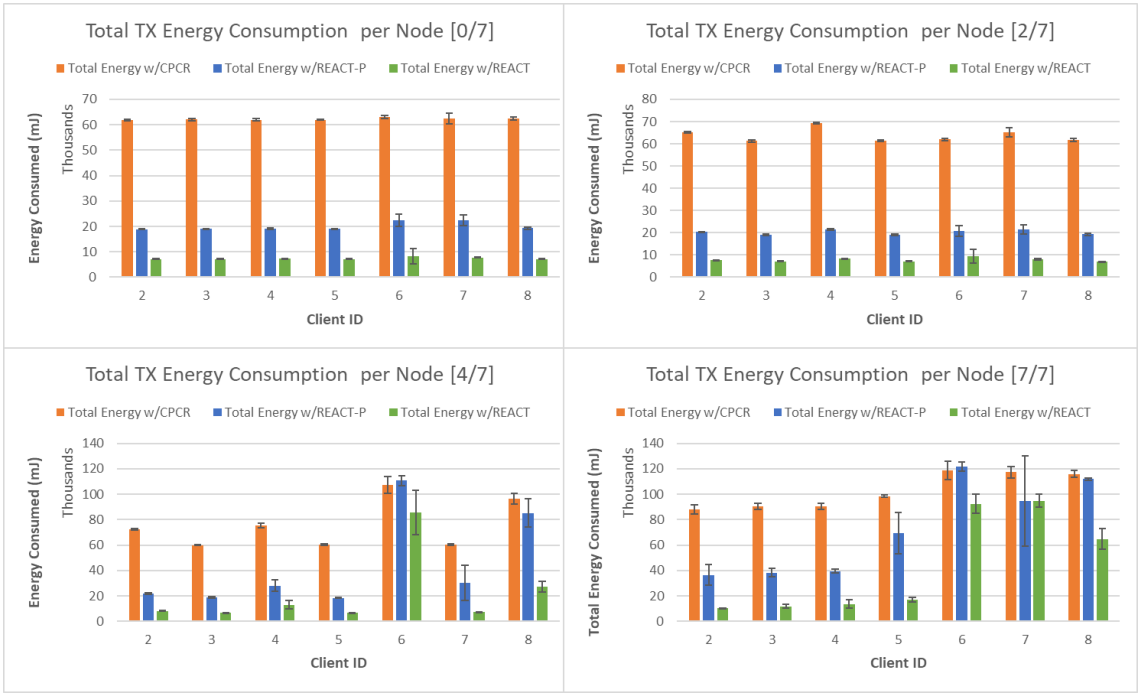

Figure 5-12: Total TX energy consumption per node

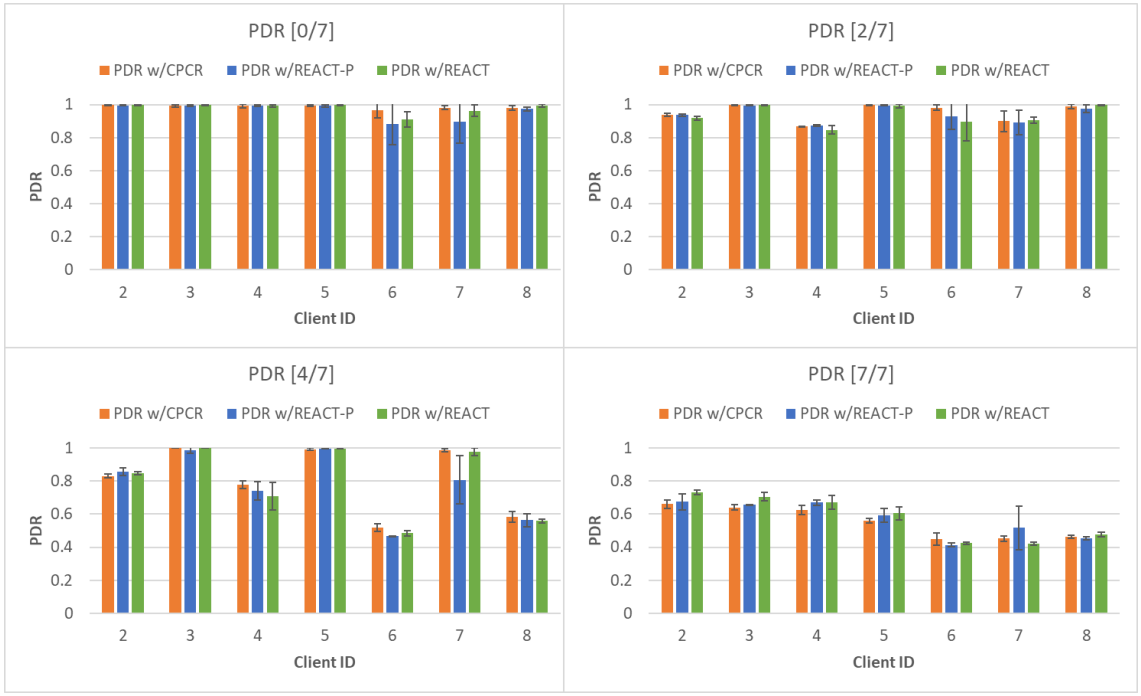

Figure 5-13: PDR per Node

5.6.3.3 Test at different Bit-rates

In all the experiments performed above, except for REACT itself, others were performed at constant bit-rate of 12.50Kbps. Now, in the following graphs, we compare their performance at different constant rate levels to verify the performance of REACT in other constant rate

modes using parameters from Table 5-5. These graphs shown in Figure 5-14 and Figure 5-15 are the particular case of 2/7 which shows that REACT performs better than just REACT-P and CPCR at different constant rates. The performance of the REACT is same as REACT-P when using at maximum rate.

Figure 5-14 shows that there is constant improvement in the energy consumption at different rates when compared with the maximum power used. On the other hand, the improvement in the energy consumption is higher when REACT is used. In Figure 5-15, it can be observed that the count of channel busy experienced by the nodes decreases with the increase in the rate level and is lowest when using REACT.

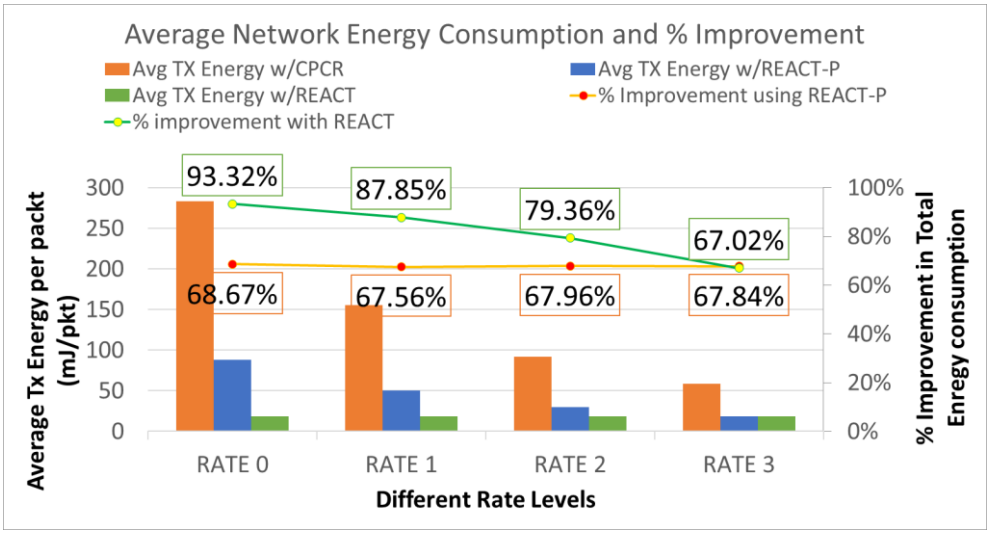

Figure 5-14: Average Network Energy consumption and % improvement w.r.t. CPCR for different constant rates for 2/7 case.

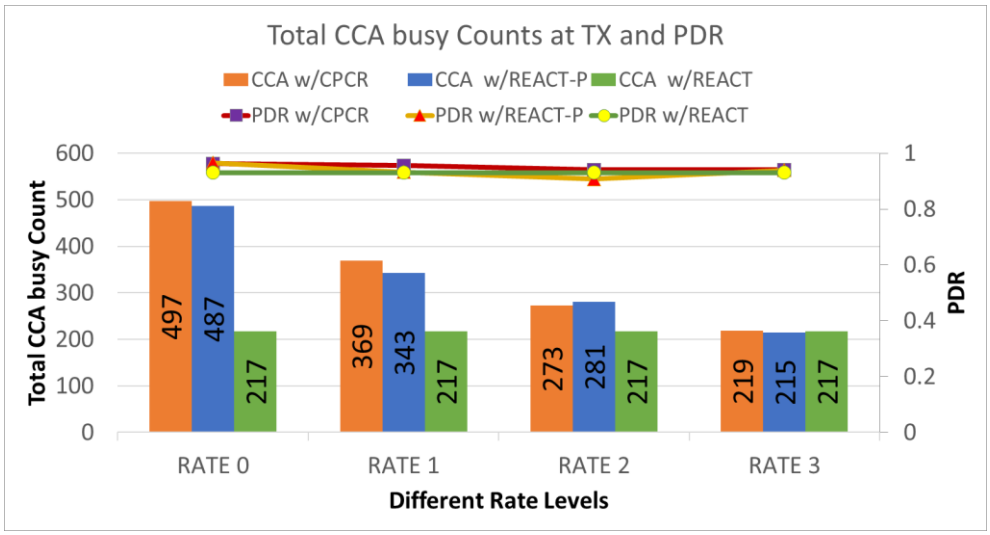

Figure 5-15: Total CCA busy counts at different rates

5.7 Conclusion

In this chapter, we have studied about the tradeoffs between the transmission power, bit-rate and the reliability. We have seen that all the existing algorithms are defined for IEEE 802.11 WLAN standard and most of them focus on improving the throughput and latency. The main objective of this chapter was to provide a responsive algorithm for LLNs that dynamically controls both transmission power and rate which helps to reduce the energy wastage without impacting too much on the other performance aspect. This chapter highlights the adjustments and extensions made to REACT-P that controls only power, to obtain the anticipated goal. REACT establishes an array with unique power-rate combination before the actual transmission starts which is used later in the bootstrap and the run-time phase. The proposed algorithm REACT-PR or simply REACT was evaluated using experimentation and compared with the REACT-P and CPCR at different rates. The results show high percentage improvement in the energy consumption and the lifetime of the nodes/network with similar packet delivery ratio. It is also shown that using REACT further helped to reduce the number of channel busy encountered by the nodes proving the reduction in the channel occupancy and interference.

6. Conclusion and Future Works

Contents

6.1 Conclusion 123

6.2 Future Works 125

6.1 Conclusion

It is a known fact that the concept of Internet of things is here to stay for a long time. The number of connected IoT devices has been increasing exponentially. For numerous applications, it is understood that the battery and IoT come side-by-side. There are various benefits of using a battery over other sources of power in terms of size, cost, flexibility, mobility, installation. However, it has some challenges as well; lifetime being the major one. Device longevity has become one of the major challenges in the successful deployment of the IoT devices.

With regards to this matter, various energy saving techniques exist in the field. Among them, this thesis focuses on reducing the radio transmission energy consumption by bringing intelligence to the edge. In this scope, this thesis aims in optimizing the transmission power and transmission bit-rate which are the two essential radio parameters that have huge impact on the energy consumption. To this end, four major research objectives were defined; each of which finally points to the global aim of developing an energy-efficient technique by adapting transmission power and rate control. These research objectives were specified in various chapters. Transmission power and transmission bit-rate have several impacts; most important being the energy consumption, interference, channel occupancy and radio connectivity.

Observing and analyzing the radio link, utilizing the results to derive predictions about the future link quality, adjusting protocol or radio parameters to satisfy the communication requirements in an energy-efficient fashion is the key idea for creating a proficient transmission power/rate control mechanism.

Wireless Mediums (RF) are highly dynamic, random and unpredictable. An efficient link quality estimation is required to analyze and anticipate the future link conditions. Various link quality metrics and their combination techniques were studied in this thesis along with their pros and cons. With a subjective evaluation, ETX (Expected Transmission Count) from the sender-side and RSSI (Received Signal Strength Indicator) from receiver-side were used in this research as a primary and a secondary metric respectively to provide better link quality estimation. The primary metric ETX provides the number of link-layer transmissions which is crucial to the design of the algorithm as it has direct impact on the energy consumption.

To obtain the desired goal with the design challenges mentioned in the Chapter 1, we proposed REACT-PR or simply REACT (Responsive Energy-efficient Adaptive Control of Transmission Power and Rate). REACT is a sender-based responsive algorithm with a feedback and it was implemented in a real IoT platform to reduce the energy wastage and efficiently improve both nodes' and networks' lifespans. It presents novel approaches in controlling the power/rate, which is easy to implement without too much of an impact on other layers or on design. The proposed algorithm uses multiple link quality information. It utilizes a direct control method during the bootstrap-phase using a simple path loss model and a step-wise control technique during the run-time phase, thereby offering a hybrid control. With various components, such as a BEW module, a link loss analyzer, a loop detector, a safe2decrease module and out of coverage detection, this algorithm provides a stable, optimal power/rate which is environment-adaptive and that aids in reducing the nodes' energy consumption.

The required additional implementation complexity for REACT is very low: because the approach only counts successful and unsuccessful transmissions, there is no expensive operation involved. The only change required at the receiver-side is to piggy-bag the RSSI information on the ACK message back to the sender. In contrast to most of the approaches discussed, neither RTS/CTS scheme nor initial overheads are required here.

We started with a design and the development of the transmission power control only at fixed data-rate as explained in Chapter 3. The performance of REACT-P was validated using both simulation and experimentation. It was compared with one of the dominant existing algorithms and the maximum constant power by simulation and compared with the maximum usable power level using experimentation. From experiment, it was perceived that PHY rate adaptation is more effective in saving energy than the transmission power control only. Hence, REACT-P was later extended to take the bit rate into account giving rise to REACT as described in Chapter 5. REACT was evaluated using the experimentation only due to the limitation of the Cooja simulator to change the bit-rate during run-time. The performance results of REACT and REACT-P show that improvement of up to 68% was possible when using REACT-P and up to 88% improvement was obtained when using REACT in terms of network TX energy consumption. It has been witnessed via graphs that such gains were achievable with a similar packet delivery ratio. This work also showed that the network lifetime, which is the average remaining life time of the nodes, could be improved by up to 4 times on average when using REACT-P and 7.5 times on average when

using REACT. This improvement in life time is higher for nodes that are closer to the sink as they can use both lower power and higher bit-rates. It was also observed that with REACT, the channel occupancy was reduced to some extent compared to REACT-P and constant power algorithms. This means, with REACT, the air time is less hence the channel is less busy and yields less interference.

The results also indicated that, without an effective collision resolution scheme, the performance gains of intelligent TPC schemes, including REACT, reduce when the number of contending stations increases. But the improvement in energy consumption is still higher when compared to using maximum constant power. With a proper channel access technique, more energy saving can be attained by applying REACT.

While this algorithm is targeted for battery operated devices, it would be equally applicable to the mains powered IoT devices as the rate and power control help to reduce interference and channel occupancy, improve the throughput and latency. Rate adaptation can further benefit by switching to higher bit rates for delay-sensitive real-time applications.

In this way, a responsive, energy-efficient and adaptive transmission power and bit-rate control algorithm was developed for LLN in order to fulfill the aim of reducing the energy consumption while ensuring a good reliability.

6.2 Future Works

This thesis has provided some contributions and has provided a control framework for adapting the power/rate level with the change in the environment. At the same time, it unfolds some research ideas and future directions. In the following, we state some open issues/ideas that can be explored in the future as a continuation of this work.

The first would be to evaluate the performance with different parameters like the packet size, traffic rate, ETX Threshold, Margin and various parameters of weights used for averaging. As the experiments in this thesis were performed with fixed data frame size, future work could involve evaluating the algorithm with variable sized packets, where the metric ETT would come into play. It is necessary to obtain the various results for different values of these parameters to understand the impact on the network performance and the energy consumption. This will help to recognize the suitable values of theses parameters for different applications. For example, an application with higher traffic rates should have different parameters than that of the application with lower traffic rates.

As this research was conducted for a star network in a single channel; future work could apply the same algorithm in a mesh network and in multi-channel environment. This may involve defining various states in a memory friendly way. The challenge here would be to understand the tradeoff between the complexity of the algorithm for maintaining various states in the constrained devices and the amount of energy efficiency attained. It may also imply channel black listing to avoid bad channels during the transmission as some fading are frequency-selective.

Next future work could be to perform an energy-efficient and accurate loss diagnosis in LLNs that can have an impact on the decision of the power/rate control and hence on the efficiency. As an example, increasing the transmission bit-rate during the loss due to collision and increasing the transmission power during the loss due to fading would be preferable. Decreasing the rate during the loss due to collision would in fact aggravate the losses as it increases the probability of collision. However, differentiating the cause of the packet loss accurately with low overhead and low energy cost would be a challenge.

Future work may further include adaptive modulation which involves changing the modulation depending on the radio link quality.

7. Publications

- **N. M. Shakya**, M. Mani, and N. Crespi, “SEEOF: Smart energy efficient objective function: Adapting RPL objective function to enable an IPv6 meshed topology solution for battery operated smart meters,” in *2017 Global Internet of Things Summit (GIoTS)*, 2017, pp. 1–6.

- **N. M. Shakya**, M. Mani, “Smart Transmission Power Control for Wireless Communication Modules”, US Patent 30134-US-PAT, December 2017 (Accepted).

- M. Lazarevskal, R. Farahbakhsh, **N. M. Shakya** and N. Crespi, "Mobility Supported Energy Efficient Routing Protocol for IoT Based Healthcare Applications," *2018 IEEE Conference on Standards for Communications and Networking (CSCN)*, Paris, 2018, pp. 1-5.

- **N. M. Shakya**, M. Mani and N. Crespi, “Responsive Transmission Power Control for Battery-operated Wireless IoT Modules” (Submitted at SECON’19)

- **N. M. Shakya**, M. Mani, N. Crespi, “REACT: Responsive Energy-efficient Adaptive Control of Transmission Power and Rate for battery-operated Wireless IoT modules” (IEEE Transaction Paper on Wireless Communication under review, awaiting reviewer’s score)

8. References

[1] "Internet of Things (IoT) History | Postscapes." [Online]. Available: https://www.postscapes.com/internet-of-things-history/.

[2] N. F. Raun, "Smart environment using internet of things(IOTS) - a review," in *2016 IEEE 7th Annual Information Technology, Electronics and Mobile Communication Conference (IEMCON)*, 2016, pp. 1–6.

[3] "Routing Over Low power and Lossy networks (roll)." [Online]. Available: https://datatracker.ietf.org/wg/roll/charter/.

[4] N. Kushalnagar, G. Montenegro, and C. Schumacher, "IPv6 over low-power wireless personal area networks (6LoWPANs): overview, assumptions, problem statement, and goals," 2007.

[5] "IEEE SA - 802.15.4e-2012 - IEEE Standard for Local and metropolitan area networks--Part 15.4: Low-Rate Wireless Personal Area Networks (LR-WPANs) Amendment 1: MAC sublayer."

[6] "IEEE SA - 802.15.4g-2012 - IEEE Standard for Local and metropolitan area networks--Part 15.4: Low-Rate Wireless Personal Area Networks (LR-WPANs) Amendment 3: Physical Layer (PHY) Specifications for Low-Data-Rate, Wireless, Smart Metering Utility Networks."

[7] "M2M Alliance." [Online]. Available: https://m2m-alliance.com/.

[8] WisunAll, "Wi-SUN Alliance." [Online]. Available: https://www.wi-sun.org/index.php/en/.

[9] A. Nordrum, "Popular Internet of Things Forecast of 50 Billion Devices by 2020 Is Outdated," *IEEE Spectrum*, 2016. [Online]. Available: https://spectrum.ieee.org/tech-talk/telecom/internet/popular-internet-of-things-forecast-of-50-billion-devices-by-2020-is-outdated.

[10] J. Howell, "Number of Connected IoT Devices Will Surge to 125 Billion by 2030, IHS Markit Says - IHS Technology," 2017. [Online]. Available: https://technology.ihs.com/596542/number-of-connected-iot-devices-will-surge-to-125-billion-by-2030-ihs-markit-says.

[11] "Press Release: Global Internet of Things market to grow to 27 billion devices, generating USD3 trillion revenue in 2025," 2016. [Online]. Available: https://machinaresearch.com/news/press-release-global-internet-of-things-market-to-grow-to-27-billion-devices-generating-usd3-trillion-revenue-in-2025/.

[12] M. Friedli, L. Kaufmann, F. Paganini, and R. Kyburz, "Energy Efficiency of the Internet of Things," *thesis*, pp. 1–66, 2017.

[13] MachNation, "Amazon, IBM, Microsoft and 18 Others Compared in MachNation's Newest IoT Platform ScoreCard," 2018. [Online]. Available: https://www.prnewswire.com/news-releases/amazon-ibm-microsoft-and-18-others-compared-in-machnations-newest-iot-platform-scorecard-300588195.html.

[14] I-scoop, “Internet of Things spending nearing $800 billion mark in 2018,” 2018. [Online]. Available: https://www.i-scoop.eu/internet-things-spending-2018/.

[15] Iot-analytics, “IoT Project List | List Of 1,600 Enterprise IoT Projects 2018 | IoT Analytics,” 2018. [Online]. Available: https://iot-analytics.com/product/list-of-1600-enterprise-iot-projects-2018/.

[16] iot-analytics, “IoT Platform Company List 2017,” 2017. [Online]. Available: https://iot-analytics.com/iot-platforms-company-list-2017-update/.

[17] “Top 50 Internet of Things Applications - Ranking | Libelium.” [Online]. Available: http://www.libelium.com/resources/top_50_iot_sensor_applications_ranking/.

[18] “IoT technology stack - IoT devices, sensors, gateways and platforms.” [Online]. Available: https://www.i-scoop.eu/internet-of-things-guide/iot-technology-stack-devices-gateways-platforms/.

[19] C. M. Team, “Internet of Things (IoT) 2018-Market Statistics, Use Cases and Trends,” pp. 1–53, 2018.

[20] R. Kotian, G. Exarchakos, and A. Liotta, “Reliable low-power wireless networks over unstable transmission power,” *2017 IEEE 14th Int. Conf. Networking, Sens. Control*, pp. 801–806, May 2017.

[21] J. Schandy, L. Steinfeld, and F. Silveira, “Average Power Consumption Breakdown of Wireless Sensor Network Nodes Using IPv6 over LLNs,” *2015 Int. Conf. Distrib. Comput. Sens. Syst.*, pp. 242–247, 2015.

[22] Web, “Powering IoT Devices: Technologies and Opportunities - IEEE Internet of Things,” 2017. [Online]. Available: http://iot.ieee.org/newsletter/november-2015/powering-iot-devices-technologies-and-opportunities.html.

[23] “LoRa Alliance.” [Online]. Available: https://lora-alliance.org/.

[24] “Sigfox - The Global Communications Service Provider for the Internet of Things (IoT).” [Online]. Available: https://www.sigfox.com/en.

[25] “Zigbee Alliance.” [Online]. Available: https://www.zigbee.org/.

[26] Z. Shelby, K. Hartke, and C. Bormann, “The Constrained Application Protocol (CoAP),” Jun. 2014.

[27] T. Winter *et al.*, “RPL: IPv6 Routing Protocol for Low-Power and Lossy Networks,” *(IETF), RFC 6550, ISSN2070-1721*, 2012.

[28] G. Montenegro, N. Kushalnagar, J. Hui, and D. Culler, “Transmission of IPv6 Packets over IEEE 802.15.4 Networks,” Sep. 2007.

[29] L. A. N. Man, S. Committee, and I. Computer, *IEEE Std 802.15.4e™-2012 (Amendment to IEEE Std 802.15.4-2011) IEEE Standard for Local and metropolitan area networks—Part 15.4: Low-Rate Wireless Personal Area Networks (LR-WPANs)—Amendment 2: Active Radio Frequency Identification (RFID) System Physical*, vol. 2012, no. April. 2012.

[30] L. a N. Man, S. Committee, and I. Computer, *IEEE Std 802.15.4g™-2 2012*

(Amendment to IEEE Std 802.15.4™-2011) Part 15 . 4 : Low-Rate Wireless Personal Area Networks (LR-WPANs), vol. 2012, no. April. 2012.

[31] Bill Schweber, "Options for Powering Your Wireless IoT Device | DigiKey," 2016. [Online]. Available: https://www.digikey.fr/en/articles/techzone/2016/apr/options-for-powering-your-wireless-iot-device.

[32] D. Feng, C. Jiang, G. Lim, L. J. Cimini, G. Feng, and G. Y. Li, "A survey of energy-efficient wireless communications," *IEEE Commun. Surv. Tutorials*, vol. 15, no. 1, pp. 167–178, 2013.

[33] T. Rault, A. Bouabdallah, and Y. Challal, "Energy efficiency in wireless sensor networks: A top-down survey," *Comput. Networks*, vol. 67, pp. 104–122, 2014.

[34] G. Anastasi, M. Conti, M. Di Francesco, and A. Passarella, "Energy conservation in wireless sensor networks: A survey," *Ad Hoc Networks*, vol. 7, no. 3, pp. 537–568, 2009.

[35] G. Miao and N. Himayat, "Cross-layer optimization for energy-efficient wireless communications: a survey," *... Mob. Comput.*, 2009.

[36] John esposito, "DZone Guide 2015 The Internet Of Things, 2015," 2015. [Online]. Available: https://dzone.com/guides/internet-of-things-1.

[37] S. Kim *et al.*, "Health Monitoring of Civil Infrastructures Using Wireless Sensor Networks," 2006.

[38] A. Mainwaring, J. Polastre, R. Szewczyk, D. Culler, and J. Anderson, "Wireless Sensor Networks for Habitat Monitoring," 2002.

[39] N. Baccour, M. Z. Antonio, H. Youssef, and C. Alberto Boano, "Radio Link Quality Estimation in Wireless Sensor Networks: a Survey," *ACM Trans. Sens. Netw*, vol. 35, 2011.

[40] S. Kostin, R. M. Salles, and C. L. de Amorim, "An approach for wireless sensor networks topology control in indoor scenarios," in *Proceedings of the 5th International Latin American Networking Conference on - LANC '09*, 2009, p. 1.

[41] K. Bannister, G. Giorgetti, S. G.-P. of the 5th W. on, and undefined 2008, "Wireless sensor networking for hot applications: Effects of temperature on signal strength, data collection and localization," *Citeseer*, 2008.

[42] M. Zennaro, H. Ntareme, and A. Bagula, "Experimental evaluation of temporal and energy characteristics of an outdoor sensor network," in *Proceedings of the International Conference on Mobile Technology, Applications, and Systems - Mobility '08*, 2008, p. 1.

[43] K. Benkic, M. Malajner, and P. Planinsic, "Using RSSI value for distance estimation in wireless sensor networks based on ZigBee," *Syst. signals*, 2008.

[44] S. Lin, J. Zhang, G. Zhou, L. Gu, J. A. Stankovic, and T. He, "ATPC: adaptive transmission power control for wireless sensor networks," in *Proceedings of the 4th international conference on Embedded networked sensor systems - SenSys '06*, 2006, p. 223.

[45] N. Reijers and G. Halkes, “Link layer measurements in sensor networks,” *Mob. Ad-hoc Sens.*, 2004.

[46] R. Draves, J. Padhye, and B. Zill, “Routing in multi-radio, multi-hop wireless mesh networks,” *Proc. 10th Annu. Int.*, 2004.

[47] “CC2420 Single-Chip 2.4 GHz IEEE 802.15.4 Compliant and ZigBee™ Ready RF Transceiver | TI.com.” [Online]. Available: http://www.ti.com/product/CC2420. [Accessed: 20-Nov-2017].

[48] “Atmel AT86RF215 Device Family Atmel AT86RF215 -DATASHEET.”

[49] F. Qin, X. Dai, and J. E. Mitchell, “Effective-SNR estimation for wireless sensor network using Kalman filter,” *Ad Hoc Networks*, vol. 11, no. 3, pp. 944–958, May 2013.

[50] R. Draves and B. Zill, “Routing in Multi-Radio , Multi-Hop Wireless Mesh Networks.”

[51] G. Hackmann, O. Chipara, and C. Lu, “Robust topology control for indoor wireless sensor networks,” *Proc. 6th ACM Conf. Embed. Netw. Sens. Syst. - SenSys ’08*, p. 57, Nov. 2008.

[52] K. Srinivasan and and P. Levis, “RSSI is Under Appreciated.” [Online]. Available: https://sing.stanford.edu/pubs/rssi-emnets06.pdf. [Accessed: 08-Sep-2015].

[53] Q. Xia and M. Hamdi, “Smart sender: A practical rate adaptation algorithm for multirate IEEE 802.11 WLANs,” *IEEE Trans. Wirel. Commun.*, vol. 7, no. 5, pp. 1764–1775, 2008.

[54] Y. Chen and A. Terzis, “Calibrating RSSI Measurements for 802.15.4 Radios.”

[55] B. Li, S. C. H. Hoi, P. Zhao, and V. Gopalkrishnan, “Radio Link Quality Estimation in Wireless Sensor Networks: a Survey,” *Proc. 14th Int. Conf. Artif. Intell. Stat.*, vol. 15, no. 212, pp. 434–442, 2011.

[56] G. Von Zengen, B. Felix, and L. Wolf, “Transmission Power Control for Interference Minimization in WSNs.”

[57] A. Cerpa *et al.*, “Statistical Model of Lossy Links in Wireless Sensor Networks Publication Date Statistical Model of Lossy Links in Wireless Sensor Networks,” 2005.

[58] M. Rondinone, J. Ansari, J. Riihijärvi, and P. Mähönen, “Designing a reliable and stable link quality metric for wireless sensor networks,” *Proc. Work. Real-world Wirel. Sens. networks - REALWSN ’08*, p. 6, 2008.

[59] C. A. Boano, M. A. Zuniga, T. Voigt, A. Willig, and K. Romer, “The Triangle Metric: Fast Link Quality Estimation for Mobile Wireless Sensor Networks,” *Proc. 19th Int. Conf. Comput. Commun. Networks, ICCCN ’10*, pp. 1–7, 2010.

[60] Y. Qin, Z. He, and T. Voigt, “Towards accurate and agile link quality estimation in wireless sensor networks,” *Ifip Amahnw*, pp. 179–185, 2011.

[61] D. S. D. Son, B. Krishnamachari, and J. Heidemann, “Experimental study of the

effects of transmission power control and blacklisting in wireless sensor networks," *2004 First Annu. IEEE Commun. Soc. Conf. Sens. Ad Hoc Commun. Networks, 2004. IEEE SECON 2004.*, pp. 1–10, 2004.

[62] L. H. a. Correia, D. F. Macedo, A. L. dos Santos, A. a. F. Loureiro, and J. M. S. Nogueira, "Transmission power control techniques for wireless sensor networks," in *Computer Networks*, 2007, vol. 51, no. 17, pp. 4765–4779.

[63] X. Liu, S. Seshan, and P. Steenkiste, "Interference-aware transmission power control for dense wireless networks," *Proc. Annu. Conf. ...*, 2007.

[64] J. K. J. Kim, S. C. S. Chang, and Y. K. Y. Kwon, "ODTPC: On-demand Transmission Power Control for Wireless Sensor Networks," in *2008 International Conference on Information Networking*, 2008, pp. 1–5.

[65] M. M. Y. Masood, G. Ahmed, and N. M. Khan, "Modified on demand transmission power control for wireless sensor networks," in *2011 International Conference on Information and Communication Technologies*, 2011, pp. 1–6.

[66] M. M. Y. Masood, G. Ahmed, and N. M. Khan, "A Kalman filter based adaptive on demand transmission power control (AODTPC) algorithm for wireless sensor networks," in *2012 International Conference on Emerging Technologies*, 2012, pp. 1–6.

[67] M. Tahir, N. Javaid, A. Iqbal, Z. A. Khan, and N. Alrajeh, "On Adaptive Energy Efficient Transmission in WSNs," *arXiv.org*, vol. cs.NI, 2013.

[68] B. Son, K. Kim, Y. Li, and Y. Choi, "Active-Margin Transmission Power Control for Wireless Sensor Networks," *Int. J. Distrib. ...*, 2014.

[69] R. Kotian, G. Exarchakos, and A. Liotta, "Data Driven Transmission Power Control for Wireless Sensor Networks," in *Proceedings of the 8th International Conference on Internet and Distributed Computing Systems - Volume 9258*, Springer-Verlag New York, Inc., 2015, pp. 75–87.

[70] A. Dunkels, F. Osterlind, N. Tsiftes, and Z. He, "Software-based on-line energy estimation for sensor nodes," *Proc. 4th Work.*, 2007.

[71] "Tutorial on Creating Charts | CanvasJS JavaScript Charts." [Online]. Available: https://canvasjs.com/docs/charts/basics-of-creating-html5-chart/.

[72] "Contiki: The Open Source Operating System for the Internet of Things." [Online]. Available: http://www.contiki-os.org/.

[73] "TMote Sky DataSheet." [Online]. Available: http://www.eecs.harvard.edu/~konrad/projects/shimmer/references/tmote-sky-datasheet.pdf.

[74] "Atmel SAM4L ARM Cortex M4 MCUs." [Online]. Available: http://www.atmel.com/products/microcontrollers/arm/sam4l.aspx. [Accessed: 20-Nov-2017].

[75] "AT86RF215 - Smart Energy - Smart Energy Wireless Communications." [Online]. Available: http://www.microchip.com/wwwproducts/en/AT86RF215.

[76] G. Hackmann, O. Chipara, and C. Lu, "Robust topology control for indoor wireless sensor networks," in *Proceedings of the 6th ACM conference on Embedded network sensor systems - SenSys '08*, 2008, p. 57.

[77] G. Holland, N. Vaidya, and P. Bahl, "A rate-adaptive MAC protocol for multi-hop wireless networks," in *ACM/ IEEE Int. Conf. on Mobile COmputing and networking (MOBICOM'01)*, 2001, p. 15.

[78] J. Jelitto, A. N. Barreto, and H. L. Truong, "Power and Rate Adaptation in IEEE 802.11a Wireless LANs," *57th IEEE Semiannu. Veh. Technol. Conf. 2003. VTC 2003-Spring.*, vol. 1, pp. 413–417, 2003.

[79] A. H. Sodhro, L. Chen, A. Sekhari, Y. Ouzrout, and W. Wu, "Energy efficiency comparison between data rate control and transmission power control algorithms for wireless body sensor networks," *Int. J. Distrib. Sens. Networks*, vol. 14, no. 1, p. 155014771775003, Jan. 2018.

[80] A. R. Rebai and M. Fliss, "A Dynamic Link Adaptation for Multimedia Quality-Based Communications in," 2010.

[81] I. Wlans, "CARA : Collision-Aware Rate Adaptation for," vol. 00, no. c, 2006.

[82] S. H. Y. Wong, S. Lu, H. Yang, and V. Bharghavan, "Robust rate adaptation for 802.11 wireless networks," *Proc. 12th Annu. Int. Conf. Mob. Comput. Netw. - MobiCom '06*, p. 146, 2006.

[83] S. Biaz and S. Wu, "ERA : An Efficient Rate Adaption Algorithm with Fragmentation," *Netw. 2008 Ad Hoc Sens. Networks, Wirel. Networks, Next Gener. Internet*, 2008.

[84] J. Choi, J. Na, Y. S. Lim, K. Park, and C. K. Kim, "Collision-aware design of rate adaptation for multi-rate 802.11 WLANs," *IEEE J. Sel. Areas Commun.*, vol. 26, no. 8, pp. 1366–1375, 2008.

[85] B. K. P. -, M. K. M. -, A. K. J. -, and A. K. N. -, "Power Aware Ad Hoc On-demand Distance Vector (PAAODV) Routing for MANETS," *J. Converg. Inf. Technol.*, vol. 6, no. 6, pp. 212–220, Jun. 2011.

[86] C. Schurgers, D. Estrin, G. Pottie, and K. Yao, "Energy-aware wireless communications PHD," 2002.

[87] D. Qiao, S. Choi, and K. G. Shin, "Interference analysis and transmit power control in IEEE 802.11a/h wireless LANs," *IEEE/ACM Trans. Netw.*, vol. 15, no. 5, pp. 1007–1020, 2007.

[88] D. Qiao, "Goodput Enhancement of IEEE 802 . lla Wireless LAN via Link Adaptation," *98*, pp. 1995–2000, 2002.

[89] H. Slimani, B. Escrig, R. Dhaou, and A.-L. Beylot, "Energy and throughput efficient transmission strategy with Cooperative Transmission in ad-hoc networks," in *2013 9th International Wireless Communications and Mobile Computing Conference (IWCMC)*, 2013, pp. 381–386.

[90] X. Ao, S. Jiang, and L. Tang, "Traffic-aware active link rate adaptation via power

control for multi-hop multi-rate 802.11 networks," *Int. Conf. Commun. Technol. Proceedings, ICCT*, no. 9351064101000004, pp. 1255–1259, 2010.

[91] J. Kim and J. Huh, "Link Adaptation Strategy on Transmission Rate and Power Control in IEEE 802 . 11 WLANs," 2006.

[92] "code2flow - online interactive code to flowchart converter." [Online]. Available: https://code2flow.com/app.

9. Appendices

Appendix-A: Related Figures

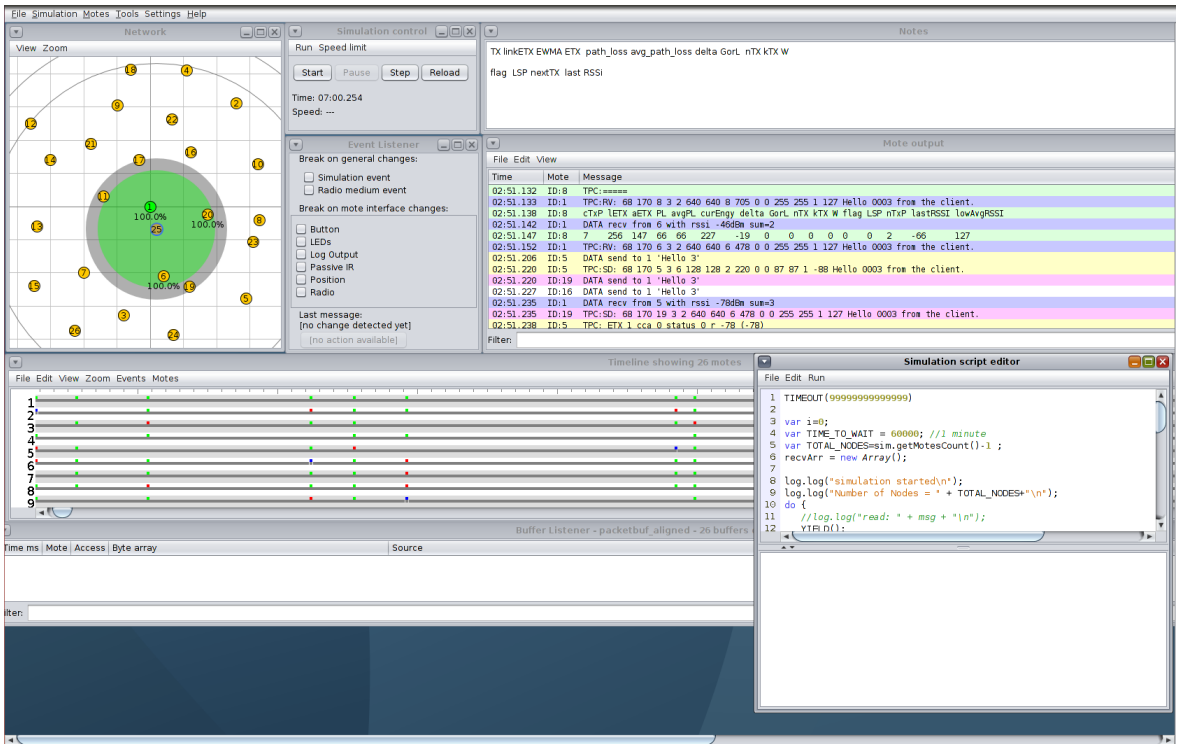

Figure 9-1: Snapshot of COOJA simulator

Appendix-B: Sorted Energy level array in the ascending order

Table 9-1: Sorted Energy level array in ascending order for REACT

Energy Levels	Rate (Kbps)	Power Level	Energy(µJ)
0	50	0	17483.04
1	50	1	19042.56
2	50	2	20602.08
3	50	3	22599.36
4	50	4	23994.72
5	50	5	26593.92
6	25	0	27259.74
7	50	6	29275.2
8	25	1	29691.36
9	25	2	32122.98
10	50	7	32722.56

11	25	3	35237.16
12	50	8	35485.92
13	25	4	37412.82
14	50	9	39535.2
15	25	5	41465.52
16	50	10	43693.92
17	25	6	45646.2
18	12.50	0	46736.46
19	50	11	48263.04
20	12.50	1	50905.44
21	25	7	51021.36
22	50	12	52284.96
23	12.50	2	55074.42
24	25	8	55330.02
25	50	13	56115.36
26	12.50	3	60413.64
27	25	9	61643.7
28	12.50	4	64143.78
29	25	10	68128.02
30	12.50	5	71092.08
31	25	11	75252.24
32	12.50	6	78259.8
33	25	12	81523.26
34	6.25	0	85766.58
35	12.50	7	87475.44
36	25	13	87495.66
37	6.25	1	93417.12
38	12.50	8	94862.58
39	6.25	2	101067.7
40	12.50	9	105687.3
41	6.25	3	110865.7
42	12.50	10	116804.6
43	6.25	4	117710.9

44	12.50	11	129019
45	6.25	5	130461.8
46	12.50	12	139770.5
47	6.25	6	143615.4
48	12.50	13	150010.1
49	6.25	7	160527.1
50	6.25	8	174083.3
51	6.25	9	193947.9
52	6.25	10	214349.3
53	6.25	11	236764.1
54	6.25	12	256494.4
55	6.25	13	275285.2

Appendix-C: Flowcharts of the proposed algorithm REACT

Code2Flow Web application [92] was used to design the flowchart for the proposed algorithm. The following shows the flowcharts of various functionalities of the algorithm.

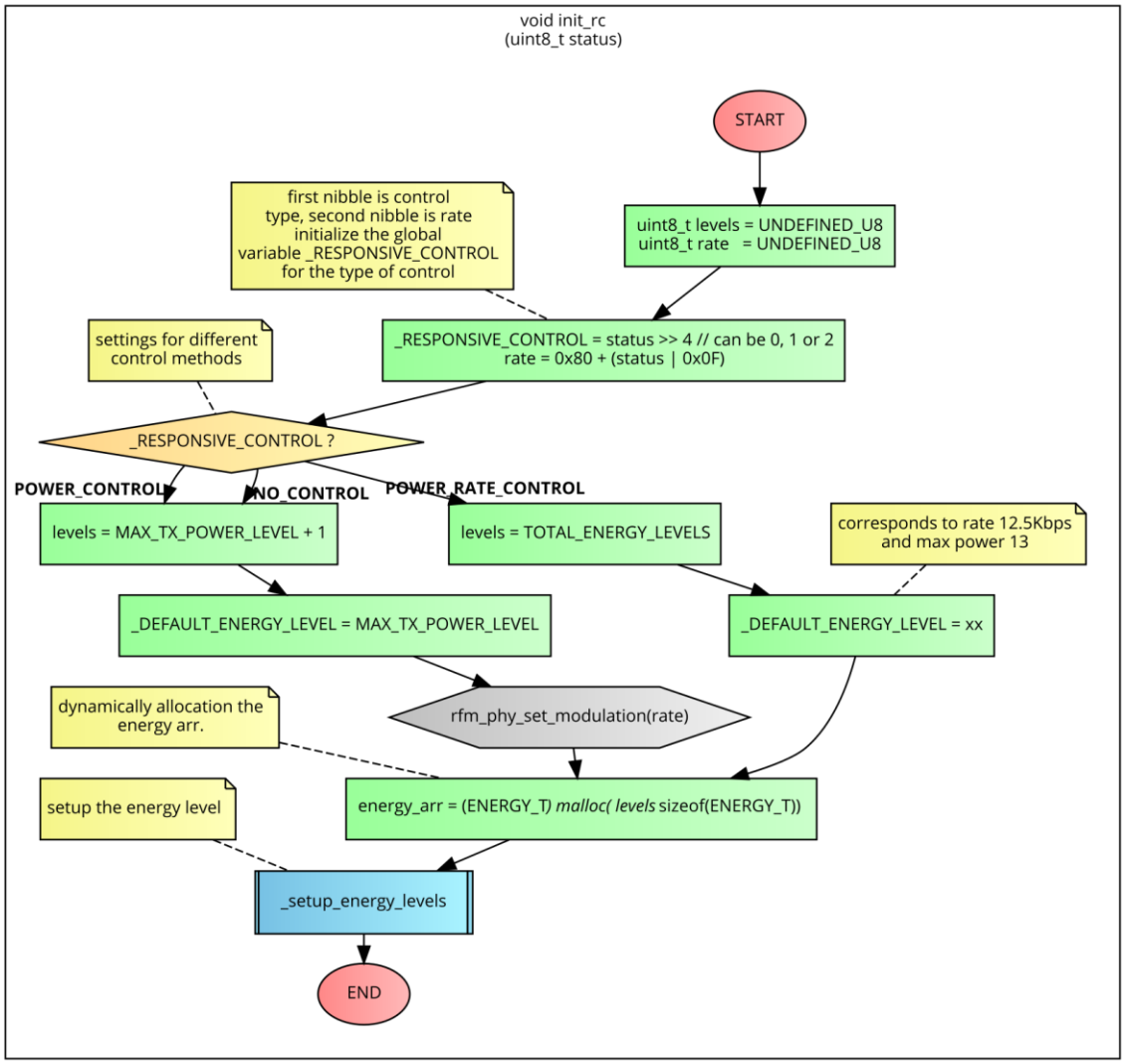

Figure 9-2: FLowchart for initializing the control mechanism

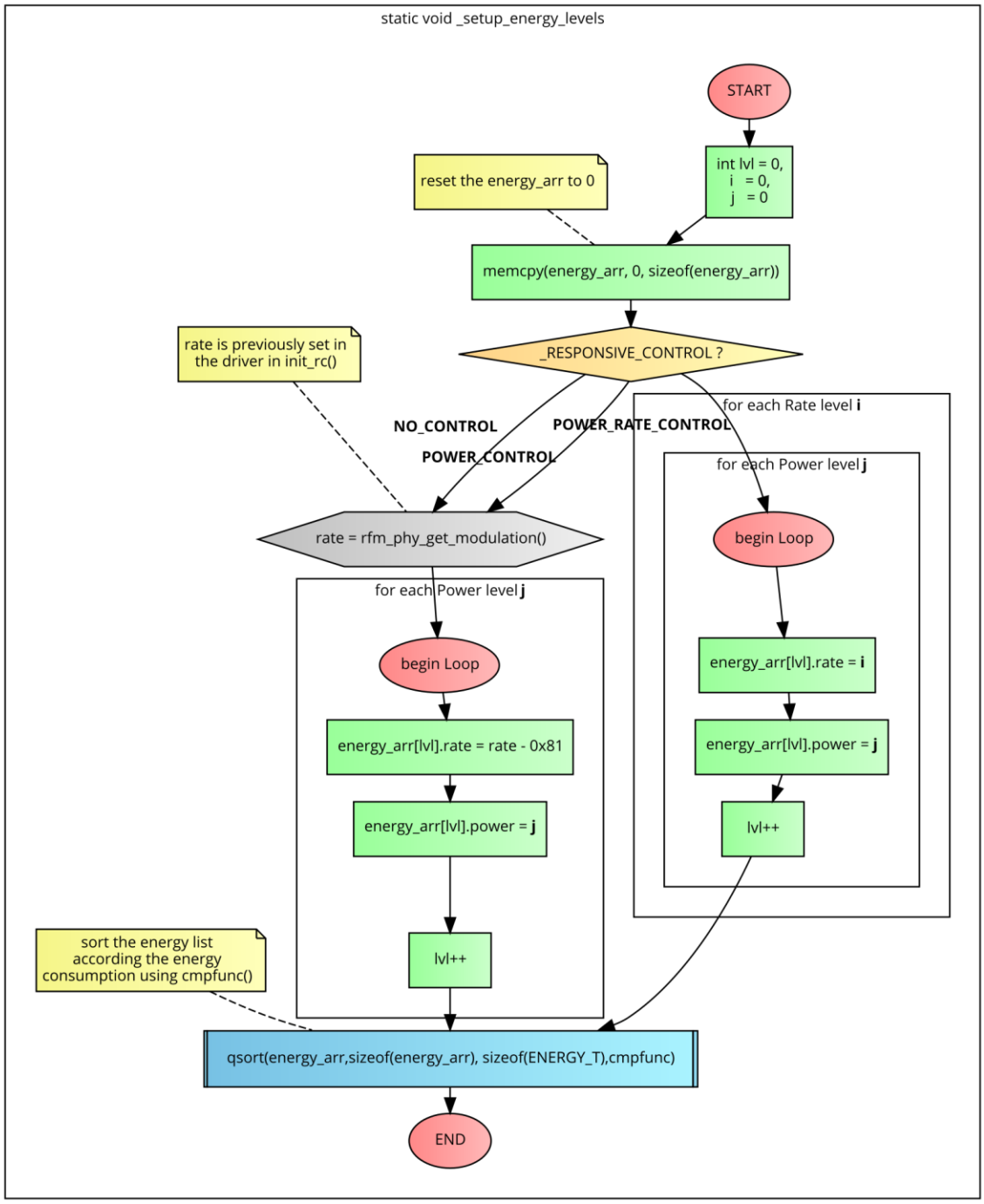

Figure 9-3: Setting up energy level array

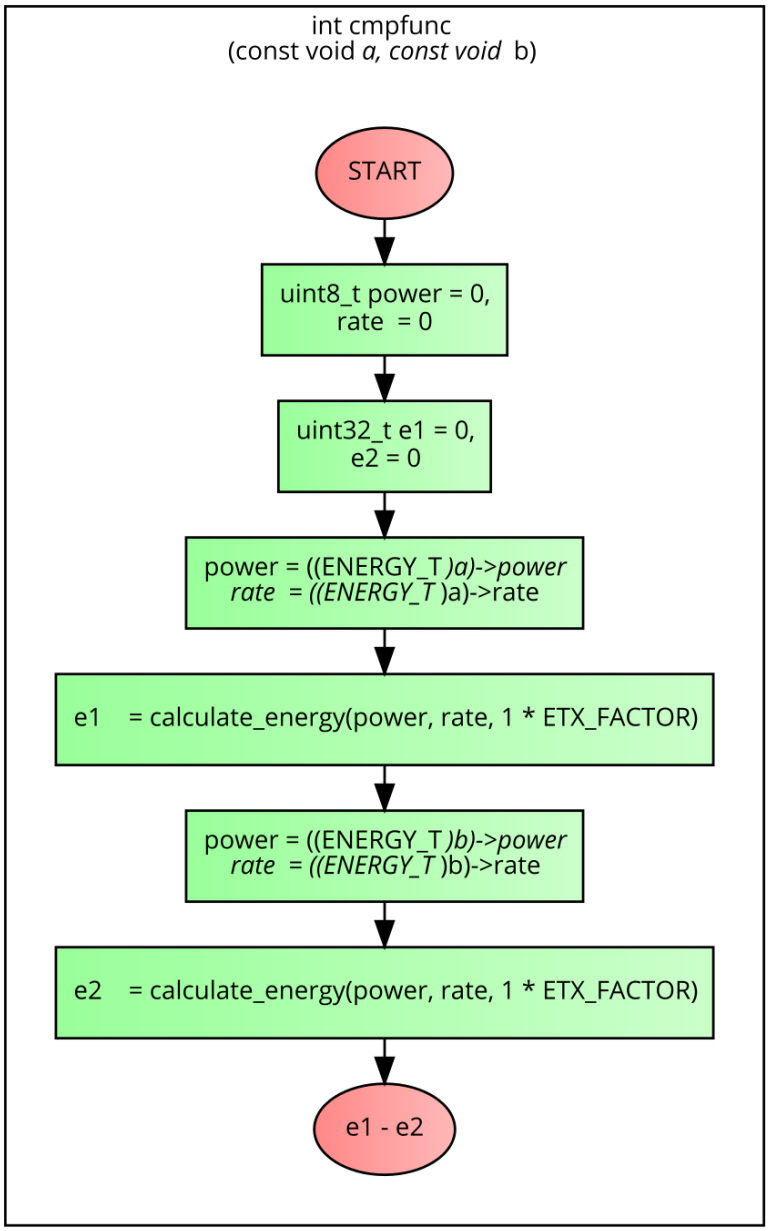

Figure 9-4: Flowchart to compare the energy levels used by qsort

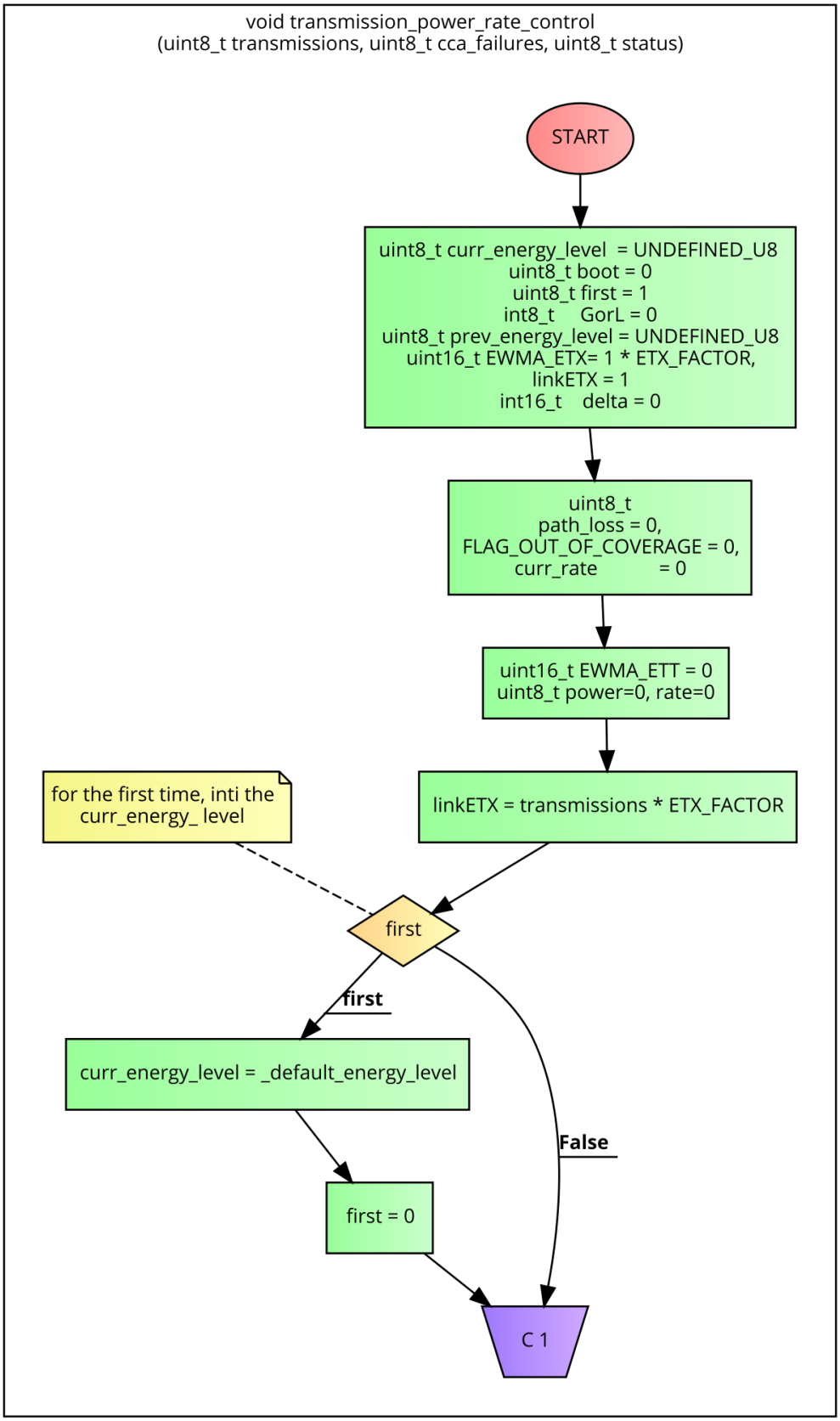
void transmission_power_rate_control
(uint8_t transmissions, uint8_t cca_failures, uint8_t status)
START
uint8_t curr_energy_level = UNDEFINED_U8
uint8_t boot = 0
uint8_t first = 1
int8_t GorL = 0
uint8_t prev_energy_level = UNDEFINED_U8
uint16_t EWMA_ETX= 1 * ETX_FACTOR,
linkETX = 1
int16_t delta = 0
uint8_t
path_loss = 0,
FLAG_OUT_OF_COVERAGE = 0,
curr_rate = 0
uint16_t EWMA_ETT = 0
uint8_t power=0, rate=0
for the first time, inti the
curr_energy_ level
linkETX = transmissions * ETX_FACTOR
first
first
curr_energy_level = _default_energy_level
False
first = 0
C 1

(a)

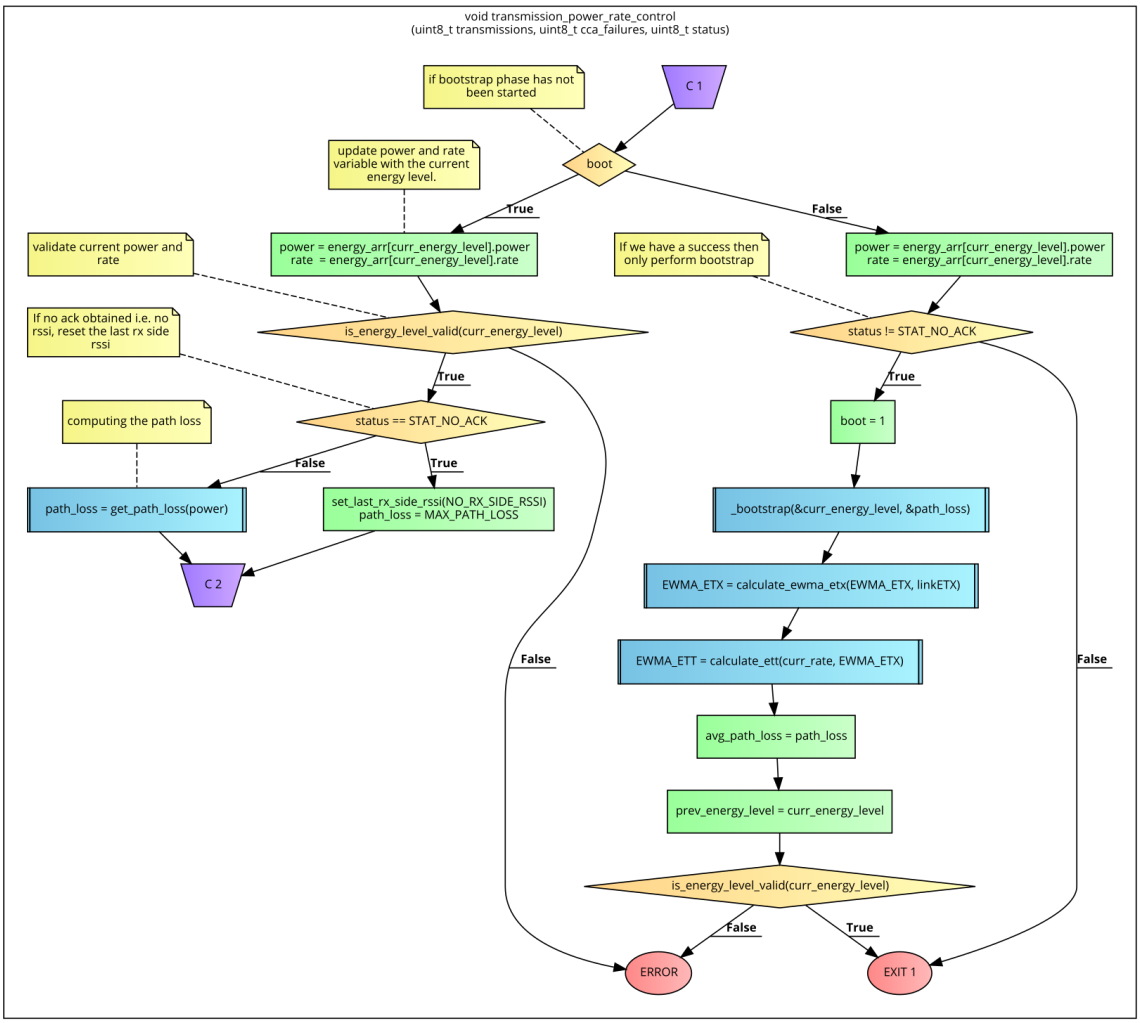
void transmission_power_rate_control
(uint8_t transmissions, uint8_t cca_failures, uint8_t status)
if bootstrap phase has not been started
C 1
update power and rate variable with the current energy level.
boot
True
False
validate current power and rate
power = energy_arr[curr_energy_level].power rate = energy_arr[curr_energy_level].rate
If we have a success then only perform bootstrap
power = energy_arr[curr_energy_level].power rate = energy_arr[curr_energy_level].rate
If no ack obtained i.e. no rssi, reset the last rx side rssi
is_energy_level_valid(curr_energy_level)
status != STAT_NO_ACK
True
True
computing the path loss
status == STAT_NO_ACK
boot = 1
False
True
path_loss = get_path_loss(power)
set_last_rx_side_rssi(NO_RX_SIDE_RSSI)
path_loss = MAX_PATH_LOSS
_bootstrap(&curr_energy_level, &path_loss)
C 2
EWMA_ETX = calculate_ewma_etx(EWMA_ETX, linkETX)
False
EWMA_ETT = calculate_ett(curr_rate, EWMA_ETX)
False
avg_path_loss = path_loss
prev_energy_level = curr_energy_level
is_energy_level_valid(curr_energy_level)
False
True
ERROR
EXIT 1

(b)

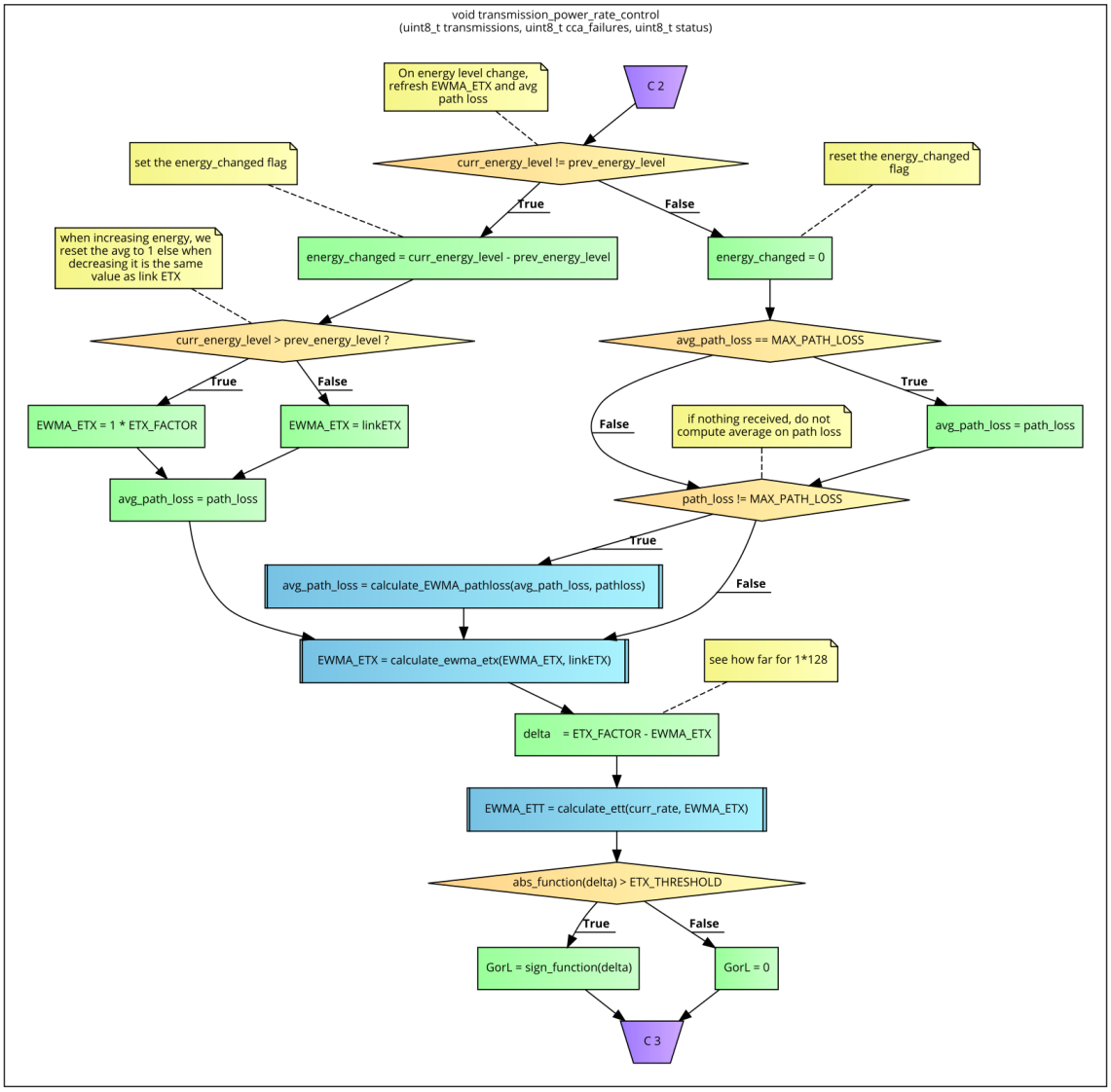
void transmission_power_rate_control
(uint8_t transmissions, uint8_t cca_failures, uint8_t status)
On energy level change, refresh EWMA_ETX and avg path loss
C 2
set the energy_changed flag
curr_energy_level != prev_energy_level
reset the energy_changed flag
True
False
when increasing energy, we reset the avg to 1 else when decreasing it is the same value as link ETX
energy_changed = curr_energy_level - prev_energy_level
energy_changed = 0
curr_energy_level > prev_energy_level ?
avg_path_loss == MAX_PATH_LOSS
True
False
EWMA_ETX = 1 * ETX_FACTOR
EWMA_ETX = linkETX
False
if nothing received, do not compute average on path loss
True
avg_path_loss = path_loss
avg_path_loss = path_loss
path_loss != MAX_PATH_LOSS
True
avg_path_loss = calculate_EWMA_pathloss(avg_path_loss, pathloss)
False
EWMA_ETX = calculate_ewma_etx(EWMA_ETX, linkETX)
see how far for 1*128
delta = ETX_FACTOR - EWMA_ETX
EWMA_ETT = calculate_ett(curr_rate, EWMA_ETX)
abs_function(delta) > ETX_THRESHOLD
True
False
GorL = sign_function(delta)
GorL = 0
C 3

(c)

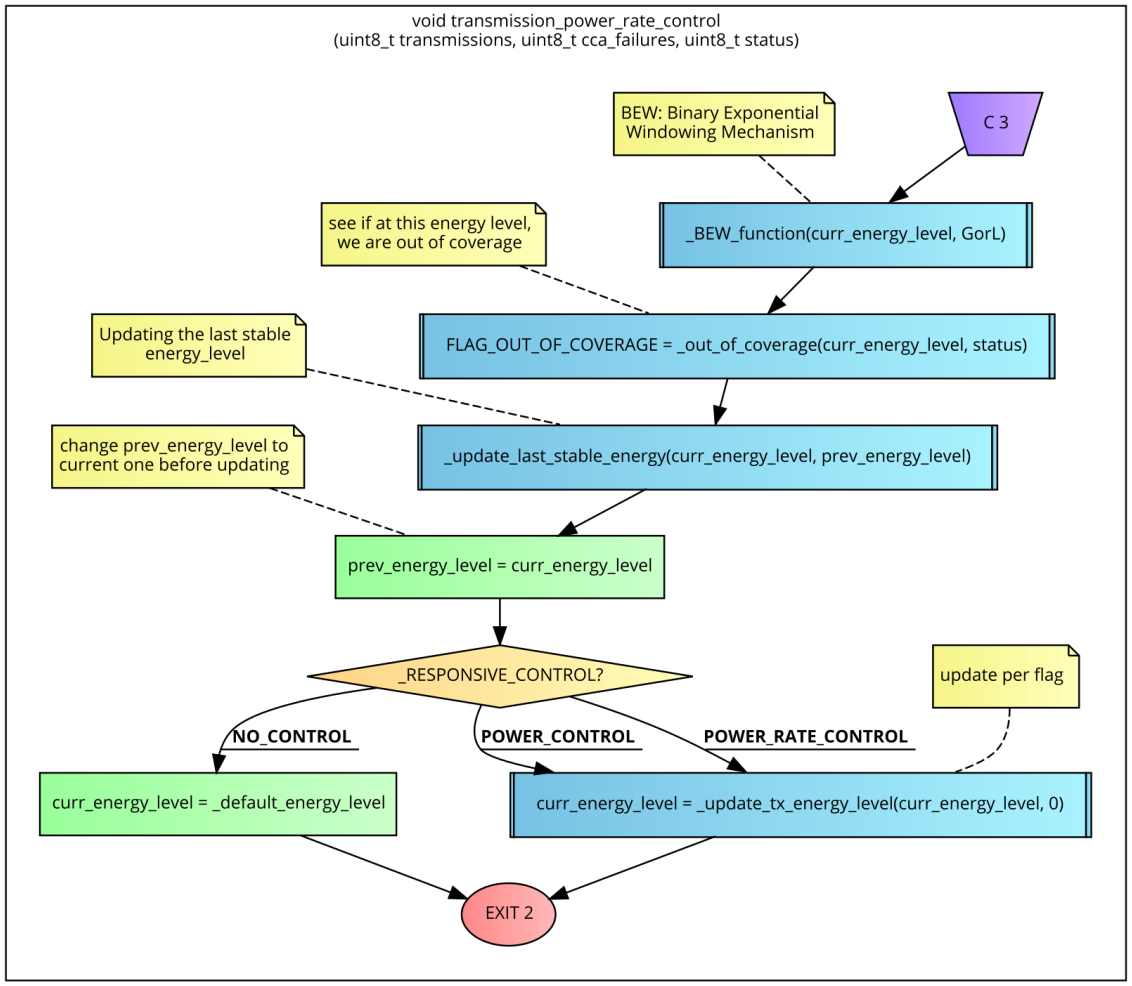

(d)

Figure 9-5: Main function of Transmission power and rate control algortihm for REACT

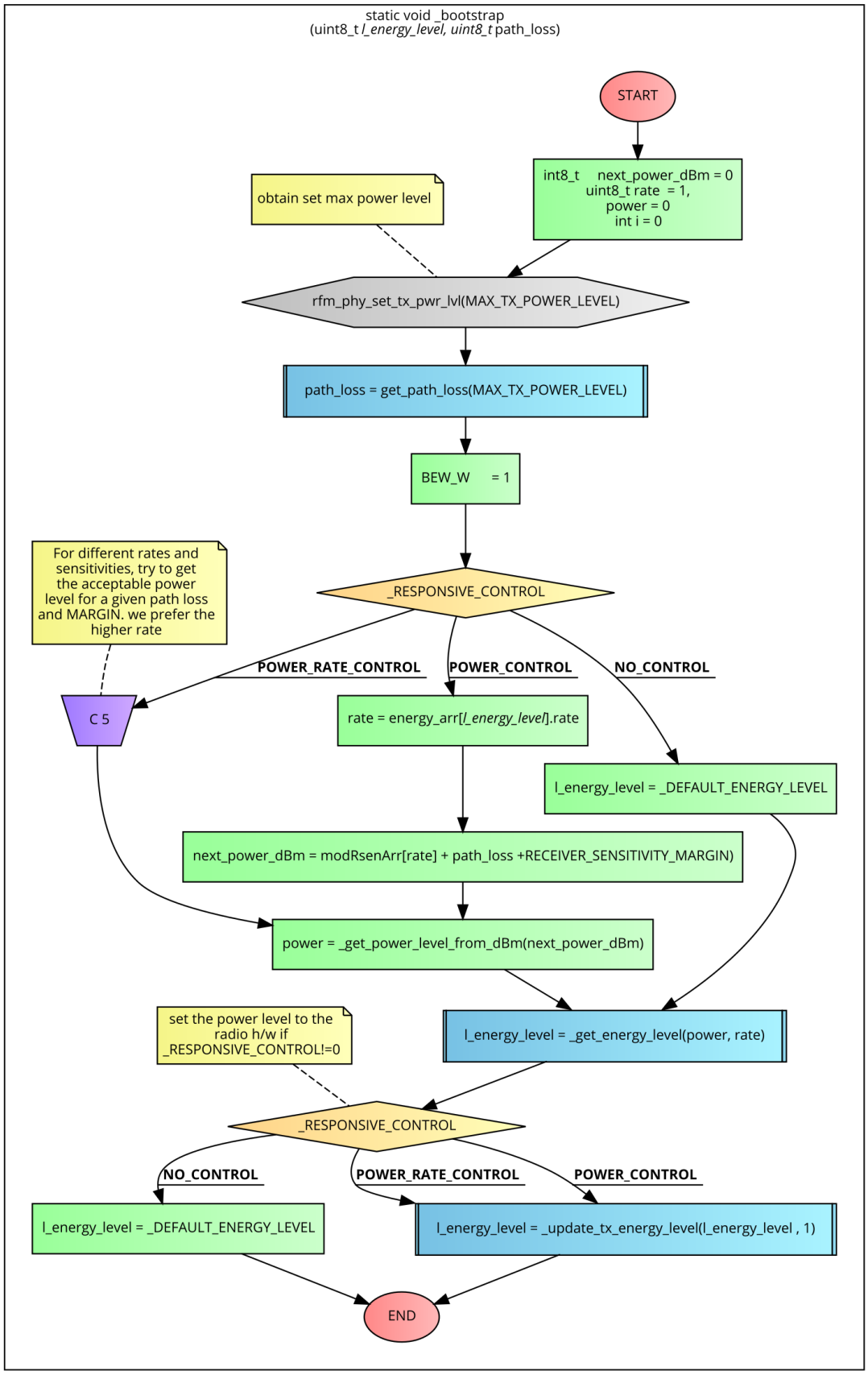
static void _bootstrap
(uint8_t l_energy_level, uint8_t path_loss)
START
int8_t next_power_dBm = 0
uint8_t rate = 1,
power = 0
int i = 0
obtain set max power level
rfm_phy_set_tx_pwr_lvl(MAX_TX_POWER_LEVEL)
path_loss = get_path_loss(MAX_TX_POWER_LEVEL)
BEW_W = 1
For different rates and sensitivities, try to get the acceptable power level for a given path loss and MARGIN. we prefer the higher rate
_RESPONSIVE_CONTROL
POWER_RATE_CONTROL
POWER_CONTROL
NO_CONTROL
C 5
rate = energy_arr[l_energy_level].rate
l_energy_level = _DEFAULT_ENERGY_LEVEL
next_power_dBm = modRsenArr[rate] + path_loss +RECEIVER_SENSITIVITY_MARGIN)
power = _get_power_level_from_dBm(next_power_dBm)
set the power level to the radio h/w if _RESPONSIVE_CONTROL!=0
l_energy_level = _get_energy_level(power, rate)
_RESPONSIVE_CONTROL
NO_CONTROL
POWER_RATE_CONTROL
POWER_CONTROL
l_energy_level = _DEFAULT_ENERGY_LEVEL
l_energy_level = _update_tx_energy_level(l_energy_level , 1)
END

(a)

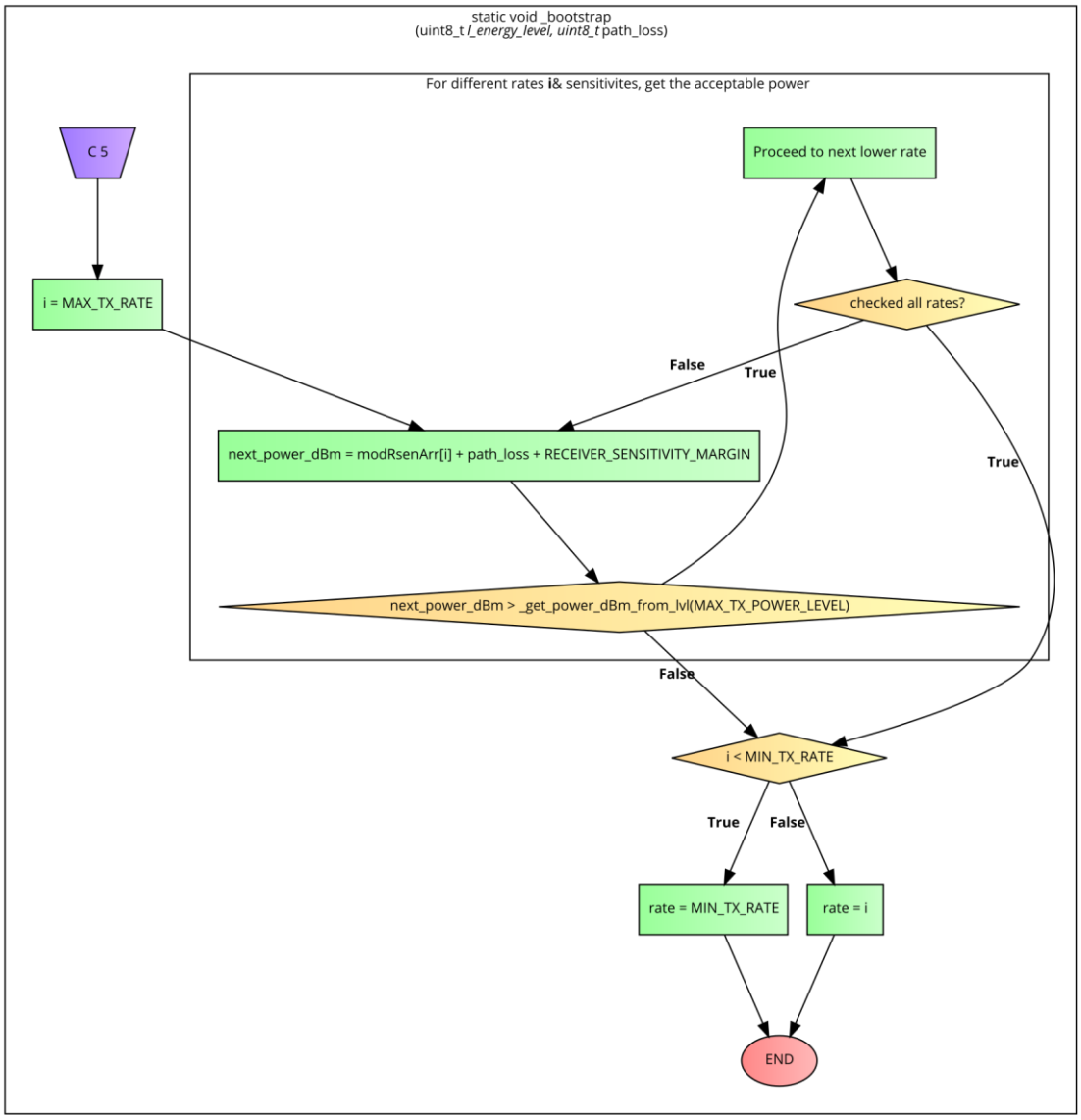

(b)

Figure 9-6: Flowchart showing the bootstrap phase

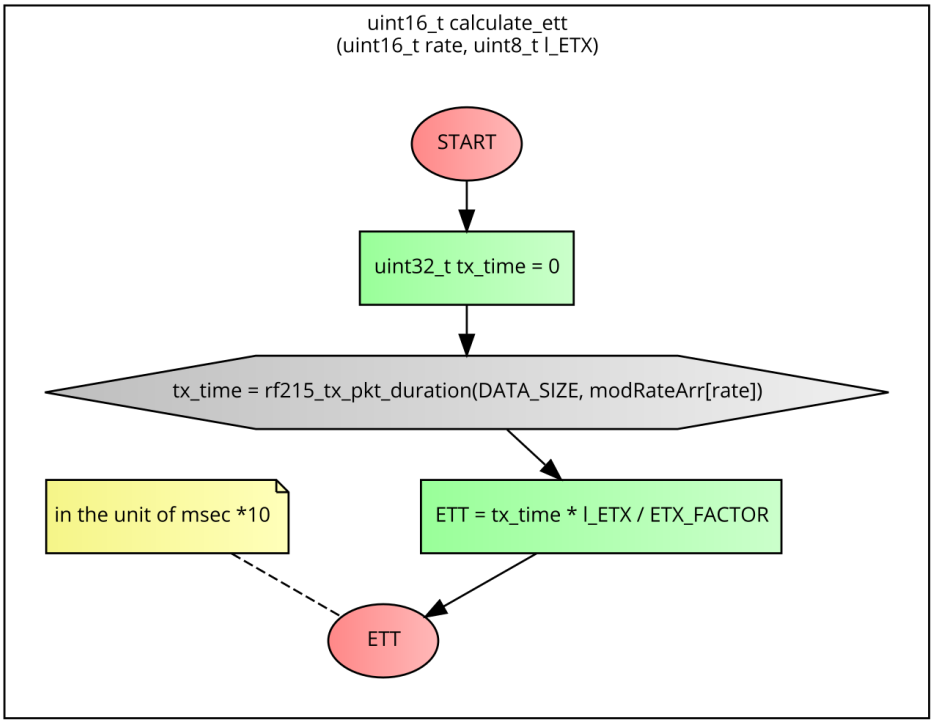

Figure 9-7: Flowchart for calculating the ETT

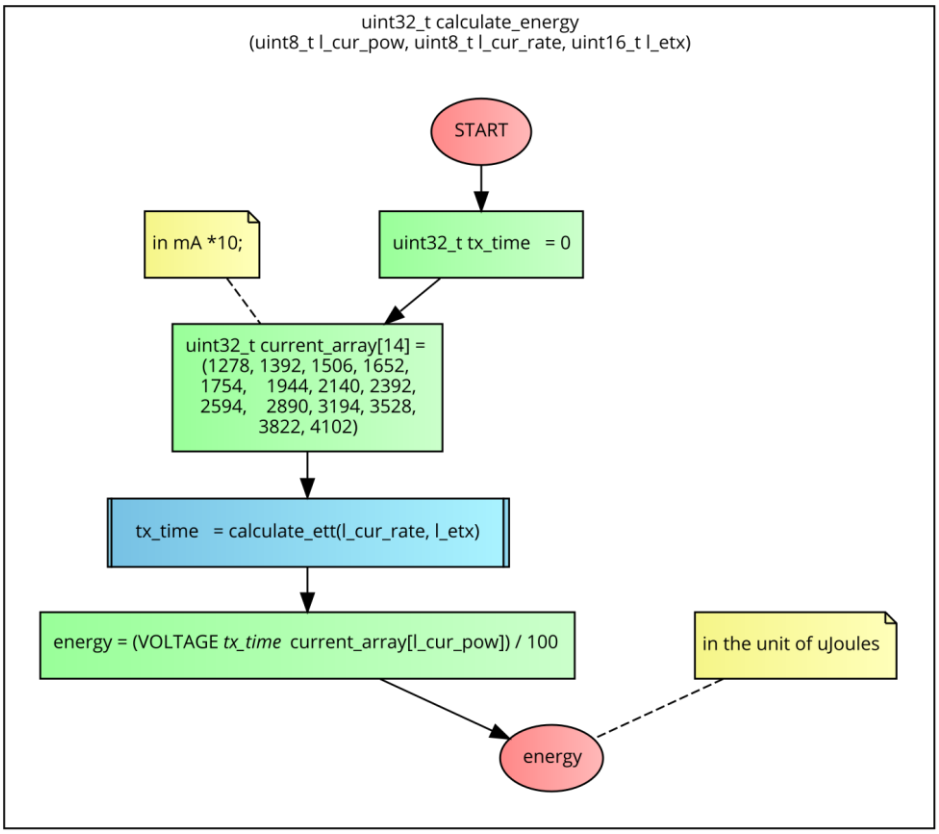

Figure 9-8: Flowchart for calculating TX Energy consumption

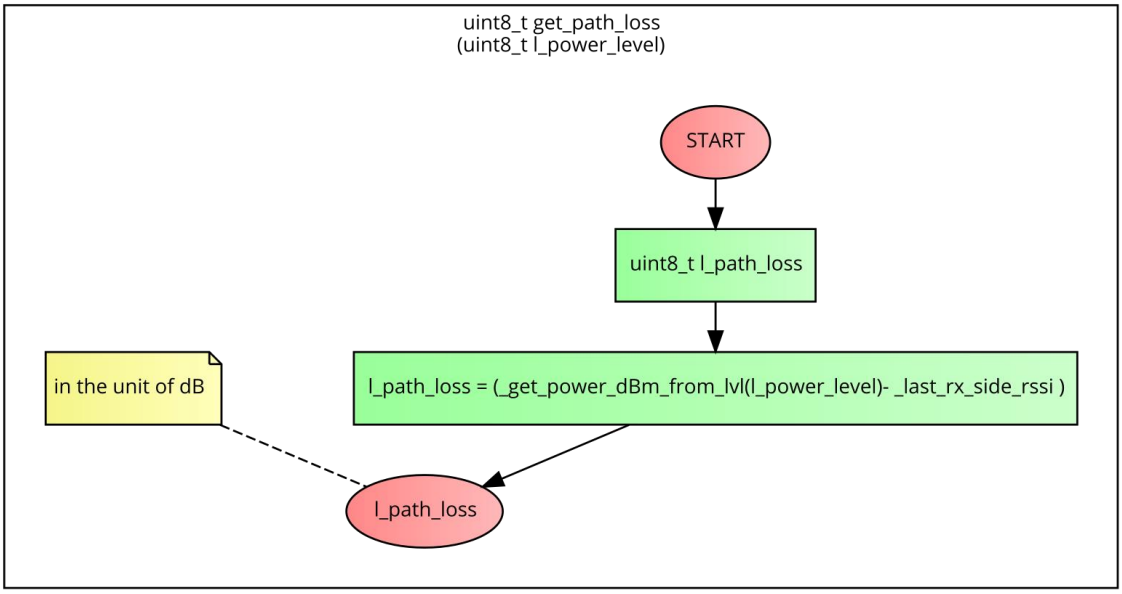

Figure 9-9: Flowchart for claculating the path loss

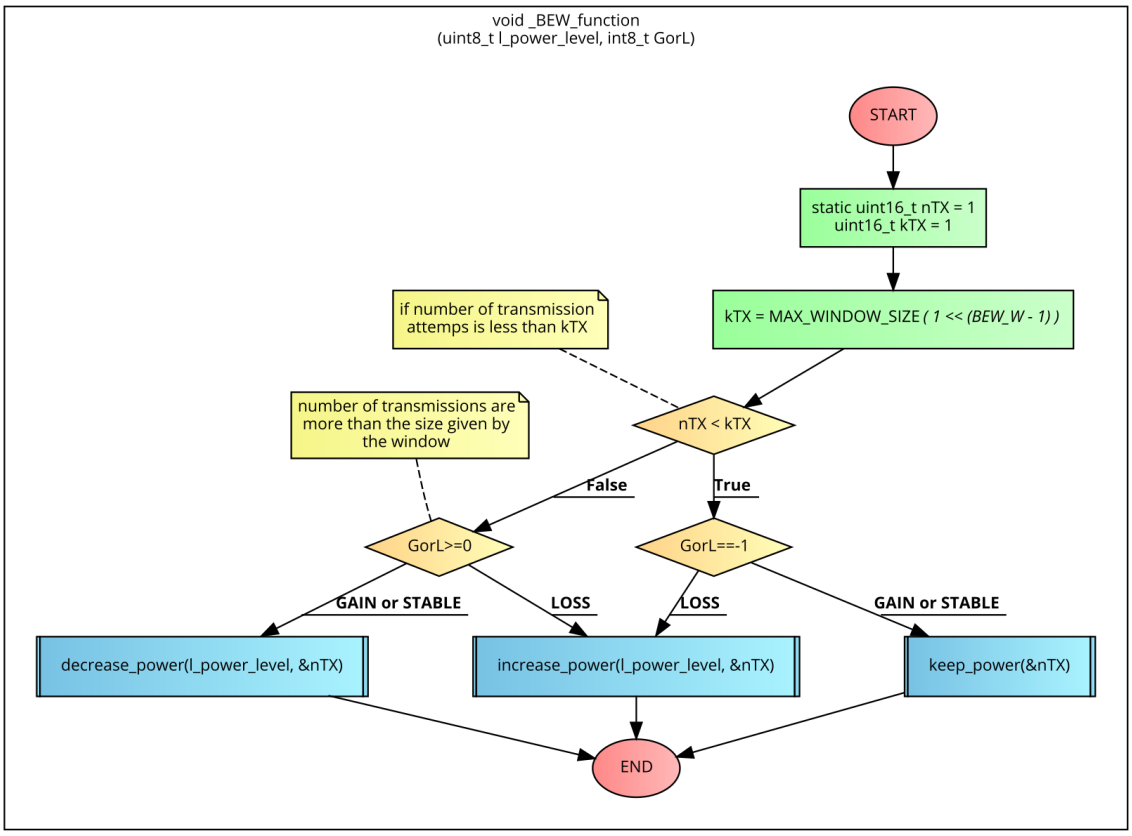

Figure 9-10: Flowchart showing BEW Mechanism

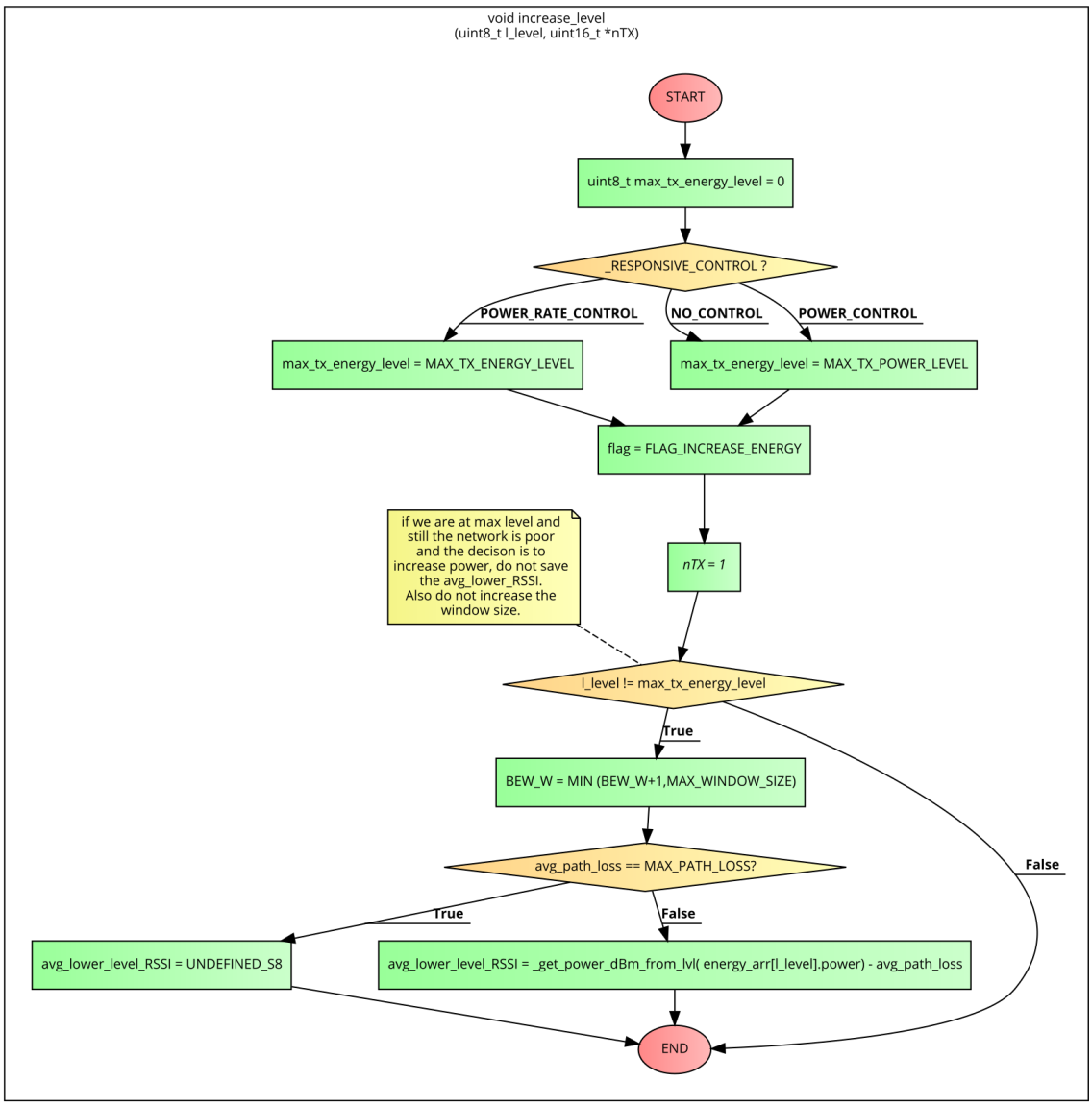

Figure 9-11: Flowchart for the actions for increasing the power/energy level

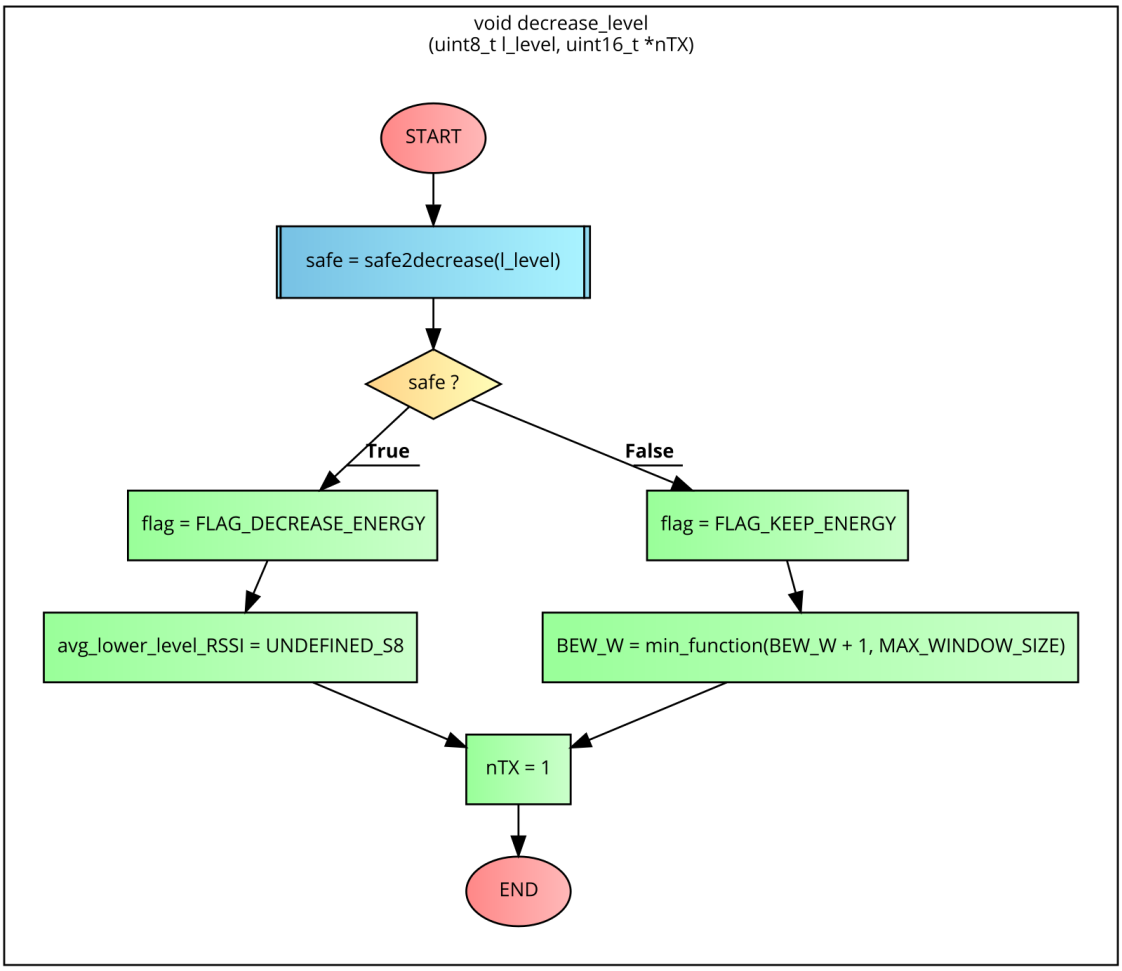

Figure 9-12: Flowchart showing the process for decresing the power/energy level

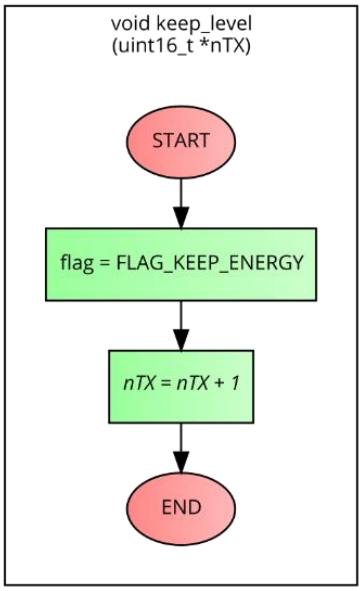

Figure 9-13: Flowchart showing process for keeping the same level

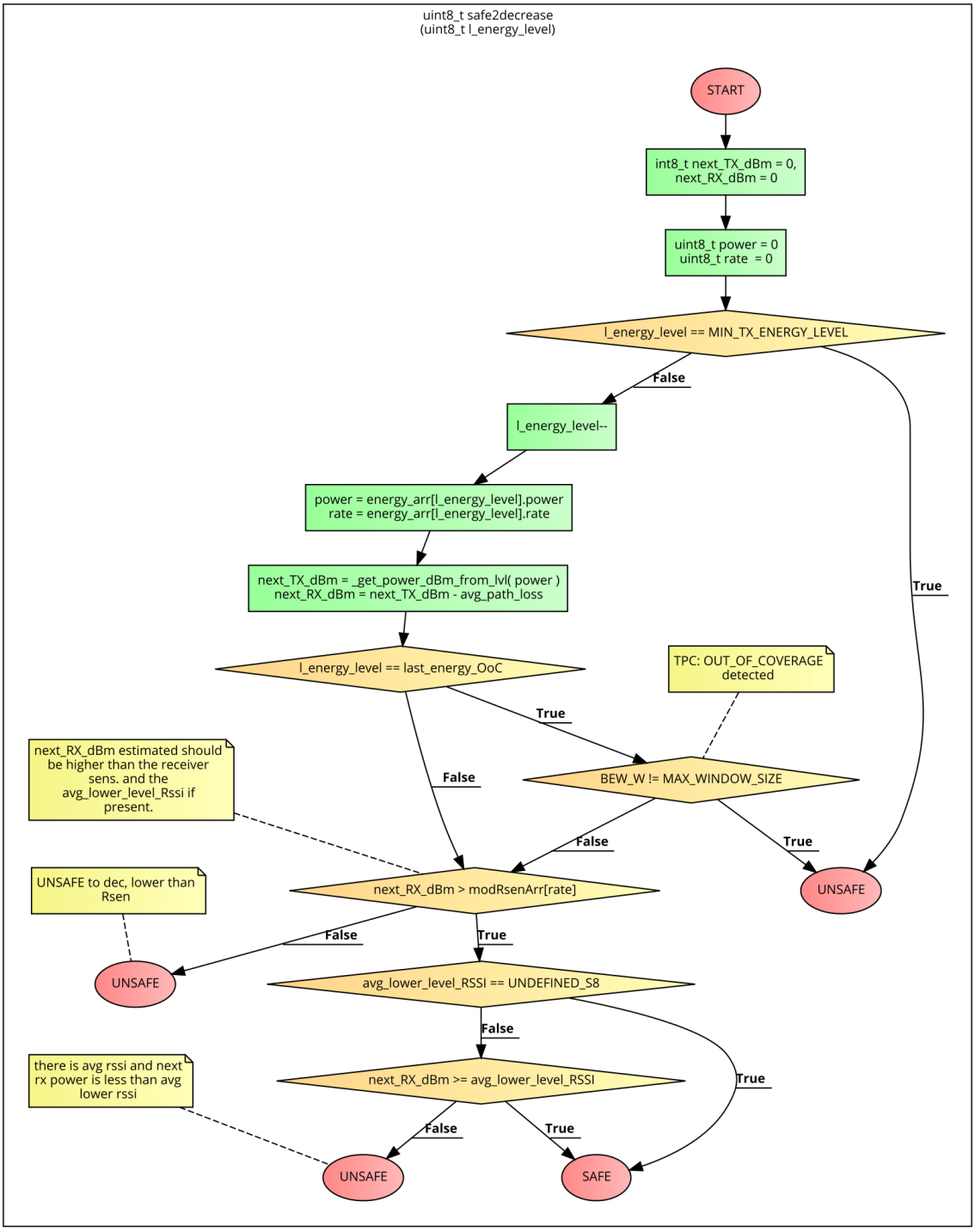

Figure 9-14: Flowchart showing safe2Decrease Module

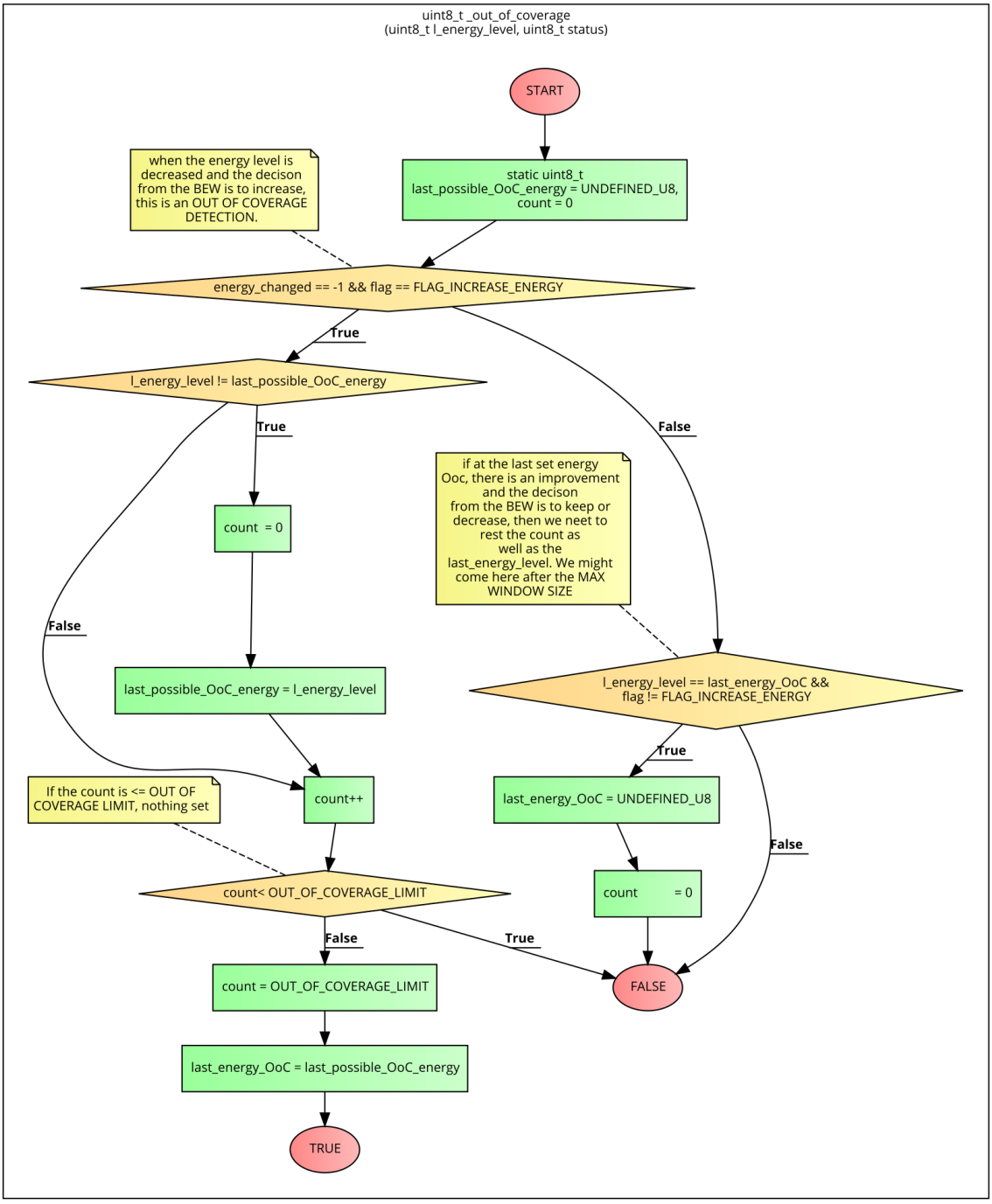

Figure 9-15: Flowchart showing out_of_coverage detection mechanism

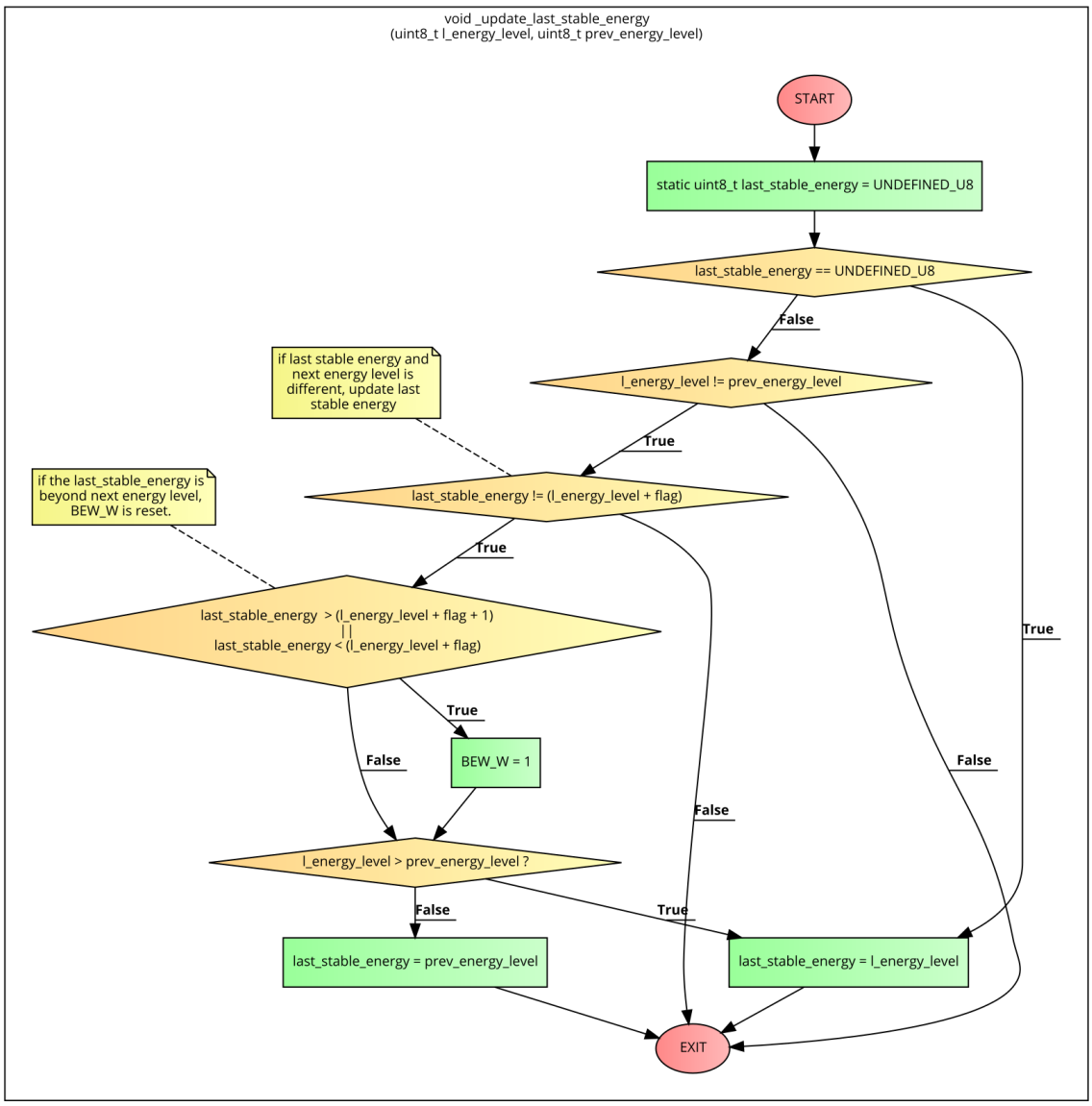

Figure 9-16: Flowchart to update the last stable energy/power level

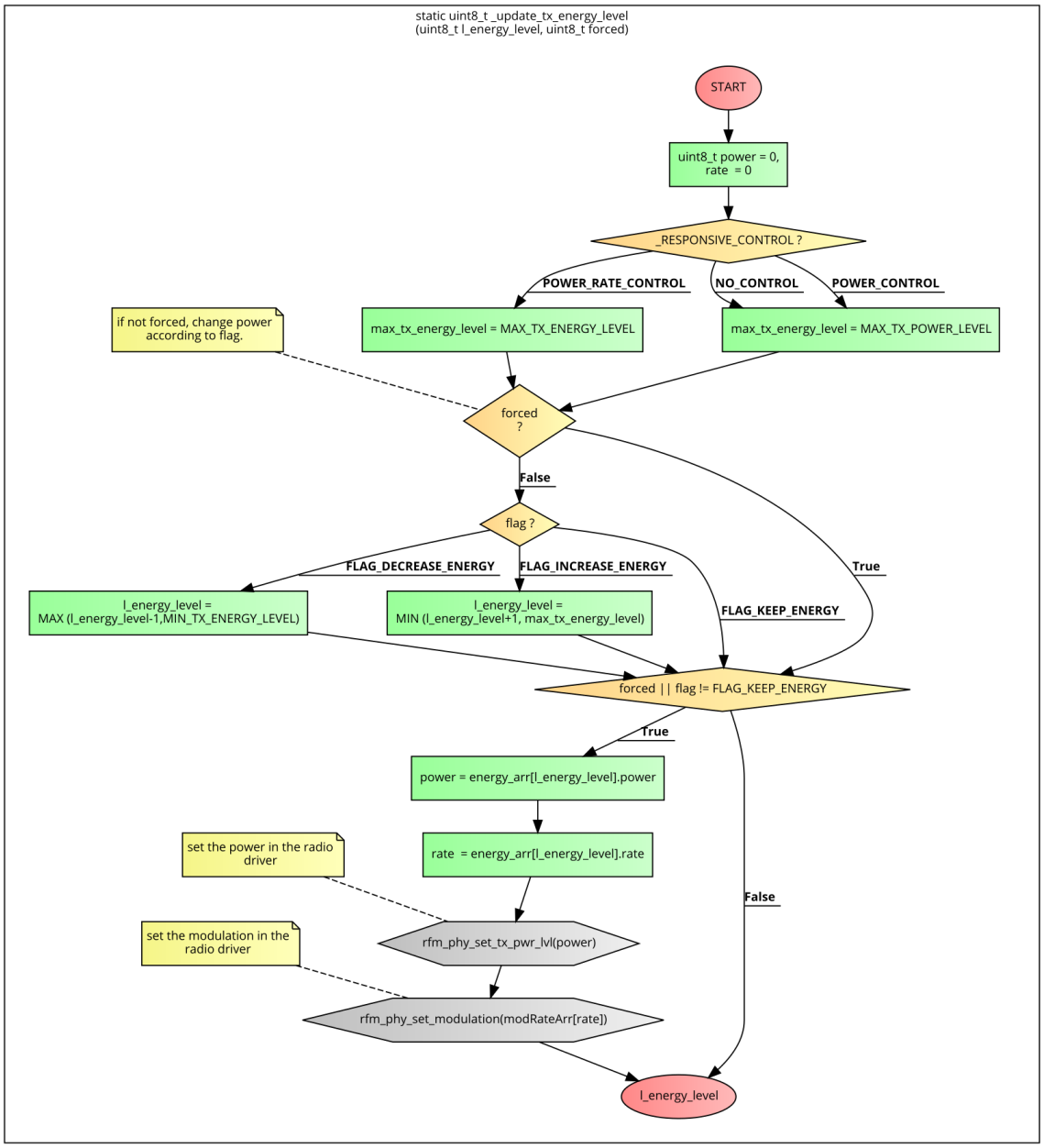

Figure 9-17: Flowchart to update the TX radio parameters (power, rate)